January 2017

Demethylation Therapy As A Novel Treatment For Human Papilloma Virus-Associated Head And Neck Cancer

Michael Hajek
Yale University

Demethylation therapy as a novel treatment for human papilloma virus-associated head and neck cancer

A Thesis Submitted to the

Yale University School of Medicine

In Partial Fulfillment of the Requirement for the

Degree of Doctor of Medicine

By

Michael A. Hajek

2017

Thesis advisor: Wendell G. Yarbrough, MD MMHC FACS

Acknowledgements

This work would not be possible without my thesis advisor, Dr. Wendell Yarbrough, as well as Dr. Natalia Issaeva, for their support and guidance through the planning, experimental procedures, and writing of this project. In particular, I would like to also thank Cyril Gary and Dr. Asel Biktasova who performed some of the experiments described herein. I would also like to thank May-Anh Nguyen her help in editing the final version of this work. Funding for this research was made possible through two NIH TL1 training grants. A version of Specific Aim 3 is published in Cancer.

Abstract

DEMETHYLATION THERAPY AS A NOVEL TREATMENT FOR HUMAN PAPILLOMA VIRUS-ASSOCIATED HEAD AND NECK CANCER. Michael A. Hajek, Natalia Issaeva, and Wendell G. Yarbrough. Section of Otolaryngology, Department of Surgery, Yale University, School of Medicine, New Haven, CT.

5-azacytidine (5-aza) and its structural analog 5-aza-2'-deoxycytidine (decitabine) are demethylating agents currently used to treat myelodysplastic syndrome and acute myeloid leukemia. In addition to demethylating DNA, they are known to cause DNA damage and activate DNA damage response pathways, but our mechanistic understanding of these processes is incomplete. Given the unique epigenetic profile of human papilloma virus-associated (HPV+) head and neck squamous cell carcinoma (HNSCC), we sought to develop demethylation therapy as a novel, targeted treatment for this subset of cancer that has less morbidity than current treatments. We wanted to characterize the DNA damage and describe the mechanism of damage induced by 5-aza in these cells, as well as the cellular response and effect on metastatic potential in cells, xenograft models, and tumors from patients treated in a clinical trial at the Yale Cancer Center. By using pulsed-field gel electrophoresis, we found that demethylation treatment induces DNA double strand break formation exclusively in HPV+ head and neck cancer cells, and that these breaks depend on active transcription, replication, and expression of a known antiviral enzyme, apolipoprotein B mRNA editing enzyme catalytic polypeptide-like 3 (APOBEC3B). Furthermore, we found that demethylation therapy also reactivates p53, downregulates HPV genes, reduces the expression of matrix metalloproteinases, and reduces the metastatic potential in cells, xenograft models, and in patient tumors.

In addition, we sought to discover biomarkers to identify a subset of HPV+ head and neck cancer patients that may be amenable to de-escalated treatment. In doing so, by analyzing The Cancer Genome Atlas (TCGA), we found that roughly one third of HPV+ head and neck tumors harbor inactivating mutations in TRAF3 (TNF receptor associated factor 3) or CYLD (cylindromatosis) that predict a lack of viral integration and improved patient survival, thus questioning the canonical model of HPV-driven carcinogenesis and identifying a group of patients that may respond to de-escalation therapy.

Table of Contents

Introduction

Introduction to Head and Neck Cancer

Head and neck squamous cell carcinoma (HNSCC) is the sixth most common malignancy worldwide and accounts for roughly 600,000 new cases diagnosed each year [3, 4]. As an aggressive cancer that tends to present late in the course of disease, HNSCC has a poor prognosis with a five-year survival rate ranging from 50-63% [5, 6]. The term "head and neck cancer" is more broad than HNSCC, and describes all soft tissue malignancies of the head and neck region, including the upper aerodigestive tract, nasal cavity, and salivary glands. HNSCC accounts for about 90% of head and neck cancers, and encompasses malignancies arising from the epithelia of the upper aerodigestive tract, namely, the oral cavity, oropharynx, hypopharynx, and larynx. Though dependent on the location, size, and extent of local metastases, patients tend to present with neck mass, dysphagia, otalgia, unexplained weight loss, hoarseness, or dyspnea. Given the anatomical location, both the natural course of disease and treatment modalities are inextricably linked to the patient's ability to breath, speak, and swallow, which adds a layer of complexity to the care of head and neck cancer patients.

The most important risk factors in the development of HNSCC are tobacco, alcohol, and infection with high risk strains of the human papilloma virus (HPV). In recent years, decreased tobacco consumption has paralleled falling rates of HNSCC in the United States. Tobacco and excessive alcohol intake can give rise to HNSCC anywhere along the upper aerodigestive tract where cells are exposed to the carcinogens. In fact, tobacco and alcohol create a synergistic effect, where years of heavy use of the two leads

to a 35- to 50-fold increase in the risk of developing HNSCC [7, 8]. HPV, on the other hand, tends to cause cancers in the oropharynx, a subsite within the head and neck that includes the tonsils and base of tongue. Roughly 70% of oropharyngeal squamous cell carcinomas (OPSCC) in the United States are caused by high risk HPV infection, and these malignancies have seen a startling increase in prevalence in recent years despite the decreased incidence of tobacco-associated HNSCC [9-11]. In fact, with an average incidence of roughly 11,000 cases of HPV-associated OPSCC and 10,700 cases of HPV+ cervical cancer annually, HPV-associated (HPV+) head and neck cancers are now the most common HPV-associated malignancies in the United States [12]. Despite arising from the same cell type, it is now widely accepted that HPV+ and tobacco-associated (HPV-) head and neck cancers comprise two distinct clinical entities that are driven by different molecular mechanisms. From a clinical standpoint, HPV+ HNSCC tends to occur in younger patients with less tobacco and alcohol exposure [13, 14]. Patients HPV+ HNSCC tend to present with smaller primary tumors (T1 and T2), as compared to patients with HPV- HNSCC, yet are more likely to present with regional lymph node metastases [15-17]. In addition, HPV+ HNSCC responds better to chemotherapy and radiation when compared to HPV- HNSCC, and HPV-associated HNSCC is associated with improved overall survival [18], likely reflecting fundamental molecular differences between the two diseases, which will be discussed below.

Current therapy for advanced HNSCC includes combinations of primary surgical resection, cervical lymphadenectomy, radiation, or radiation given with platin drugs or cetuximab, depending on the stage, location, and pathologic features of the tumor; however, National Comprehensive Cancer Network guidelines state that HPV status

should not change treatment strategies outside of clinical trials [19]. Treatment for advanced HNSCC includes chemotherapy and radiation, which causes long-term side effects, such as swallowing and speech dysfunction, neck muscle fibrosis, xerostomia, accelerated dental decay, and lymphedema. To decrease the morbidity associated with therapy, a major goal of the head and neck oncology community is to de-escalate therapy for HPV-associated tumors. Trials such as ECOG 331, which risk stratifies HPV+ HNSCC patients to identify patients that will benefit from reduced doses of post-operative radiation, are underway. Currently, identification of appropriate patients for de-escalation depends only on the absence of aggressive histologic tumor characteristics and history of minimal tobacco use. Despite the relatively good prognosis associated with HPV-associated HNSCC, up to 25% of patients with HPV-positive tumors suffer recurrent or metastatic disease despite aggressive and morbid therapy.

The burden of HPV+ HNSCC is likely to continue to rise; in fact, Chaturvedi et. al predict that the rates of oropharyngeal cancer in the U.S. will almost double by 2030 [10]. Given the latency between infection and the development of HPV+ HNSCC, Gillison et. al estimate that the effect of the HPV vaccine will not be reflected in OPSCC prevalence until 2060 [20]. Thus, there is a great need for the development of efficacious treatments that can take advantage of the inherent molecular difference between HPV+ and HPV- tumors to treat this growing population of patients in a manner that reduces the extensive morbidity from current treatment paradigms. Given that the overall prevalence of oral HPV-16 infection is 1% of the US population ages 14 to 69 years (6.9% prevalence of all HPV subtypes) and the majority of adults have been infected with HPV

at some point in their lives [21], understanding the molecular mechanisms of HPV-induced carcinogenesis in the head and neck is of utmost importance.

Carcinogenesis of HPV-associated HNSCC

Human papilloma viruses represent a family of ~8kb, non-enveloped, double stranded DNA viruses known to also be a major causative agent of cervical and anogenital cancers [9, 22-25]. Of the more than 100 subtypes, most are referred to as "low risk," a fraction of which can cause benign, neoplastic papillomas of the skin or mucosal membranes. Benign papillomas of the upper aerodigestive tract including recurrent respiratory papillomas of larynx are most commonly associated with HPV types 6 and 11. "High risk" HPV, on the other hand, include the subtypes 16, 18, 31, 33, among others, and are classified as such based on their oncogenic potential [26]. Much of the current knowledge regarding HPV carcinogenesis in the oropharynx has been coopted from studies in cervical cancer, but emerging evidence from our lab and others suggests that there are more fundamental differences than originally thought, which will be discussed in more detail. As an example, 90-95% of HPV+ head and neck cancers are caused by HPV 16, while HPV+ cervical cancers are associated with a wider variety of high risk HPV subtypes, as only 70% are caused by either HPV 16 or 18 [27-29].

The HPV genome comprises two "late genes," L1 and L2, which code for the viral capsid, as well as six "early genes," E1, E2, E4, E5, E6, and E7 [30]. E6 and E7 are the most widely studied of the HPV genes and are considered the most important oncogenes in carcinogenic transformation. The HPV E6 protein binds and leads to the degradation of p53, arguably the most important human tumor suppressor. This inhibits

the host cell's transcription of genes in pro-apoptotic and growth inhibitory pathways, as well as prevents p53's direct stimulation of the mitochondrial apoptotic pathway [31-34]. The HPV E7 oncoprotein binds the pRb tumor suppressor and Rb family members and promotes their degradation, thus releasing the inhibition of E2F transcription factors [35, 36]. Together, the loss of p53 and pRb activity allows cellular proliferation and inhibits cell death even in the presence of DNA damage or genetic alterations and allows mutations to accrue [37, 38].

In the canonical model of HPV carcinogenesis (which was largely developed based on studies of cervical cancer), HPV gains access to the basal, least differentiated cells of the epithelia, either through microabrasions of the genital tract or through the tonsillar crypts in the oropharynx [39]. After initial infection of these cells, the HPV genome is maintained in its episomal form, where it is kept at a low copy number. In the normal HPV life cycle, episomal expression of HPV E1, E2, E4, and E5 genes leads to viral amplification. As cells differentiate and reach the luminal epithelial layer, HPV L1 and L2 are expressed, thus encapsidating the virus, which then can be released [39]. In contrast, in HPV-driven carcinogenesis, the high risk HPV genome is thought to integrate randomly into the host cell genome. As this occurs, it is thought that the E2 open reading frame is disrupted, which releases its inhibition of E6 and E7 transcription [39-41]. Integration of the HPV genome is a critical step for this model of HPV-induced carcinogenesis since it is seen upon transition from CIN2 (cervical intraepithelial neoplasia 2) to the imminent premalignant CIN3 state in the uterine cervix [40, 42]. Recent whole genome sequencing of The Cancer Genome Atlas (TCGA) HPV+ HSCC

samples revealed that approximately 30% lacked viral integration, suggesting that at least a portion of these tumors may have a different pathway to carcinogenesis [27, 43].

Mutational landscape in HPV+ HNSCC

HPV+ cancers contain significantly different mutational landscapes when compared to HPV- HNSCC [27, 43-46]. The majority of HPV- HNSCC contain mutations and genetic alterations classically associated with tobacco and alcohol exposure, including loss of function mutations in TP53 (84%) and inactivating mutations in CDKN2A (54%), an important cell cycle regulator. In contrast, genetic alterations in these genes are exceedingly rare in the HPV+ subset (TP53 - 3%; CDKN2A - 0%) [43]. Though it was thought that the overall mutational burden in HPV+ HNSCC was significantly lower than in tobacco associated head and neck cancer [47, 48], recent analysis of TCGA data sets reveal that the mutation burden was roughly equal [43]. In contrast to HPV- HNSCC, a distinct mutational signature is found in HPV+ tumors that is associated with a family of antiviral proteins known as apolipoprotein B mRNA editing enzyme catalytic polypeptide-like 3 (APOBEC3). The APOBEC3 enzymes are upregulated in response to viral infection, where they serve as important components of anti-viral innate immunity. APOBECs are cytidine deaminases and elevated APOBEC activity is thought to drive the majority of PIK3CA mutations in virally-associated HNSCC [43, 46, 49-52]. Mutations driven by APOBEC activity in HPV+ HNSCC likely contribute to distinct carcinogenic events distinguishing HPV+ and HPV- HNSCC.

A seminal finding of TCGA head and neck study identified tumor necrosis factor receptor-associated factor 3 (TRAF3) as one of the most commonly mutated and deleted genes in HPV+ HNSCC [43]. Interestingly, TRAF3 gene alterations are infrequent in HPV-negative HNSCC, suggesting that TRAF3 inactivation is required only for HPV-driven carcinogenesis in HNSCC. TRAF3 is a member of the TRAF family of proteins that serve as both crucial intracellular adaptors and E3 ubiquitin ligases that mediate signaling downstream of various cell surface and intracellular receptors. Receptors that signal through TRAF proteins include those involved in inflammation, innate immune responses, and cell death, most notably: tumor necrosis factor receptors (TNFR), Toll-like receptors (TLR), RIG-1-like receptors (RLR), and interleukin-1 receptors (IL-1R) [53]. These receptors initiate signaling that ultimately leads to activation of the innate immune response and nuclear factor-κB (NF-κB). NF-κB is a potent transcription factor central to control of apoptosis, inflammation, and several aspects of the immune response [53, 54]. TRAF3's function is unique and thought to not be replicated by other TRAFs in that it negatively regulates canonical and non-canonical NF-κB pathways while simultaneously stimulating a potent antiviral response, mediated through type I interferon (IFN) signaling [53, 55]. Reported here, we found mutations/deletions of the cylindromatosis gene (CYLD), which like TRAF3 inhibits NF-κB pathways [56], is also mutated in a subset of HPV+ HNSCC that did not overlap with the subset containing TRAF3 mutations. Inactivating mutations or deletions in TRAF3 and CYLD leading to constitutive activation of NF-κB have been identified in other cancers such as multiple myeloma; however, amongst solid tumors, inactivating TRAF3/CYLD gene defects were most common in HPV+ HNSCC [57]. The absence of frequent mutations of these genes

in uterine cervical cancer [58, 59] provides yet another difference between HPV-associated tumor types.

In Specific Aim 3, through in-depth analysis of TCGA HNSCC dataset, we propose that inactivating mutations in TRAF3 or CYLD identify a distinct subset of HPV+ HNSCC with associated constitutive activation of NF-κB signaling and depleted innate immune signaling. This previously undescribed subtype of HPV+ HNSCC marked by TRAF3 or CYLD mutations is associated with the absence of integrated HPV and improved patient survival.

Epigenetics and Demethylation Therapy

Epigenetics refers to reversible, heritable modifications to the DNA and histones that alter gene transcription without changing the actual base sequence of DNA [60]. Often, these changes reflect a dynamic process by which environmental and cellular factors can influence gene expression and cellular differentiation. Epigenetic changes generally affect the relative accessibility of DNA to transcription factors, and can function at a chromosomal level, as is the case in X-inactivation in XX cells [61], as well as the gene level, as single genes can be upregulated or downregulated based on both the three dimensional structure of the DNA molecule and the accessibility of transcription factors to the gene's promoter [62]. Catalyzed by DNA methyltransferase (DNMT) enzymes, DNA methylation at CpG dinucleotides represents one of the most important examples of epigenetic changes that cells utilize to alter gene transcription [63, 64]. At CpG loci located at gene promoters, DNA methylation generally results in gene silencing,

whereas DNA methylation in gene bodies is more complicated and can have differential effects [63-65].

Many studies have described the link between DNA methylation and cancer. In fact, HPV- HNSCC tend to have relatively low levels of DNA methylation, which is correlated with genomic instability [66, 67], while HPV+ HNSCC harbor distinctly hypermethylated genomes [44, 68-70]. HPV has been shown to induce aberrant hypermethylation in HPV-driven anal squamous cell carcinoma [71], and it is thought that de-novo methylation at the E2 binding site plays a role in the HPV life cycle and changes throughout the course of the host cell differentiation process in HPV-driven carcinogenesis [72]. Moreover, studies have found associations between specific gene methylation patterns and overall survival [73], as well as the presence of nodal metastases [74], in HPV+ head and neck cancer. Taken together, while HPV- HNSCC seems to be driven largely by the accrual of carcinogen-induced mutations, evidence suggests that epigenetic changes, namely genomic hypermethylation, likely mediate both cellular and viral factors necessary for HPV-mediated carcinogenesis [43].

High levels of DNA methylation at CpG loci in HPV-driven cancers, which has been implicated in immune evasion in virally infected cells, transcriptional repression of tumor suppressor genes, and dysregulation of DNA repair genes [44, 68-71, 75, 76] raises the idea of demethylation therapy as a potential treatment in HPV+ HNSCC. 5-azacytidine (5-aza) and its structural analog, 5-aza-2'-deoxycytidine (decitabine), are U.S Food and Drug Administration (FDA) approved, global DNA demethylating agents that are used in clinic to treat myelodysplastic syndromes (MDS) and refractory cases of acute myelogenous leukemia (AML), two neoplastic hematologic processes with aberrant

genome hypermethylation [77, 78]. As cytidine analogs (known as azanucleosides) that incorporate into newly synthesized DNA, these drugs bind to and inactivate the major enzyme responsible for maintaining DNA methylation at CpG loci, DNA methyltransferase 1 (DNMT1), resulting in global demethylation of the cellular genome [79]. Though known to demethylate DNA, the link between demethylation and the therapeutic effects of these drugs is weak [79]. Tumor suppressor genes that were previously silenced through promoter methylation can be transcriptionally activated by azanucleosides as a mechanism through which these drugs can induce cell death in cancer cells [80]. DNA demethylation plays a complex role in transcriptional regulation, however, as methylation of CpG loci within gene bodies can paradoxically cause increased transcription [65]. Furthermore, as 5-aza is also incorporated in RNA [81, 82], the drug can alter expression independently of its effect on transcription, as its incorporation can affect mRNA stability [83]. In addition, azanucleosides have also been shown to stimulate a type I interferon response as another mechanism of activity [84]. Finally, 5-aza and decitabine have been reported in some cells to cause DNA damage and stimulate the DNA damage response (DDR), though the exact type of DNA damage has not been fully characterized and is likely cell type dependent [85-87]. The use of demethylating drugs in solid tumors is still in its infancy, though initial clinical trial results show the highest response rates to decitabine in cervical carcinoma (36%) and pleural carcinoma (14%); however, HNSCC has not been tested [88]. To date, there are no FDA approved epigenetic therapies for head and neck cancer; however, results from the ongoing window clinical trial at the Yale Cancer Center utilizing 5-aza in HNSCC are detailed in Specific Aim 2.

DNA damage and DNA damage response

Many exogenous and endogenous sources damage cellular DNA. Endogenous DNA damage routinely happens due to spontaneous DNA base loss (e.g. depurination or depyrimidination), as a consequence of enzymatic reactions (e.g. deamination), during metabolic processes producing free radicals, or by means of replication errors or augmented transcriptional activity. Known sources of environmental DNA damage include ultraviolet radiation that biochemically alters DNA, creating pyrimidine dimers and 6-4 photoproducts, and ionizing radiation directly producing breaks in DNA and indirectly injuring DNA via production of free radicals and stalling replication forks. In addition, DNA-DNA and DNA-protein crosslinks arise from an exposure to platinated compounds (e.g. cisplatin), nitrogen and oxygen atoms of DNA bases are modified by alkylating agents (e.g. nitrogen mustards) that covalently attaches methyl or alkyl groups, intercalating agents (e.g. doxorubicin) twist DNA leading to nucleotides insertions and deletions during replication. DNA double strand breaks (DSBs), classified as either primary when produced by ionizing radiation or secondary when formed by stalled and collapsed replication forks, represent the most lethal type of DNA damage.

The maintenance of genome fidelity is essential for the proper function and survival of all organisms; therefore, cells have developed a complex DNA damage response network to recognize damage to DNA and transduce signals to effector molecules that initiate DNA damage repair, arrest the cell in a particular phase of cell

cycle to acquire the necessary time for recovery, or promote cell death in the case of severe damage [89].

DNA damage recognition is initiated by the transient relocation of DNA damage sensor proteins to the sites of injured DNA. The MRE11/RAD50/NBS1 (MRN) complex is recruited to DSBs, activating ATM (ataxia–telangiectasia mutated), a member of the family of phosphoinositide-3-kinase-related kinases [90]. Three other members of the same kinase family, DNA-dependent protein kinase (DNA–PK), ATR (ATM and Rad3 related), and SMG1 (human suppressor with morphogenic effect on genitalia), are also recruited to DNA DSBs, are activated, and participate in the response to DSBs [91-95]. DNA DSB-activated kinases phosphorylate proteins that are present in close proximity to the sites of DNA damage. One of the first targets for phosphorylation is histone H2AX (called γH2AX once phosphorylated) that is crucial for chromatin-remodeling processes that allow damaged DNA to become available for repair.

Two major pathways, homologous recombination repair (HR) and non-homologous end joining (NHEJ), repair DNA DSBs in mammalian cells. HR is an high fidelity pathway that corrects chromosomal DSBs using the homologous sequence on the paired chromosome [96-98]. Homologous recombination is also required in the replication process to re-establish stalled or broken replication forks [99-102]. Rad51 is the central HR protein in eukaryotes, which forms nucleoprotein filaments on single stranded DNA (ssDNA) regions and mediates homologous pairing and strand exchange between the DNA duplexes. Following DNA damage, Rad51 molecules form nuclear foci that can be observed by immunofluorescence.

Cancer cells have several phenotypic features that distinguish them from normal healthy cells in the body. One common feature of cancer cells is an increased level of genomic instability, which allows them to break and rearrange chromosomes, resulting in new oncogene fusions and the inactivation of tumor suppressor genes. In order to elevate the level of genomic instability, a cancer cell must tolerate DNA damage. This can be achieved through the loss of DNA damage signaling and checkpoints, and by acquiring defects in the major DNA repairs pathways. Virtually all types of cancer have some defect in the DNA damage response and/or repair that weakens the ability of the cancer cell to properly replicate DNA; in particular, HPV+ HNSCC have been shown to be partially deficient in HR repair [103, 104].

Statement of Purpose

The purpose of this study was to develop demethylation therapy as a rational targeted approach to the treatment of HPV-associated head and neck cancer through understanding of cellular and molecular effects. In doing so, we hope to change the current treatment guidelines so that the HPV status of a HNSCC tumor guides clinical decision-making and treatment paradigms. This work is subdivided into three specific aims to achieve this goal, as described below.

Specific Aims

1. To characterize the DNA damage and describe mechanisms of damage induced by demethylating agents in HPV+ HNSCC cells
2. To assess the cellular response and effect on metastatic potential of demethylation therapy in HPV+ HNSCC cells, xenograft models, and clinical trial patients
3. To discover biomarkers that identify a subset of HPV+ HNSCC patients that may be amenable to de-escalation therapy

Methods

The methods used in the study include cell culture of cell lines, primary HNSCC cells, shRNA transfection, CRISPR/Cas9 gene knockout, immunoblotting, pulsed-field gel electrophoresis (PFGE), immunofluorescence, fluorescence-activated cell sorting (FACS), quantitative real-time polymerase chain reaction (qRT-PCR), colony formation assays, clonogenic survival, DNA purification, subcellular fractionation, mass spectrometry, use of xenografted tumors in mice, immunohistochemistry (IHC), analysis of mutations through cBioportal, and gene set enrichment analysis. The specific details of these methods are described in detail within each specific aim section. I performed the immunoblots with the exception of one, PFGE with the exception of one, shRNA transfections, FACS, qRT-PCR with the exception of two, survival assays, and subcellular fractionation (exceptions performed by Natalia Issaeva or Asel Biktasova). CRISPR knockout was performed by Natalia Issaeva. All cell culture was performed by either myself or Natalia Issaeva. All *in vivo* mouse work was performed by myself, Cyril Gary, and Asel Biktasova. Mutational and gene set analysis was performed by myself,

Dr. Wendell Yarbrough, and Natalia Issaeva. IHC and mass spectrometry was performed by the Yale core facilities.

SPECIFIC AIM 1: To characterize the DNA damage and describe the mechanism of damage induced by demethylating agents in HPV+ HNSCC cells

Methods

Cell lines, constructs and chemicals

HPV-negative (HPV-) (SCC61, SCC25, UNC7, and JHU012) and HPV+ (SCC090, UMSCC47) HNSCC cell lines were used. All HPV- cells were cultured in DMEM/F12 medium supplemented with 0.4μg/mL hydrocortizone, and all HPV+ cell lines were grown in DMEM with nonessential amino acids. V-C8 and V-C8B2 cells were previously described [105]. All media was supplemented with 10% FBS (Invitrogen), 50 μg/mL penicillin, and 50μg/mL streptomycin (Invitrogen). All cell lines have been tested negative for mycoplasma and authenticated by microsatellite testing.

To establish *primary HNSCC cultures*, surgical specimens were collected from consented patients in PBS within 30 min of resection. Tissue was cut into ~5 mm^3 pieces, disinfected by immersion in 70% ETOH for ~1 min, rinsed with PBS four times, and digested in 0.05% trypsin-EDTA supplemented with Collagenase type 1A (200 units/ml) (Sigma C-9722) in a vented flask at 37^0C with 5% CO_2 for 10-20 min. Digestion was

stopped by adding 1 volume of FBS (Sigma). After centrifugation at 1500 rpm x 5 min, the supernatant was aspirated, the cells were resuspended in keratinocyte serum-free medium with supplements and 10% FBS, strained through a 100 μm nylon cell strainer (Falcon; Becton Dickinson Labware), plated in keratinocyte serum-free medium with supplements (Gibco/Invitrogen) and 10% FBS onto 0.1% gelatin (Millipore) coated plates, and grown at 37^0C in a 5% CO_2 incubator. The next day, cells were washed with PBS and grown in keratinocyte serum-free medium with supplements until they reached ~90% confluence. After near confluence, the cells were detached with 0.05% trypsin-EDTA, the reaction was stopped with defined trypsin inhibitor (Gibco), and the cells were plated on uncoated plates in keratinocyte serum-free medium with supplements for experimental use.

Cells were transfected using Lipofectamine 2000 (Invitrogen) according to manufacturer recommendations.

Olaparib, veliparib, and AZD6738 were from Selleckchem. 5-Azacytidine, mirin, hydroxyurea, aphidicolin, triptolide, DRB, Actinomycin D, and cycloheximide were obtained from Sigma.

Establishing APOBEC3B CRISPR cells.

UMSCC47 were co-transfected with APOBEC3B CRISPR/Cas9 KO (Santa Cruz) and APOBEC3B HDR (Santa Cruz) plasmids. 70 hours after transfection, cells were plated at low density in growth media supplemented with 2μg/ml puromycin (Invitrogen). 7 days later, individual clones were collected, propagated, and tested for

APOBEC3B mRNA expression using primers ordered from IDT with the following sequences:

Forward: CCTGATGGATCCAGACACATT
Reverse: GCTCCAGGAGATGAACCAAG

Forward: TTTGCATACTGCTGGGAAAA
Reverse: GCTCCACCTCATAGCACAAG

Establishing UNC7 Rad51 shRNA expressing cells

UNC7 were transfected with Rad51 shRNA plasmids (Origene). 70 hours after transfection, the cells were plated at low density in growth media supplemented with 2μg/ml puromycin (Invivogen). 7 days after, individual clones were collected, propagated and tested for Rad51 expression in immunoblotting.

Immunoblotting

Cells were collected by trypsinization and lysed in radioimmunoprecipitation assay (RIPA) lysis buffer (Sigma) with the addition of protease inhibitors (Roche) and phosphatase inhibitors (Sigma) for 15 minutes on ice. Insoluble material was removed by centrifugation at 14,000 rpm for 15 minutes at 4°C. Proteins were separated in Tris-glycine polyacrylamide gels (Mini-PROTEAN; Bio-Rad) and electrophoretically transferred onto polyvinylidene fluoride membranes. Membranes were blocked with 3% BSA in PBS and incubated with antibodies against γH2AX (Abcam), Rad51, tubulin or actin (Santa Cruz). After incubation with primary antibodies, membranes were washed, incubated with secondary DyLight anti-mouse and anti-rabbit antibodies (Thermo Scientific), and signals was visualized using a Bio-Rad imager.

Pulsed-field gel electrophoresis

Cells were treated with indicated drugs, collected by trypsinization, resuspended in 1% InCert-agarose (in 37°C PBS) to a final concentration of 1.5 million cells/100μL and agarose plugs were separated by pulsed-field gel electrophoresis as previously described [106].

Immunofluorescence

Cells were grown in chamber slides, treated, fixed, immunostained, and analyzed as previously described [103]. Cells with more than 10 foci were determined as positive. The primary antibodies used were mouse anti-γH2AX (Abcam) at a dilution of 1:2,000 and rabbit anti-Rad51 (Santa Cruz) at a dilution of 1:500. Secondary anti-mouse Alexa 555 and anti-rabbit Alexa 488 were from Invitrogen and were used at a dilution 1:1000.

Fluorescent activated cell sorting (FACS)

Cells were collected by trypsin and fixed in ice-cold 70% ethanol over night at −20°C. Ethanol was removed by centrifugation and the cells were rehydrated in PBS and pelleted. The pellets were resuspended in 25μg/ml propidium iodide (PI) (Sigma) in PBS containing 100 μg/ml RNase A (Invitrogen) and stained for 30 min at room temperature. The DNA content was analyzed by FACSCalibur flow cytometer (BD Biosciences). Samples were gated on the single cell population, and 10,000 cells were collected for each sample.

To simultaneously determine γH2AX intensity and cell cycle distribution, cells were collected by trypsin and fixed in 3% paraformaldehyde in PBS for 15 min at room

temperature. Paraformaldehyde was removed by centrifugation and the cells were permeabilized in 0.3% Triton X100 in PBS for 10 min at room temperature, pelleted and washed 2X with PBS. The pellets were stained with Alexa Fluor® 488 Mouse anti-H2AX (pS139) (BD Biosciences) according to the manufacturer recommendation. After the staining, the cells were washed once with PBS, resuspended with 25μg/ml propidium iodide (PI) (Sigma) in PBS containing 100μg/ml RNase A (Invitrogen) and stained for 30 min at room temperature. ɣH2AX staining (FL1 channel) and the DNA content (FL2 channel) were analyzed by FACSCalibur flow cytometer (BD Biosciences). Samples were gated on the single cell population, and 30,000 cells were collected for each sample.

RNA extraction and quantitative RT-PCR

Total RNA was extracted from cells by Qiagen RNA extraction kit and cDNA was synthesized using iScript cDNA Synthesis Kit (Bio-Rad) according to the manufacturer's instructions. Quantitative real-time reverse transcription (qRT-PCR) was done using iQ SYBR Green Supermix (Bio-Rad) and primer pairs indicated in the Table 1 on the iCycler iQ Real-Time PCR Detection System (Bio-Rad). Each qRT-PCR reaction was done in at least duplicate, and the ΔΔCt method was used to analyze the data.

Colony formation assay

Cells were plated into six well plates at a density of 500 cells/well. The next day, the cells were treated with indicated drugs. After 1 week, when colonies could be observed, colonies were fixed and stained with methylene blue in methanol (4g/L). Colonies consisting of more than 30 cells were subsequently counted.

DNA purification and restriction

DNA was purified using DNeasy Blood & Tissue Kits (Qiagen). 0.5µg of DNA was incubated with or without restrictases from EpiTect Methyl II DNA Restriction Kit (Qiagen) at 37ºC for 6 hours, the enzymes were inactivated at 65ºC for 20 minutes following the digestion, the reactions were run in 1% agarose (Invitrogen) gel, and DNA was visualized with ethidium bromide (Biorad).

Subcellular fractionation

Subcellular Protein Fractionation Kit for Cultured Cells (Thermofisher Scientific) was used to isolate cytoplasmic, nuclear soluble, chromatin bound, and membrane proteins from the same cells according to manufacturer's suggested protocol.

Mass Spectrometry

Mass spectrometry was performed at the Yale Mass Spectrometry and Proteomics Core on the chromatin bound fraction, obtained as described above. Results were deemed significant at 95% confidence.

Results

5-azacytidine causes DNA double strand breaks in HPV-associated HNSCC

5-azacytidine and decitabine cause replication-associated DNA damage that requires homologous recombination (HR) for repair [85], suggesting that cells with deficiencies in HR may be more sensitive to these therapies. Since HPV+ head and neck

squamous cell carcinoma (HNSCC) cells have impaired homologous recombination [104, 107], response of HPV+ HNSCC cells to 5-azacytidine was determined. Based on proliferation assays, cell lines and patient-derived HPV+ HNSCC cells were found to be significantly more sensitive to 5-azacytidine than HPV- HNSCC cell lines or primary cultures (Fig. 1A). To begin exploring the increased sensitivity of HPV+ HNSCC to 5-azacytidine, we determined DNA damage over a time course after treatment. We used doses in line with previous research studying azanucleoside-induced DNA damage [85]. As indicated by the induction of γH2AX, a phosphorylated histone that binds DNA damage sites [108], 5-azacytidine induced DNA damage in both HPV+ and HPV- cell lines over the course of 72 hours [85, 86] (Fig. 1B). Rad51 is required for homologous recombination-based repair and co-localizes with γH2AX to stalled replication forks caused by 5-aza or decitabine [85, 86, 109]. As expected, 5-aza treatment of HPV- cells resulted in nuclear foci containing co-localized γH2AX and RAD51 (Fig. 1C). In contrast, similar treatment of HPV+ cells revealed that the vast majority of nuclear foci contained primarily γH2AX alone with a paucity containing both γH2AX and RAD51 foci. These data are consistent with HPV+ cells having defects in homologous recombination following DNA demethylation therapy.

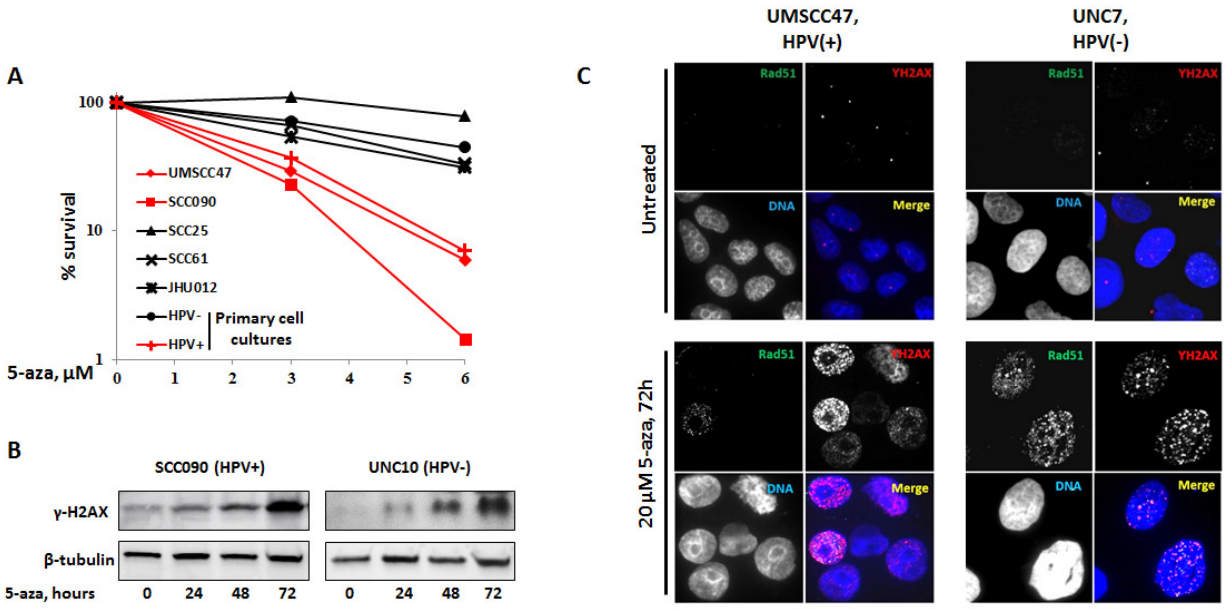

Figure 1: *HPV+ HNSCC cells are sensitive to 5-azacytidine and induces DNA damage in cells, yet does not induce Rad51 foci in HPV+ cells* (A) Survival after increasing doses of 5-aza after 10 days was determined in HPV+ cell lines UMSCC47 and SCC090, HPV- cell lines SCC25, SCC61, JHU012, as well as HPV+ and HPV- primary cell cultures. HPV+ cells labeled in red, HPV- cells labeled in black. Note log scale. (B) HPV+ cell line SCC090 and HPV- cell line UNC10 were treated with 20 μM 5-aza for 24, 48, and 72 hours and immunoblotted with antibodies against γH2AX and β-tubulin as a control. (C) HPV+ UMSCC47 and HPV- UNC7 cell lines were treated with 20 μM for 72 hours and subsequently fixed and immunostained with γH2AX and Rad51 antibodies; representative images shown above.

To characterize DNA damage marked by γH2AX, HPV+ and HPV- cells were treated with 5-aza and genomic DNA subjected to pulsed-field gel electrophoresis (PFGE) to detect double strand breaks. PFGE is a technique that allows large DNA fragments created by double strand breaks to be released into the gel while intact chromosomal DNA remains in the well (Fig. 2). In HPV- HNSCC cell lines (UNC7 and UNC10), there was no evidence of DNA DSB formation after treatment with 30 μM 5-aza for 0, 24, 48, and 72 hours (Fig. 2A, left). Intriguingly, DSBs were detected after

treatment with 5-aza for 72 hours in HPV+ HNSCC cell lines (SCC090 and UMSCC47) (Fig. 2A, right). Sensitivity of HPV+ HNSCC cells to DSB formation was examined following exposure to increasing concentrations of 5-aza. Double strand breaks were detected at all concentrations tested (starting at 5μM, data not shown) and increased in a concentration-dependent manner (Fig. 2B, left gel).

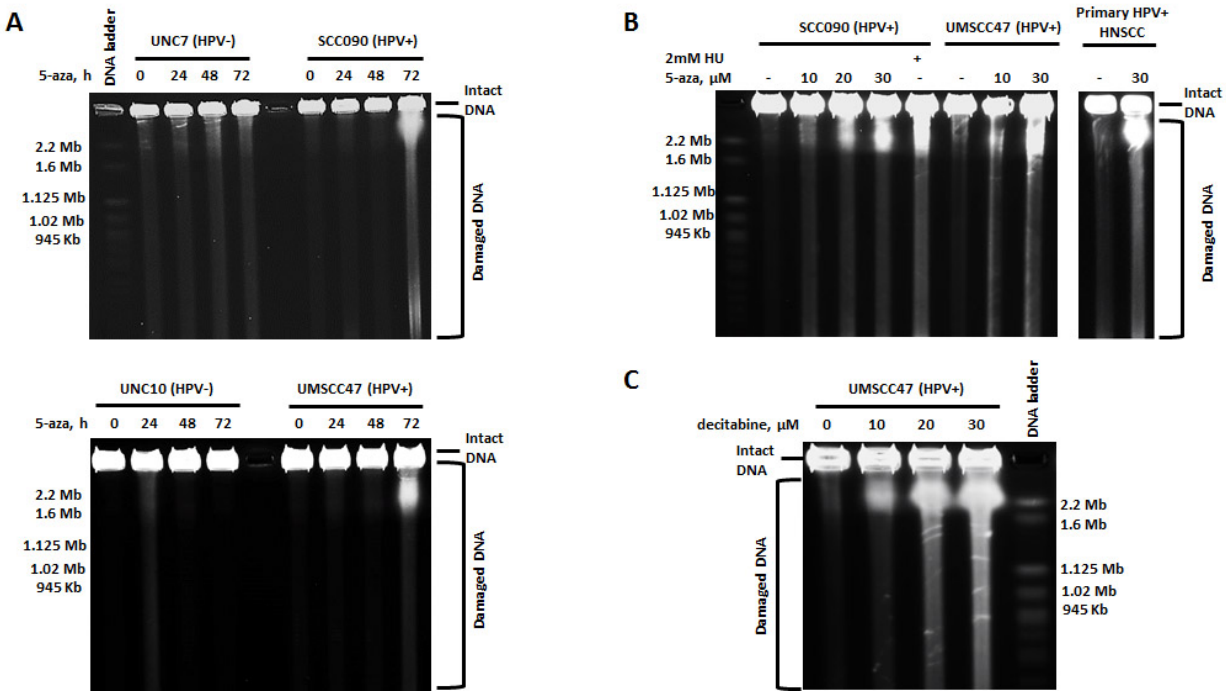

Figure 2: *5-azacytidine and decitabine treatment caused DNA double strand breaks in HPV+ but not HPV- HNSCC cells* (A) Pulsed-field gel electrophoresis (PFGE) depicting HPV- UNC7 cells and HPV+ SCC090 cells (top gel), as well as HPV- UNC10 cells and HPV+ UMSCC47 cells (bottom gel), after treatment with 30 μM 5-aza for 0, 24, 48, or 72 hours. (B) PFGE depicting HPV+ cell lines SCC090 and UMSCC47 (left gel) and primary, early passage, HPV+ tonsillar cancer cell culture after treatment with increasing doses of 5-aza for 72 hours. Treatment of cells for 72 hours with 2 mM hydroxyurea (HU) was used as positive control. (C) PFGE depicting HPV+ cell line UMSCC47 after increasing doses of decitabine for 72 hours.

Like other azanucleosides, incorporation of 5-aza into DNA is required for its demethylating effects, but roughly 80% of 5-aza is incorporated into RNA. To determine if incorporation of 5-aza into RNA is required for DSB formation in HPV+ HNSCC cells,

cells were treated with the 5-aza analogue, decitabine (5-aza-2'-deoxycytidine), which is only incorporated into DNA [81, 82]. As observed with 5-aza, increasing doses of decitabine also induced DSBs in a concentration-dependent manner (Fig. 2C). To ensure that generation of DSBs in HPV+ HNSCC cells following therapy with demethylating agents are not related to establishment of immortal cell lines, a primary, early passage HPV+ tonsillar squamous cell carcinoma (passage 3) was tested. In these primary cells, double strand breaks were detected by PFGE following 72 hr of 5-aza treatment (Fig 2B, right gel).

Dysfunctional homologous recombination is not sufficient for 5-aza to induce DSBs

Compared to HPV- HNSCC, HPV+ HNSCC are more sensitive to DNA damaging agents, and reports show that HPV+ HNSCC cells have impaired homologous recombination [104, 107]. Given that demethylation therapy induced DNA damage in both HPV+ and HPV- cells, but that HPV+ cells did not form damage foci with co-localized RAD51 (Fig. 1C), we hypothesized that dysfunctional double strand break repair in HPV+ HNSCC may be responsible for the observed DSBs following 5-aza treatment (Fig. 2). To test this hypothesis, sensitivity of Chinese hamster ovary cells with defective HR due to BRCA2 deficiency (VC8 cells) and VC8 cells with reconstituted BRCA2 (labeled as VC8 B2) to 5-aza was tested [105]. Clonogenic survival (Fig. 3A) revealed that VC8 cells with defective HR were significantly more sensitive to 5-aza than isogenic cells with BRCA2 restored (Fig. 3A). To determine if the sensitivity of VC8 cells deficient in homologous recombination correlated with DSB formation after 5-aza

therapy, cells were exposed to 30μM of 5aza for 72 hours. No DNA DSBs were detected after 5-aza in either VC8 or VC8 B2 cells (Fig. 3B). Similarly, HPV- HNSCC cells with defective HR created via stable shRNA-mediated RAD51 knockdown did not form DSB following 5-aza treatment (Fig. 3C). Together, these data reveal that cytotoxicity following 5-aza therapy is at least partially dependent on HR (Fig. 3A), but that defective HR repair is not sufficient to cause the DNA breaks seen after 5-aza treatment of HPV+ HNSCC cells.

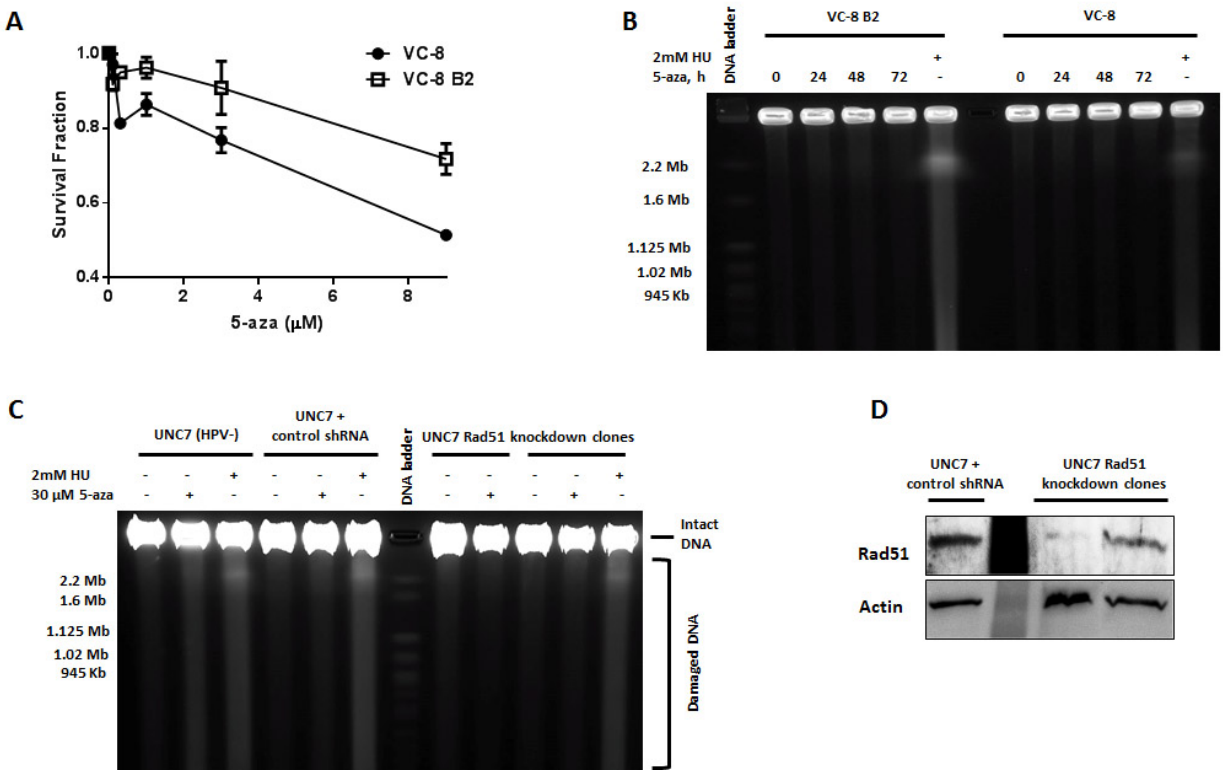

Figure 3: *Dysfunctional homologous recombination is not sufficient for induction of DNA DSB by 5-aza therapy* (A) Survival of Chinese hamster ovary cells with deficient BRCA2 (VC-8) and restored BRCA2 (VC-8 B2) was tested after treatment with increasing doses of 5-aza. Standard deviation calculated from 2 independent experiments. (B) PFGE depicting VC-8 and VC-8 B2 cells after 30μM 5-aza for 72 hours. 72 hours of 2mM hydroxyurea (HU) was used as positive control. (C) HPV- UNC7 cells were stably transfected with Rad51 or control shRNA and subjected to PFGE after 72 hours of 30 μM 5-aza treatment as indicated. 72 hours of 2mM HU used as positive control. (D) Immunoblot with antibodies for Rad51 and actin confirming Rad51 knockdown in lysates from same UNC7 clones as shown in C.

Azacytidine and decitabine are used to treat patients with myelodysplastic syndrome (MDS) and refractory cases of acute myelogenous leukemia (AML). Interestingly, MDS cells can be transformed to AML through a process involving aberrant genome methylation [110]. Hypermethylation of the host cell genome is also a distinct feature of HPV+ HNSCC, but its role in transformation is not known since HPV+ HNSCC lack a known precursor lesion [44, 67-70]. To determine if the hypermethylated state of AML cells sensitized them to DSB as observed in HPV+ HNSCC, AML and lymphoma cells were treated for 72 hours with azacytidine. As opposed to HNSCC, 5-aza did not induce DNA DSBs in these cells (Supp. Fig. 1). Thus, increased levels of genome methylation are unlikely to be sufficient to cause 5-aza-induced DNA DSB formation.

Transcription and replication are required for 5-azycytidine induced DNA double strand breaks

Demethylating agents markedly increase global transcription [111, 112], and recent evidence points to aberrantly active transcription as a source of DNA DSBs leading to increased genomic instability [113]. To determine if transcription is required for development of DSBs, cells were treated with transcriptional inhibitors. Transcription inhibition is toxic to cells and results in cell cycle arrest [114]. To allow 5-aza incorporation into DNA before cell cycle arrest initiated by transcriptional inhibition, cells were treated with 5-aza for 48 hours before treatment with transcriptional inhibitors. Transcriptional inhibition was scheduled at 48 hours of 5-aza therapy because DSBs have not been observed at this time point. In addition, doubling times of all cell lines used

ensured 5-aza incorporation into DNA with 48 hours of therapy (Schema in Fig. 4A). Three inhibitors of transcription with varying mechanisms of action were used: 1) 1μM triptolide, an RNA polymerase inhibitor [115], 2) 1.25μg/ml actinomycin D, an RNA elongation inhibitor [116], and 3) 10μM dichloro-beta-D-ribofuranosylbenzimidazole (DRB), which prevents mRNA synthesis [117]. Regardless of the agent used, transcription inhibition markedly reduced or completely inhibited DSB formation following 5-azacytine therapy (last 3 lanes, Fig. 4B). These data reveal that induction of double strand breaks in HPV+ HNSCC cells following 5-aza treatment is dependent on active transcription. Actinomycin D treatment alone causes DNA double strand breaks [118], but interestingly, DSBs induced by actinomycin D in the absence of 5-azacytine were prevented in cells treated with 5-aza (Fig. 4B).

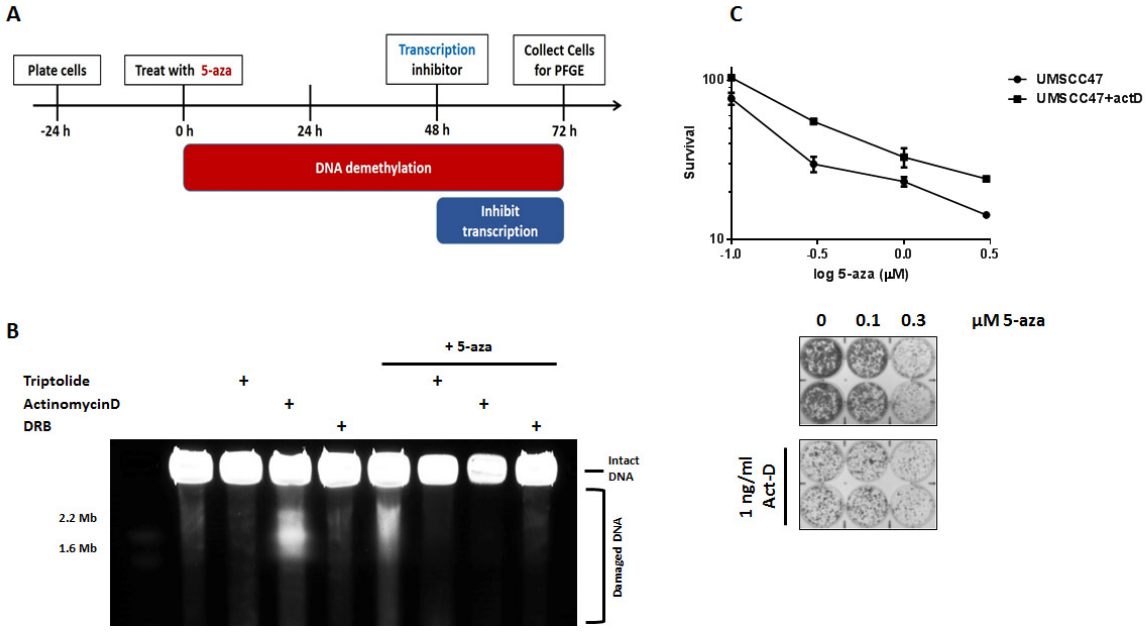

Figure 4: *5-aza induced DNA double strand breaks in HPV+ HNSCC depend on active transcription* (A) Schema of 72 hour 5-aza treatment of cells with 24 hours of transcriptional inhibition. (B) PFGE depicting HPV+ UMSCC47 cells after 72 hours of 20 μM 5-aza and addition of 1μM triptolide, 1.25μg/ml actinomycin D, or 10μM for the last 24 hours (C) Clonogenic survival of UMSCC47 cells either treated or not with 1ng/ml actinomycin D 48 hours after initiation of increasing doses of 5-aza treatment (log scale). Plates of cells stained with methylene blue shown below, quantification shown above. Standard deviations calculated from two independent experiments.

Although transcriptional inhibition is toxic to cells, its ability to prevent demethylation-induced DSBs may protect HPV+ HNSCC cells from 5-azacytidine. To determine if blocking the formation of DSB in HPV+ cells through transcriptional inhibition changes sensitivity to 5-aza, clonogenic survival assays were performed using increasing doses of 5-aza in the presence of a low concentration (1ng/ml) of actinomycin D (Fig. 4C, top). Given that we plate 500 cells per well in clonogenic survival assays and 1.5 million per well in the PFGE experiments, as well as the longer time required for survival experiments, lower doses of 5-aza and actinomycin D were used to prevent the death of all cells. Despite inherent cytotoxicity, the percentage of cells remaining (as a fraction of the control) in cells treated with actinomycin D was higher than in those treated with 5-aza alone (Fig. 4C, bottom). Taken together, these data suggest that 5-aza induced DSBs in HPV+ HNSCC cells are responsible for the observed cytotoxicity.

The finding that induction of DSBs by 5-aza was dependent on transcription suggested at least two potential mechanisms through which transcription enables DSBs after demethylation: 1) though transcription leading to the de-novo translation of a protein required for the formation of a DSB (a nuclease, for example), or 2) through the physical process of transcription. To begin distinguishing these possibilities, HPV+ cells (UMSCC47) were treated with 5-azacytidine in the presence of an inhibitor of protein translation, cycloheximide. Cycloheximide did not reduce the amount of DSB formed after 5-aza treatment (Supp. Fig 2), suggesting that 5-aza induced DSBs are mediated by the physical process of transcription itself, rather than simply from the translation of a specific protein. DNA demethylation increases the amount of transcriptional activity, so

it is also possible that there is a threshold effect where low levels of transcription could be tolerated, but high levels of transcription lead to DNA double strand breaks.

Collision of transcriptional machinery with advancing replication forks can result in genomic instability and double strand breaks [119-122], and previous reports indicate that 5-aza induces DNA lesions that are dependent on active replication [85]. To determine whether the DSB observed in HPV+ cells after DNA demethylation may also be dependent on replication, cells were treated with 5-aza and then replication inhibitors (aphidicolin and hydroxyurea). After prolonged exposure, hydroxyurea therapy itself results in double strand breaks through collapse of replication forks [123]. Here, short-interval therapy with hydroxyurea was designed as a replication inhibitor rather than as an inducer of DNA damage. Because azanucleosides must be incorporated into DNA during replication to cause demethylation through inhibition of methyl transferases [81], 5-aza was allowed to incorporate for 48 hours before HPV+ cells (UMSCC47) were treated with replication inhibitors (schema in Fig. 5A). Interestingly, treatment of UMSCC47 cells with aphidicolin completely inhibited the formation of DNA double strand breaks, while treatment with hydroxyurea partially inhibited the formation of 5-aza induced DSBs (Fig. 5B). These results indicate that 5-aza induced DNA double strand breaks in HPV+ HNSCC are dependent on active replication of cellular DNA.

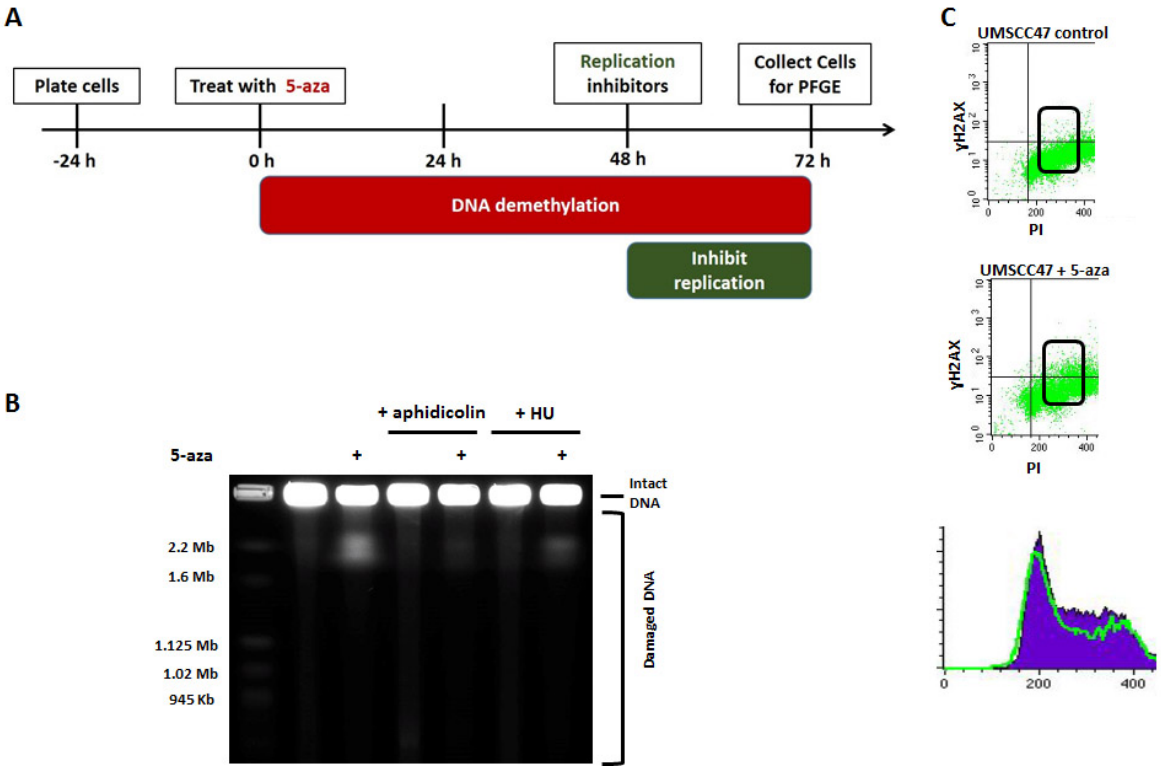

Figure 5: *5-aza induced DNA double strand breaks in HPV+ HNSCC depend on active replication and occur in S-phase* (A) Schema of 72 hour 5-aza treatment of cells and inhibition of replication during last 24 hours of 5-aza. (B) PFGE depicting HPV+ UMSCC47 cells after treatment with 20μM 5-aza for 72 hours and 24 hours of 3.3μM aphidicolin or 1mM hydroxyurea (HU) as indicated. (C) Fluorescence activated cell sorting (FACS) of HPV+ UMSCC47 cells after 72 hours of 20μM 5-aza treatment (middle) or not (top) stained with propidium iodide to indicate cell cycle and γH2AX as a marker of DNA damage. Flow cytometry of same cells indicating cell cycle, purple indicates control cells, green line indicates treatment with 20μM 5-aza (bottom).

To confirm that 5-aza was incorporated and resulted in DNA demethylation in cells treated with replication inhibitors, DNA from treated cells was exposed to methylation dependent nucleases. DNA from UMSCC47 cells treated continuously with 5-aza (72 hours) and with aphidicolin for the entire experimental time or for only the last 24 or 48 hours of 5-aza therapy was incubated with restriction enzymes that cut DNA only at methylated CpG sites ("dependent restriction") or only at unmethylated CpG sites ("sensitive restriction") (Supp. Fig. 3). In untreated cells, a large band was observed after

the sensitive restriction but not after dependent restriction, implying that at baseline, genomic DNA is largely methylated. After treatment with 5-aza alone, the sensitive restriction band was slightly diminished and the dependent restriction band became detectable, confirming that 5-aza therapy resulted in DNA demethylation. In 5-aza treated cells exposed to aphidicolin during the last 24 or 48 hours of treatment, a similar pattern was detected, confirming that the replication inhibition schema shown in Fig. 5A did not prevent 5-aza incorporation nor the demethylating activity of 5-aza (Supp. Fig. 3).

To determine if double strand breaks observed after 5-aza treatment occurred preferentially in a particular phase of the cell cycle, UMSCC47 cells were treated with 5-aza for 72 hr and cell cycle position correlated with DNA damage using flow cytometry. As expected, treatment with 5-aza resulted in many cells with increased levels of DNA damage as marked by γH2AX, and propidium iodine co-staining revealed that the cell population with DNA damage was markedly enriched during S-phase, as compared to G1 or G2/M (Fig. 5C, compare top and middle). These data imply that 5-aza induced DNA damage occurs preferentially during S-phase, consistent with the finding that 5-aza induced DNA double strand breaks are dependent on active replication.

5-azycytidine induced DNA double strand breaks are not mediated through MRN complex, ATR, or PARP-1 activity

The process of DNA replication leaves cellular DNA particularly vulnerable to DNA damage, as DNA polymerases and other proteins must traverse the billions of base pairs and replicate the entire genome during each cell division [124]. Any impediment to

the replication machinery can cause replication stress, which is a major source of DNA DSBs and chromosomal instability during replication. There exist many conditions that can lead to replication stress, including the depletion of nucleotides (the mechanism of DNA damage with hydroxyurea treatment), DNA-RNA hybrids, collision of replication and transcription machinery, and DNA-protein crosslinks [125, 126]. The mechanism of action of azanucleosides involves the trapping of DNMT1 to cellular DNA at the site of their integration causing DNA-protein crosslinks [79, 127, 128]. Fork stalling and collapse at the site of a DNA-protein cross-link, especially in the case of azanucleoside-induced DNMT1 trapping, is repaired through homologous recombination in mammalian cells [129]. This repair requires the nuclease and end priming activity of the protein complex consisting of MRE-11, Rad50, and Nbs1 (MRN) [130]. Given that MRE-11 was found on the chromatin fraction in 5-aza treated HPV+ HNSCC cells (Supp. Fig 4), this pathway was investigated further. Homologous recombination necessarily involves the transient formation of DNA DSB, so it is possible that the DSBs observed in HPV+ HNSCC after 5-aza treatment are the result of physiologic repair of collapsed replication forks. To exclude this possibility, HPV+ UMSCC47 cells were treated with 10 μM of mirin, a small molecule inhibitor of the MRN complex that prevents homology-dependent recombination and the activation of ataxia telangiectasia-mutated (ATM) [131], for 48 hours and subjected to pulsed-field gel electrophoresis. Treatment with mirin in the presence of 5-aza did not prevent the formation of 5-aza induced DSBs in HPV+ cells (Fig. 6A), suggesting that these double strand breaks are not simply the result of MRN-dependent nuclease activity following replication fork stalling.

The processing of stalled replication forks is complicated and depends on a number of pathways which have recently been described. Ataxia telangiectasia and Rad3 related (ATR) is a kinase central to the cellular response to replication stress [132]. ATR is recruited to regions of ssDNA at stalled forks, phosphorylates γH2AX, inhibits cell cycle progression [133], and promotes fork stability [125, 134, 135]. Stalled replication forks can be converted into DNA double strand breaks in a number of ways that depend on the activity of the ATR pathway in replication stress. These include the stabilization and restart of an early stalled replication fork into an intermediate that can be repaired without recombination [123, 136], the dissociation of secondary structures that arise as a consequence of replication and transcription machinery collision [122, 137], and the coordination of replication fork firing in large genes known as "common fragile sites" that are prone to translocations and instability [138, 139]. Thus, given its importance to the recognition and signaling in replication associated stress, the effect of ATR inhibition on DSB formation in HPV+ HNSCC cells in the presence and absence of 5-aza induced replication stress was tested. Not surprisingly, after 48 hr of 5μM of ATR inhibition with AZD6738 (from AstraZeneca, referred to as "ATRi") [140], a moderate amount of DNA DSBs was detected in the absence of 5-aza, as ATR activity stabilizes the replication fork in S-phase in the absence of DNA damage. However, when cells were treated with both 5-aza and ATRi, the level of DSBs as detected by PFGE were not increased compared to 5-aza treatment alone (Fig. 6A). Together, these data suggest that while ATR inhibition itself caused DSBs, the 5-aza induced DSBs in HPV+ HNSCC cells is independent of ATR activity.

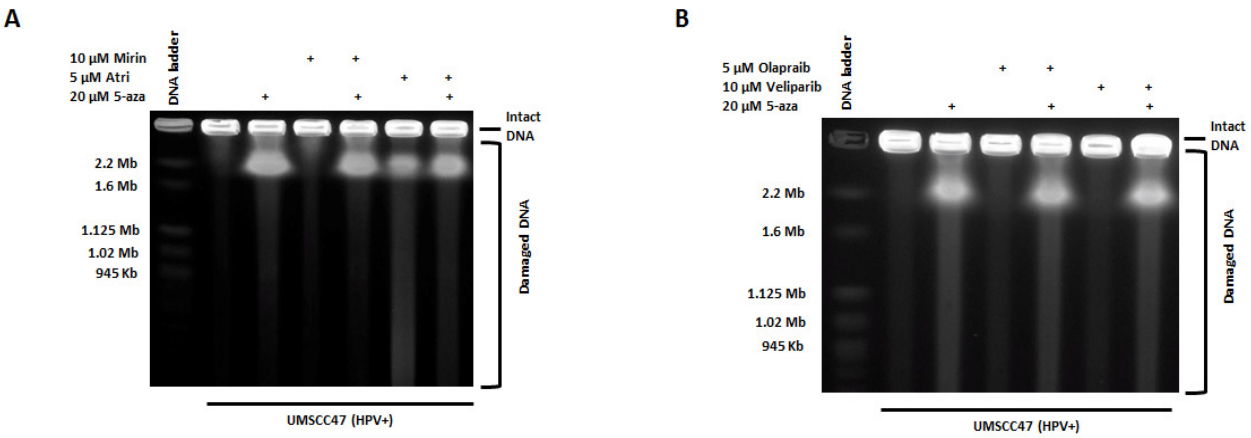

Figure 6: *5-aza induced DSBs do not depend on MRN, ATR, or PARP activity* (A) PFGE depicting HPV+ UMSCC47 cells treated with 72 hours of 20µM 5-aza as indicated, with or without 10µM mirin or 5µM ATR inhibitor during last 48 hours of 5-aza treatment, as indicated. (B) PFGE depicting HPV+ UMSCC47 cells treated with 72 hours of 20µM 5-aza as indicated, with or without either of two PARP inhibitors (5µM olaparib or 10µM veliparib) during last 48 hours of 5-aza treatment.

While also involved in the mammalian immune system, single strand break repair, and cell cycle progression, recent evidence points to poly(ADP-ribose) polymerase-1 (PARP-1) as a key mediator of coordinating the DNA damage response and fork reversal at stalled replication forks [141-144]. In mammalian cells, PARP-1 has been shown to prevent the degradation of a stalled replication forks after genotoxic stress, as well as to inhibit fork restart, presumably to allow the cell to repair the initial DNA lesion giving rise to the replication stress [141, 144]. Given that HPV+ HNSCC express genes involved in DNA repair, especially PARP-1, at much higher levels than HPV- cells [145], it is possible that in the context of dysfunctional HR and lack of Rad51 foci at the sites of DNA damage (Fig. 1C), excessive PARP-1 activity leading to fork stability may contribute to DSB formation. Thus, we sought to determine the effect of PARP inhibition

on 5-aza induced DSBs in HPV+ cells. HPV+ UMSCC47 cells were exposed to either olaparib (5μM) or veliparib (10μM), two PARP-inhibitors, during the last 48 hours of the 72 hr treatment of 20μM 5-aza and were subjected to PFGE. Exposure to PARP-inhibitors did not induce the formation of DSB in HPV+ cells in the absence of 5-aza, and PARP inhibition did not prevent the induction of 5-aza induced DNA DSBs (Fig. 6B). These results suggest that the overactive PARP-1 seen in HPV+, but not HPV-, HNSCC cells is not the fundamental driving factor behind the demethylation induced DNA DSBs seen only in HPV+ HNSCC.

ABOBEC3B is induced after 5-aza treatment and is involved in the formation of DNA DSBs in HPV+ HNSCC

To uncover potential mechanisms underlying the replication- and transcription-dependent DNA DSB formation after 5-aza treatment, tandem mass spectrometry was performed to reveal the 5-aza-induced changes in the proteomic environment of the chromatin fraction in HPV+ HNSCC cells. Of the proteins found with a 95% confidence interval only in the 5-aza treated group in HPV+ cells, APOPEC3B was identified as an enzyme commonly associated with HPV-related malignancies and was investigated further (Supp. Fig. 4) [46, 51].

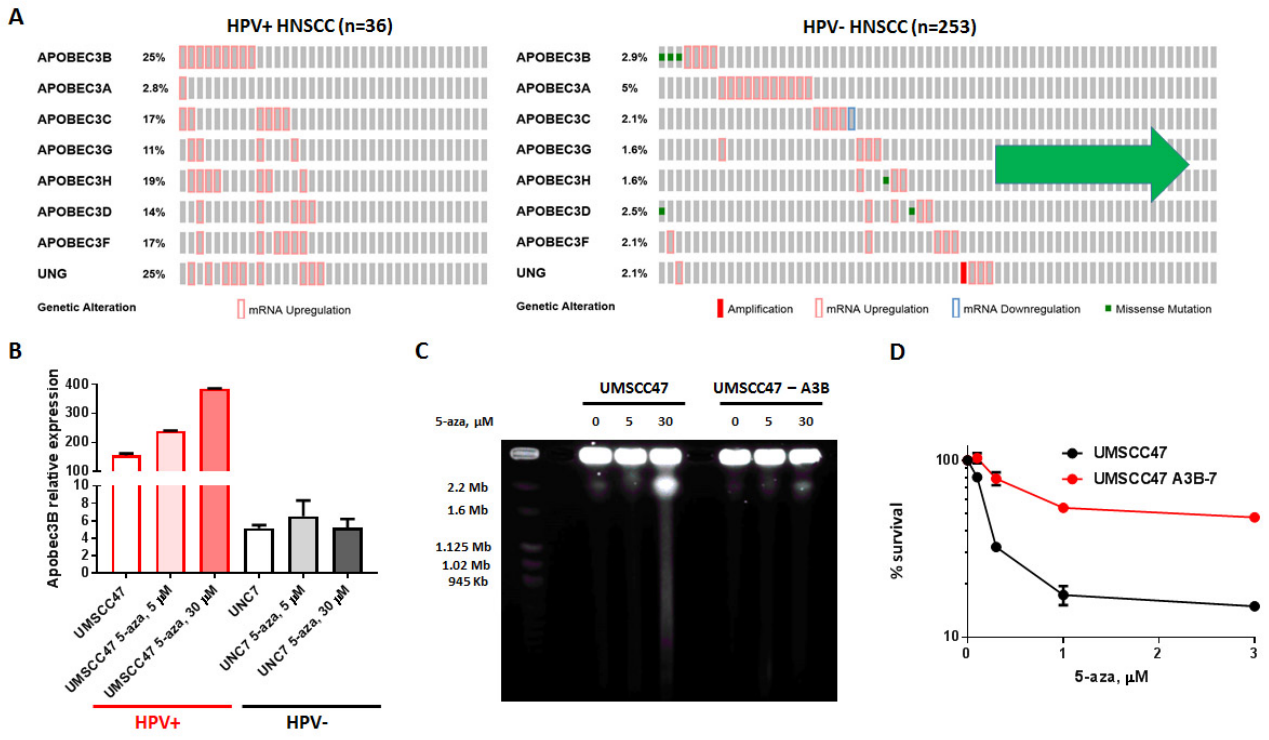

Figure 7: *5-aza-induced DSBs depend on APOBEC3B expression, and HPV+ HNSCC cells overexpress APOBEC3s* (A) Expression of APOBEC3s and UNG in HPV+ (left) and HPV- (right) HNSCC tumors as determined by RNAseq, with individual tumors depicted as vertical columns. Figures adapted from www.cbioportal.org using TCGA database [1, 2] (B) Expression of APOBEC3B in the HPV+ cell line UMSCC47 and the HPV- cell line UNC7 after 48 hours of 5 μM or 30 μM 5-aza treatment determined by rt-PCR and normalized to GAPDH expression. (C) HPV+ UMSCC47 cells with depleted APOBEC3B (through CRISPR/Cas9 system, labeled "UMSCC47-A3B") treated with increasing doses of 5-aza and subjected to PFGE. (D) Quantification of clonogenic survival of HPV+ UMSCC47 and APOBEC3B CRISPR UMSCC47 cells (UMSCC47-A3B) treated with increasing doses of 5-aza.

As known antiviral enzymes that restrict viral ssDNA, the APOBEC3 family is upregulated both in response to viral infection and in HPV-related malignancies [46, 50-52, 146, 147]. Consistent with this, querying TCGA database revealed that all 7 members of the APOBEC-3 family with the exception of APOBEC3A, are upregulated at the mRNA level in HPV+ HNSCC, as compared to HPV- HNSCC (Fig. 7A). APOBEC 3B was overexpressed in 25% of HPV+ tumors but only in 1.5% of HPV- tumors (although it was mutated in another 1%), making it the most disparately expressed APOBEC family

member. Consistent with TCGA data, APOBEC3B was much more highly expressed in HPV+ HNSCC cell lines compared to HPV- cells (Fig. 7B). Despite high basal expression of APOBEC3B in HPV+ cells, it was further upregulated following 5-aza treatment. Conversely, 5-aza therapy did not alter expression of APOBEC3B in HPV- cells (Fig. 7B).

APOBEC3 enzymes are a part of the cellular defense against viruses, but their cytidine deaminase activity is not limited to viral ssDNA. In fact, their activity on host cellular DNA is well documented and is implicated as the cause of characteristic clusters of mutations (termed "kataegis," after the Greek word for thunder) in certain cancers. These clusters of mutations have been implicated in activation of the DNA damage response and breaks in genomic DNA [49, 148-151]. Given that APOBEC3B was detected on chromatin only after 5-aza treatment and that it was highly expressed at baseline and further induced by 5-aza in HPV+ HNSCC cells, we sought to determine if APOBEC3B could mediate the 5-aza-induced DSB. APOBEC3B-depleted cells were created using the CRISPR/Cas9 system in HPV+ cells. In clones selected following CRISPR/Cas9 deletion, the absence of both APOBEC3B mRNA and protein expression was confirmed using rt-PCR and immunoblotting (Supp. Fig. 5). Amazingly, APOBEC3B knockout prevented the formation of DNA double strand breaks following treatment with 5-aza (Fig. 7C), implying that APOBEC3B is central to the demethylation-induced DNA DSBs in HPV+ HNSCC cells. As determined by clonogenic survival, APOBEC3B knockout conferred marked resistance to 5-aza in HPV+ cells (Fig. 7D), which mirrors the lack of DSB formation. Intriguingly, in untreated cells, APOBEC3B knockout significantly decreases clonogenic survival (Supp. Fig. 6). Taken

together, these data provide evidence that HPV+ HNSCC cells rely on APOBEC3B for survival, and that this unique nuclear microenvironment leads to DSB formation and cell death when treated with 5-aza.

Discussion

DNA damaging drugs and radiation have been a mainstay of cancer therapy, especially for patients with head and neck squamous cell carcinoma; however, damage to normal tissues from these therapies cause lifelong morbidity and resulting functional deficits. Avoidance of acute toxicities from chemotherapy and radiation also limits the dose and effectiveness of these therapies. It is largely accepted that HPV+ and HPV- head and neck cancer are two distinct diseases that arise from different mechanisms, yet treatment paradigms do not take this into consideration at this time [19]. Thus, designing treatment options that selectively target the cells of a patient's subtype of head and neck cancer is of utmost importance.

Given the sensitivity of HPV+ HNSCC to 5-aza treatment (Fig. 1A), and the tolerable side effect profile of the FDA-approved drug, 5-aza emerges as an attractive therapy for this subtype of head and neck cancer. Here, we present 5-azacytidine as a potential novel therapy for HPV+ HNSCC that selectively targets these cells through their inherent molecular vulnerabilities to azanucleoside treatment, namely their hypermethylated genome and overexpression of APOBEC3B, an antiviral protein. In addition to its described effects to release transcriptional inhibition of tumor suppressors and to stimulate non-specific DNA damage, we propose an additional model by which

treatment with the demethylating drugs 5-aza and decitabine cause widespread and pathologic DNA double strand breaks in HPV+ head and neck cancer cells.

In line with previous research studying other cells [85, 86], treatment with 5-aza and decitabine induce DNA damage in both HPV+ and HPV- cells, as shown by the induction of γH2AX (Fig. 1B, C). Despite causing DNA damage and activating DNA damage response in both subtypes of HNSCC, 5-aza treatment causes massive induction of DNA DSBs only in HPV+ head and neck cancer cells (Fig. 2), which correlates with the striking sensitivity of HPV+ to 5-aza (Fig. 1A). The differential effects on the DNA damage response in HPV+ and HPV- cells, evidenced by the expected co-localization of Rad51 and γH2AX in HPV-, yet lack of co-localization of Rad51 staining in HPV+ cells, confirms previous studies showing that HPV+ HNSCC harbor dysfunctional homologous recombination repair [104, 107]. Despite the absence of Rad51-mediated homologous recombination in HPV+ cells following treatment that is known to cause a lesion that requires HR for repair [85, 86], it is not sufficient to explain the selective formation of DSB in HPV+ cells, since impaired HR in control cells does not lead to the accumulation of DSB (Fig. 3B, C). However, in agreement with previous work [85], HR deficient cells are indeed more sensitive to 5-aza (Fig. 3A). Together, these data suggest that while dysfunctional homologous recombination does not explain the formation of DSB in HPV+ cells, it likely enhances HPV+ HNSCC sensitivity to 5-aza.

The finding that 5-aza-induced DNA double strand breaks in HPV+ HNSCC cells depended on active transcription (Fig. 4B) was both surprising and informative to the mechanism of damage. Given that the DSBs did not depend on new protein synthesis (Supp. Fig. 2), the mechanism of DNA DSB formation after azanucleoside treatment in

HPV+ HNSCC was likely a complex process involving stress either created or potentiated by the transcription itself, rather than the products of this process. The physical process of transcription creates vulnerable DNA structures and can predispose cellular DNA to damage. It has been shown that the ssDNA exposed in the transcription bubble is susceptible to spontaneous deamination and mutagenic events; thus, transcription itself can create stretches of DNA that vulnerable to DNA damage at highly transcribed genes due to the nature of the transcription bubble [152, 153]. The dependence on active transcription also provides evidence against a model involving replication fork collapse due to DMNT1 trapping to chromatin, as these lesions would only require DNA replication and would theoretically still arise in the context of inhibited transcription, given that the timing of transcriptional inhibition would not cause cell cycle arrest at this point [79, 127, 128].

The finding that DSB formation after 5-aza in HPV+ HNSCC also depend on active replication and occur in S-phase (Fig. 5B, C) is in line with previous research showing that 5-aza toxicity depends on replication [85]. Moreover, this mechanistically agrees with studies demonstrating that transcription-associated double strand breaks often involve conflict between the transcription and replication machinery [119, 121, 122, 137, 154-156]. In eukaryotic cells, these lesions generally arise from two general mechanistic etiologies: 1) through DNA-RNA hybrids that form from the hybridization of the newly transcribed mRNA with template DNA, thus causing an impediment to replisome progression [122, 157, 158], and 2) topological stress created by the anchoring of eukaryotic DNA to nuclear pore complexes at sites of transcription that does not allow the free rotation of DNA as the DNA and RNA polymerases traverse the DNA [122,

137]. Both of these scenarios can result in replication fork collapse and the induction of transcription-associated recombination, leading to DSB formation [121, 122]. Given that Rad51 foci are not formed in HPV+ HNSCC cells after 5-aza treatment (Fig. 1C) and that preventing MRN complex-mediated end resection necessary for recombination after replication fork collapse did not prevent the detection of DSB after 5-aza (Fig. 6A), it is unlikely that the phenomenon of 5-aza induced DSB formation occurs through transcription-associated recombination. Moreover, the finding that 5-aza induced DSBs do not depend on ATR activity (Fig. 6A) implies that the mechanism behind these DSBs is not solely due to conflict between replication and transcription machinery, because the ATR pathway is central to both the dissociation of transcribed genes from the nuclear pore complex in the context of torsional stress [159, 160] and the stabilization of replication forks during replication stress [125, 134-136, 161]. This suggests that the transcription and replication dependent DNA double strand breaks in HPV+ head and neck cancer cells after demethylation treatment arise through a more complex mechanism, and not simply from the collision of replication and transcription.

A question central to 5-aza induced DSBs remained: what key molecular differences between HPV+ and HPV- HNSCC allow the DSB formation in HPV+, but not HPV-, HNSCC cells after demethylation therapy? As mentioned above, deficiency in homologous recombination seen in HPV+, but not HPV- cells was not responsible; however, a potential mechanism was suggested from the findings that HPV+ HNSCC harbor overexpressed APOBEC3 that is further increased upon exposure to 5-aza (Fig. 7A and 7B), and that APOBEC3B is associated with chromatin only in 5-aza treated HPV+ cells (Supp. Fig. 4). A key finding in this study is that APOBEC3B depletion

prevented 5-aza-induced DSB formation in HPV+ cells (Fig. 7C). These data reveal that APOBEC3B is required for 5-aza induced DSBs in HPV+ cells, and combined with requirements for transcription and replication led to a model of DSB formation in HPV+ HNSCC (Fig. 8). Due to the hypermethylated genome of HPV+ HNSCC cells, demethylation therapy triggers a massive increase in levels of global transcription, and a resultant increase in ssDNA at the newly formed transcription bubbles. The already overexpressed APOBEC3B, which is further upregulated after 5-aza treatment, then has access to the ssDNA, where it aberrantly deaminates cytosine residues to uracil. Deaminated DNA bases are then removed by uracil-DNA glycosylase (UNG, sometimes referred to as UDG), leaving behind a single strand break at the site of base excision [149]. Single strand breaks within close proximity on complimentary strands could result in double strand breaks [113, 162]; however, DSB dependence on active replication (Fig. 5B) suggest that it is more likely that unrepaired single strand breaks cause replication fork stalling and collapse, leading to the formation of double strand breaks in S phase (Fig. 5C), [163-167].

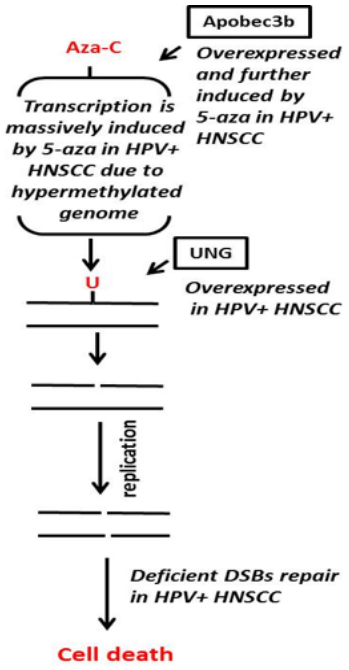

Figure 8: *Model of 5-aza induced DNA DSB in HPV+ HNSCC.* Massive transcription induced by 5-aza treatment simultaneously upregulates APOBEC3B and provides genomic ssDNA as a substrate for APOBEC3B. APOBEC3B activity results in cytidine deamination of host cell DNA, and as part of the base excision repair pathway, UNG creates a single strand break. Single strand breaks cause replication fork stalling and collapse during S-phase, leading to cytotoxic DSB formation

The concept of synthetic lethality, where perturbation of either of two pathways is compatible with survival, yet the loss of both results in cell death, has long been an attractive strategy in cancer therapy [168]. This is exemplified by the hypersensitivity of BRCA1 or 2 deficient cells to PARP inhibitors, since BRCA1 or 2 deficient cells depend on PARP activity for survival [169]. Synthetic lethal interactions allow clinicians to effectively target cancer cells with systemic therapy, as the unique deficiencies of specific cancer cells renders them unable to survive treatment, while non-cancer cells with an intact second pathway can survive. The finding that depletion of APOBEC3B is toxic to HPV+ HNSCC cells in the absence of 5-aza (Supp. Fig. 6), yet APOBEC3B expression greatly increases the sensitivity to 5-aza (Fig. 7D), raises the possibility of 5-aza as a synthetic lethal-like treatment for HPV+ head and neck cancer. HPV genomic DNA, as well as expression of the high risk E6 oncoprotein, triggers the upregulation of

APOBEC3B [170] and creates a cellular state yielding HPV+ HNSCC cells dependent on APOBEC3B expression for survival (Supp. Fig. 6). The reliance on APOBEC3B, then, becomes an "Achille's heel" for the cells, as APOBEC3B mediates the demethylation induced DSBs (Fig. 7C). Furthermore, global transcription is increased to a higher extent upon demethylation treatment in HPV+ HNSCC cells due to the inherent genomic hypermethylation [44, 67-70], providing more ssDNA as a substrate for APOBEC3B activity. This model involving the creation of single strand breaks through aberrant APOBEC3B-mediated deamination of cellular DNA and subsequent replication fork collapse is also in line with the increased sensitivity of homologous recombination deficient cells to 5-aza (Fig. 1A, 3A), as recombination is required to resolve these collapsed forks [85, 123, 167]. Thus, HPV+ HNSCC cells are both prone to generating DNA damage from demethylation therapy and are at least partially deficient in repair pathways required to repair the damage. We have demonstrated that these transcription/replication DNA DSBs occur in both cell lines and patient derived cells; however, it remains to be tested if these DSBs occur in HPV+ head and neck tumors after patients are treated with 5-aza. Analysis of specimens from the 5-aza window clinical trial currently taking place at the Yale Cancer Center may help us to answer this question.

Another important piece of experimental evidence supporting our model would be the involvement of UNG in the formation of DNA DSBs after 5-aza treatment. UNG is overexpressed in 25% of HPV+, but not HPV- HNSCC (Fig. 7A), which provides some indirect evidence that it is involved in the DNA damage response in HPV+ head and neck tumors, however direct testing would strengthen our model. UNG will be inhibited using both stable and transient expression of UNG shRNAs, as well as with transient and stable

expression of uracil glycosylase inhibitor (UGI) of Bacillus subtilis bacteriophage PBS1 [149, 171] in two HPV+ HNSCC cell lines, UMSCC47 and SCC090. These cells will then be evaluated for the presence of DSB formation after treatment with 5-aza by both PFGE and γH2AX foci formation. If DNA DSBs are abrogated in UNG inhibited cells after 5-aza, then the requirement of UNG activity will be confirmed. If DSBs are still able to form in UNG inhibited HPV+ HNSCC after demethylation treatment, the involvement of the DNA mismatch repair (MMR) pathway will be evaluated, as MMR-induced gaps in the DNA can also cause replication fork stalling and collapse [172]. This can be accomplished by using shRNAs targeted to single-strand selective monofunctional uracil-DNA glycosylase (SMUG), thymine DNA glycosylase (TDG), and methyl-CpG-binding domain protein 4 (MBD4), the three other glycosylases that recognize U/G mismatches [173-175]. Analyzing the effect of uracil glycosylase inhibition on demethylation-induced DNA double strand break formation in HPV+ HNSCC cells will both allow further characterization of the mechanism of DNA damage and provide insight into excision repair pathways utilized by these cells.

Results presented here provide evidence for a novel application of demethylation treatment in HPV+ HNSCC and serve as a model for further mechanistic understanding of the selective induction of DNA double strand breaks in these cells. Further work is needed to determine which subsets of HPV+ HNSCC tumors are susceptible to 5-aza toxicity through DSB induction, though intuitively, tumors with globally hypermethylated promoters, upregulated APOBEC3B expression, and deficiencies in homologous recombination may help identify the responsive subset.

SPECIFIC AIM 2: To assess the cellular response and effect on metastatic potential of demethylation therapy in HPV+ HNSCC cells, xenograft models, and clinical trial patients

Methods

Cell lines, constructs and chemicals

HPV- (SCC61, SCC25, JHU012) and HPV+ (SCC090, UMSCC47) HNSCC cell lines were used. All HPV- cells were cultures in DMEM/F12 medium supplemented with 0.4μg/mL hydrocortizone, and all HPV+ cell lines were grown in DMEM with nonessential amino acids. All media was supplemented with 10% FBS (Invitrogen), 50μg/mL penicillin, and 50μg/mL streptomycin (Invitrogen). All cell lines have been tested negative for mycoplasma and authenticated by microsatellite analyses.

To establish primary HNSCC cultures, surgical specimens were collected from consented patients in PBS within 30 min of resection. Tissue was cut into ~5 mm^3 pieces, disinfected by immersion in 70% ETOH for ~1 min, rinsed with PBS four times, and digested in 0.05% trypsin-EDTA supplemented with Collagenase type 1A (200units/ml) (Sigma C-9722) in a vented flask at 37^0C with 5% CO_2 for 10-20 min. Digestion was stopped by adding 1 volume of FBS (Sigma). After centrifugation at 1500 rpm x 5 min, the supernatant was aspirated, the cells were resuspended in keratinocyte serum-free medium with supplements and 10% FBS, strained through a 100μm nylon cell strainer (Falcon; Becton Dickinson Labware), plated in keratinocyte serum-free medium with supplements (GIBCO/Invitrogen) and 10% FBS onto 0.1% gelatin (Millipore) coated

plates, and grown at 37^0C in a 5% CO_2 incubator. The next day, cells were washed with PBS and grown in keratinocyte serum-free medium with supplements until they reached ~90% confluence. After that, the cells were detached with 0.05% trypsin-EDTA, the reaction was stopped with defined trypsin inhibitor (Gibco), and the cells were plated onto uncoated plates in keratinocyte serum-free medium with supplements and used in experiments.

P53 luciferase reporter, p-super and p-super p53 shRNA expressing vectors were a gift from Galina Selivanova.

Cells were transfected using Lipofectamine 2000 (Invitrogen) according to manufacturer recommendations.

5-Azacytidine, zeocin, carboplatin and pifithrin-α were obtained from Sigma.

P53 reporter

UMSCC47, UNC7, and SCC35 cells were grown in 6 well plate and transfected with p53 luciferase reporter plasmid; 6 hours after, the cells were treated or not 3μM of 5-aza. The cells were collected 24 or 48 hours after the treatment and lysed in Luciferase Cell Culture Lysis Reagent (Promega). 10μg of each cell lysate and 100μl of Luciferase Assay Reagent (Promega) were used to measure luminescence in the plate-reading luminometer.

Immunoblotting

Cells were collected by trypsinization and lysed in radioimmunoprecipitation assay (RIPA) lysis buffer (Sigma) with the addition of protease inhibitors (Roche) and

phosphatase inhibitors (Sigma) for 15 minutes on ice. Insoluble material was removed by centrifugation at 14,000rpm for 15 minutes at 4°C. Proteins were separated in 10% Tris-glycine polyacrylamide gels (Mini-PROTEAN; Bio-Rad) and electrophoretically transferred onto polyvinylidene fluoride membranes. Membranes were blocked with 3% BSA in PBS and incubated with antibodies against p53, GPDH, and PARP-1 (Santa Cruz) and DNMT1 from Cell Signaling. After incubation with primary antibodies, membranes were washed, incubated with secondary DyLight anti-mouse and anti-rabbit antibodies (Thermo Scientific), and signals was visualized using a Bio-Rad imager.

Zymography

100,000 of UMSCC47 or SCC090 cells were plated in growth media in 12 well plates. The next day, cells were treated or not with 5-aza in 0.5 ml of DMEM media supplemented with 1% FBS. 24 or 48 hours after the treatment the media was collected, the cells were trypsinated, collected, and counted using Trypan Blue (Invitrogen) and treated. Volumes of media corresponding to 10,000 live cells were mixed with 2XNovex® Tris-Glycine SDS Sample Buffer (Invitrogen), incubated for 10 min at room temperature and loaded in a Novex™ 10% Zymogram (Gelatin) Protein Gels. After electrophoresis, gels were incubated in 1X Zymogram Renaturing Buffer (Invitrogen) for 30 minutes at room temperature with gentle agitation, equilibrated in 1X Zymogram Developing Buffer (Invitrogen) for 30 minutes at room temperature with gentle agitation, developed at 37°C in a fresh developing buffer overnight and stained with SimplyBlue™ Safestain (Invitrogen).

Survival assay

All cells lines, except of SCC090 and primary cultures, were seeded in 12 well plates at a density of 1000 cells/well in duplicates and treated with increasing doses of 5-

aza the following day. SCC090 and primary cultures were plated at a density 10,000cells/well. After 7 days, the cells were trypsinized and counted using Trypan Blue Solution (Invitrogen) to determine the number of alive cells. Alternatively, we used Cell Titer Glo reagent (Promega). The data presented were obtained from at least 2 independent experiments. Two-tailed t-test was used to determine statistical significance of the differences between untreated cells and cells treated with the various concentrations of 5-aza.

RNA extraction and quantitative RT-PCR

Total RNA was extracted by Qiagen RNA extraction kit and cDNA was synthesized using iScript cDNA Synthesis Kit (Bio-Rad) according to the manufacturer's instructions. Quantitative real-time reverse transcription polymerase chain reaction (qRT-PCR) was done using iQ SYBR Green Supermix (Bio-Rad) and primer pairs indicated in the Table 1 on the iCycler iQ Real-Time PCR Detection System (Bio-Rad). Each qRT-PCR reaction was done in at least duplicate, and the ΔΔCt method was used to analyze the data. RT-PCR primers for MMP1, MMP10, and MMP12 were from Origene.

In vivo experiments

The in vivo study was approved by the local animal experimental ethical committee. Exponentially growing UMSCC47 or SCC090 cells were injected subcutaneously into the sacral area of female NUDE mice. Each mouse was inoculated with 2×10^5 cells in 50% matrigel and 50% PBS at a volume of 100μL. Body weight,

tumor growth, and general behavior were monitored. Tumor volumes were measured every 3 days. Mice were sacrificed when the tumor exceeded a size of 1 cm^3.

Immunohistochemistry

Specimens were fixed with 10% formalin and embedded in paraffin per routine of the surgical pathology division. Sectioning, hematoxylin & eosin staining, and immunostaining with the antibody against Ki67 were performed by the Yale Pathology Core Facility.

Statistical analysis

Two-way ANOVA analysis was used to compare 5-aza treated and untreated mouse groups. Other statistical analyses were done using Fisher exact and t-test.

Results

HPV+ head and neck cancer cells are sensitive to 5-aza partially due to stabilization and activation of p53.

To determine a response of HNSCC cells to 5-aza, two HPV+ HNSCC cell lines and one HPV+ primary culture, as well as three HPV- cell lines and one HPV- primary culture were compared. While both HPV+ and HPV- cells responded, HPV-associated cell lines and primary culture were markedly more sensitive (Figure 9A, note log scale).

The 5-aza structural analog 5-aza-2′-deoxycytidine (decitabine) was recently found to upregulate protein levels of tumor suppressor p53 in HPV+ cervical and head and neck cancer cells [176]. Restoring p53 protein expression and its tumor suppressor

functions has been suggested as a promising strategy to combat HPV+ cancer. Indeed, several studies showed that p53 stabilization in HPV+ cervical carcinoma by silencing E6 or E6AP resulted in the death of cancer cells [177]. The combination of leptomycin B and actinomycin D reduced expression of E6 mRNA and induced apoptosis via p53 upregulation [177]. Furthermore, a chemical library screen identified two small molecules that suppress the growth of HPV-driven cervical carcinoma cells by inhibiting E6 [178]. In addition, a synthetic peptide that binds E6 and inhibits its activity has been identified [179]. Finally, RITA, a small molecule that protects p53 from HDM2 degradation [180] also protected p53 from E6-mediated degradation and killed cervical cancer cells [181]. p53 is a powerful transcription factor able to transactivate pro-apoptotic and growth inhibitory genes, as well as induce apoptosis through transcriptional repression of another set of genes and through direct activation of the mitochondrial apoptotic pathway [31-34, 182]. Since the transcriptional transactivation function of p53 is important for the induction of apoptosis, whether 5-aza treatment enhances p53's transactivation function was investigated. Forty-eight hours of treatment with 20μM 5-aza resulted in a significant (~6 times) increase in luciferase activity in HPV+ UMSCC47 cells expressing a p53-responsive luciferase reporter, while only moderately activating (~2 times) the p53 reporter in HPV-negative UNC7 cells (Figure 9A).

To determine if the increased sensitivity of HPV+ HNSCC to 5-aza is due to activation of p53, UMSCC47 cells were transiently transfected with constructs expressing control or p53 shRNAs. Depletion of p53 caused UMSCC47 cells to become partially resistant to 5-aza treatment (Figure 9C), as did pretreatment of the cells with p53 inhibitor pifithrinα [183] that inhibits p53's transactivation function (Figure 9D). In line

with elevated p53 transactivation activity (Figure 9B), 5-aza stabilized p53 protein levels in HPV+ UMSCC47 cells, an effect that was abrogated by p53 shRNA expression (Figure 9E). Increased PARP-1 cleavage following 5-aza treatment of UMSCC47 cells suggested that the reduced survival after 5-aza was accompanied by apoptosis (Figure 9E). Knockdown of p53 by shRNA decreased cleaved PARP-1 after 5-aza treatment in UMSCC47 (Figure 9E), suggesting that apoptotic cell death in 5-aza treated HPV+ cells is partially driven by p53 reactivation.

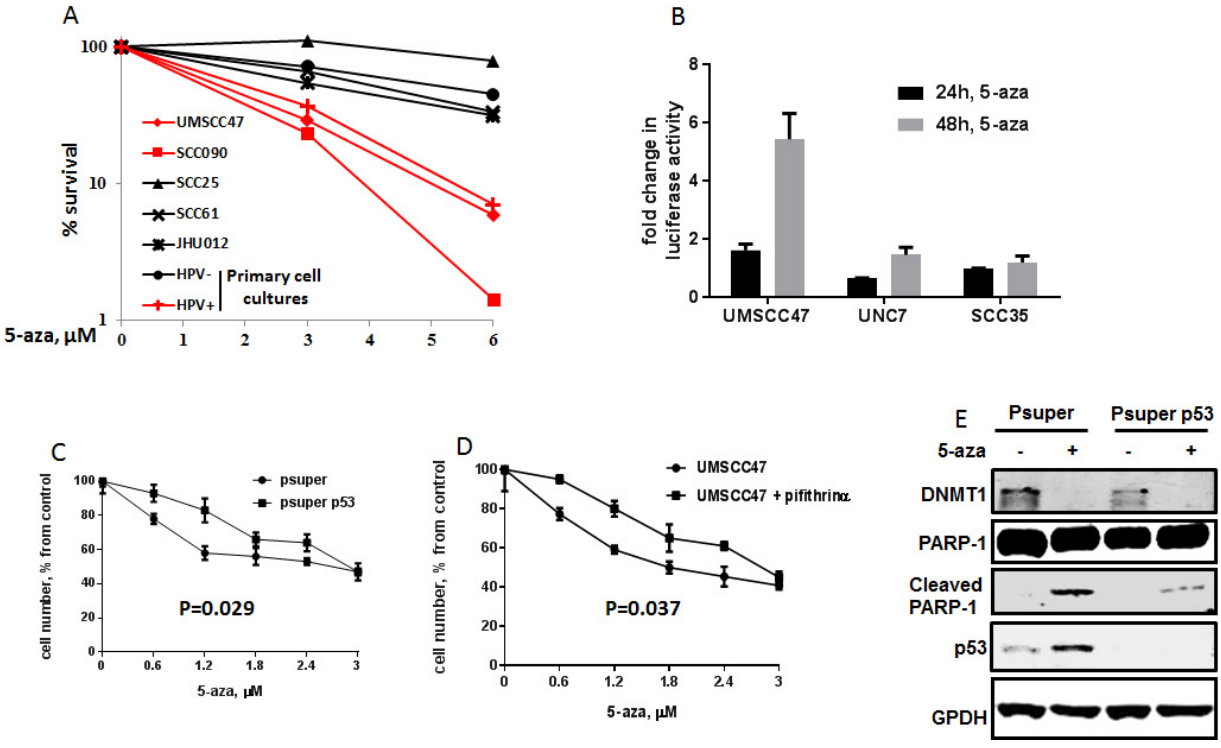

Figure 9: *HPV+ head and neck cancer cells are sensitive to 5-aza partially due to stabilization and activation of p53.* (A) HPV+ and HPV- head and neck cancer cells (cell lines and primary cells derived from patient specimens) were treated with increasing concentrations of 5-aza; cell viability was assessed by trypan blue exclusion 7 days after treatment. 2 independent experiments are presented. (B) Fold induction in p53 transactivation activity (luciferase) in p53 luciferase reporter expressing HPV+ (UMSCC47) and HPV- (UNC7 and SCC35) cells treated with 3μM of 5-aza as compared to untreated cells. 3 independent experiments are presented. (C) Survival of UMSCC47 cells, expressing psuper vector or psuper p53 shRNA and treated with increasing concentrations of 5-aza. Data from 2 independent experiments are presented. (D) Survival of UMSCC47 cells pretreated with p53 inhibitor, pifithrin α, and treated with 5-aza. Data from 2 independent experiments are presented. (E) DNMT1, p53 and cleaved PARP-1 immunoblot of lysates from UMSCC47 expressing control (psuper) or p53 (psuper p53) shRNAs cells treated or not with 5-aza.

5-aza treatment reduces expression of all HPV genes in head and neck cancer cells.

As the p53 protein is controlled by HPV E6, HPV E6 mRNA levels were determined after 5-aza treatment. Similar to recently reported decitabine treatment [176], after 48 or 72 hours, 5-aza decreased HPV E6 expression in HPV+ HNSCC cells in a dose dependent manner (Figure 10). E6 and E7 expression are critical for HPV tumorigenesis and for HPV+ cancer cells to avoid apoptosis [184-186], and depletion of E6 and E7 via shRNAs restores p53 and pRB levels and induces apoptosis in HPV-associated HNSCC cells [184]. Although not well studied, the expression of HPV genes other than E6 and E7 may affect proliferation, viability and survival of HPV+ cancer cells [187-190]. In addition to inhibiting HPV E6 and E7 expression, 5-aza treatment downregulated the expression of all HPV genes in UMSCC47 cells (Figure 10) and another HPV+ head and neck cancer cell line SCC090 (Supp. Fig. 7). In contrast, the DNA damaging drugs zeocin, which is a radiomimetic, and carboplatin, which functions as a crosslinker, did not significantly alter HPV mRNAs levels (Figure 10). This suggests that the reactivation of p53 in 5-aza treated HPV+ HNSCC is not simply the cell's reaction to DNA damage.

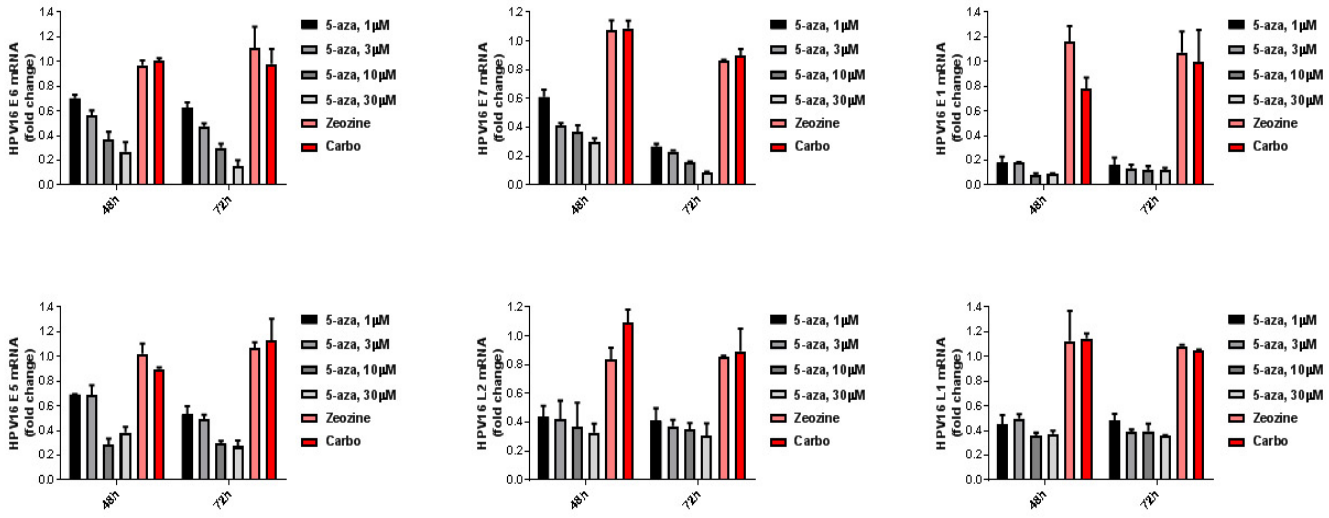

Figure 10: *5-aza treatment reduces expression of all HPV genes in head and neck cancer cells in a dose dependent manner.* Fold change in expression of HPV16 genes 48 and 72 hours after treatment with 5-aza, 20μg/ml of zeocin or 3μg/ml of carboplatin. Data from 3 independent experiments are presented.

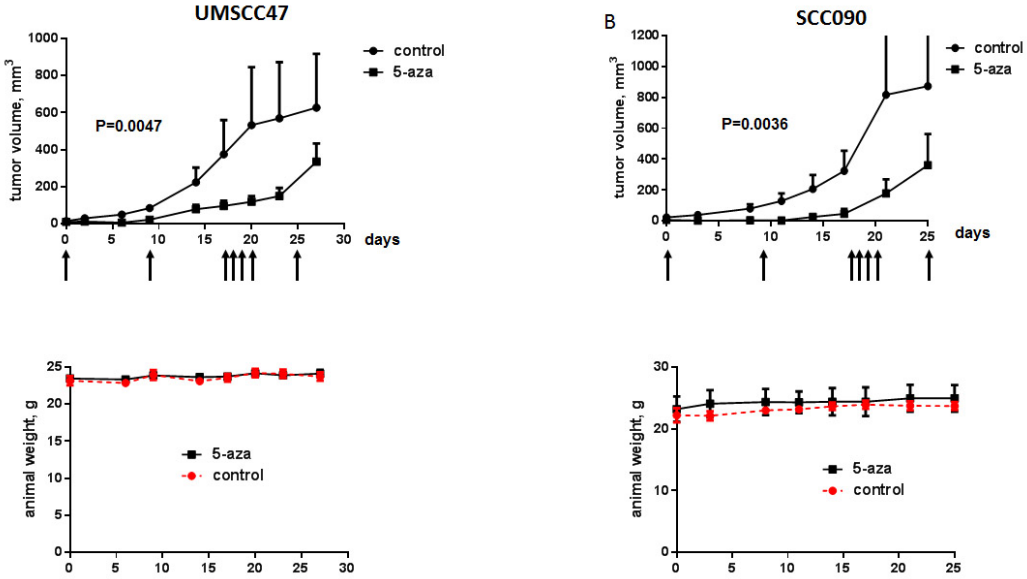

Figure 11: *5-aza delays HPV+ tumor growth in mice.* HPV+ UMSCC47 (A) or SCC090 (B) cells were inoculated subcutaneously into the flanks of NUDE mice. When tumors became palpable, mice were treated with 2mg/kg of 5-aza or vehicle (5 mice in each group) at days indicated by arrows. Tumor volume (top, p value calculated with ANOVA) and animal weight (bottom) are presented.

5-aza delays HPV+ tumor growth and inhibits cancer cell invasion in a mouse model.

To investigate the activity of 5-aza against HPV+ tumors *in vivo*, mice bearing HPV-associated head and neck UMSCC47 or SCC090 xenografts were treated with 2mg/kg of 5-aza. 5-aza treatment significantly suppressed the growth of tumors without causing any mouse weight loss (Fig. 11A, B). In addition, 5-aza inhibited proliferation in HPV+ xenografts, as measured by the percentage of Ki-67 positive cells (Figs. 12 and 13). To begin investigating the ability of HPV+ xenografted tumors to invade mouse blood vessels, expression of human GPDH in cDNA isolated from blood collected from UMSCC47 tumor-bearing mice was determined. Here, human genetic material found in mouse blood samples was taken as evidence of tumor intravasation, although exosomes from xenografted tumors containing RNA could present another explanation. Human GPDH mRNA was found in the blood of 4/5 (80%) of control mice, but in only one 5-aza treated mouse (Figure 14A), most likely due to decreased circulating tumor cells following 5-aza therapy of mice with xenografted HPV+ HNSCC tumors.

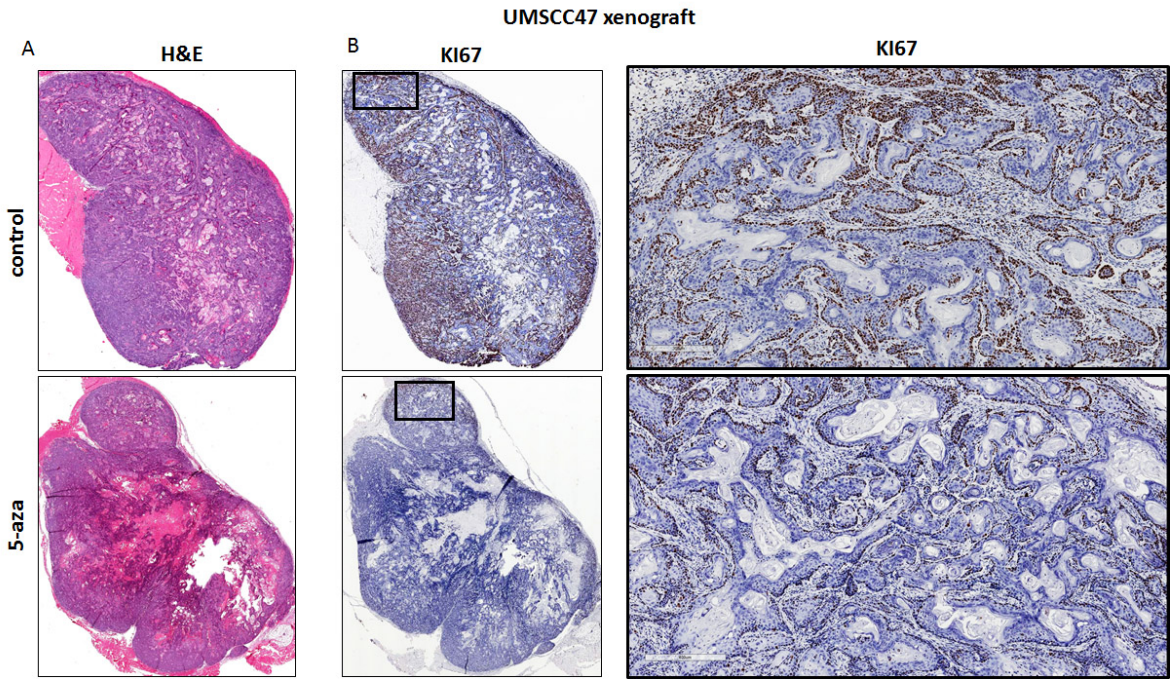

Figure 12: *5-aza constrains proliferation in HPV+ tumors*. H&E and KI67 staining of representative tumors (UMSCC47) from Figure 10.

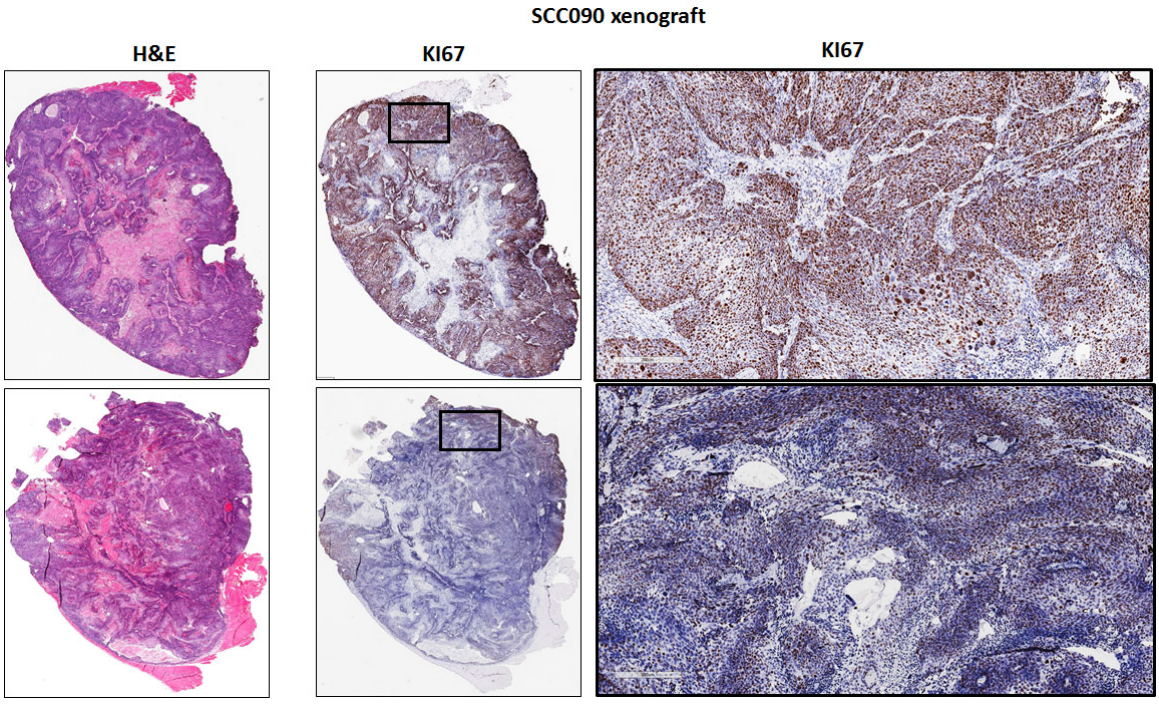

Figure 13: *5-aza constrains proliferation in HPV+ tumors*. H&E and KI67 staining of representative tumors (SCC090) from Figure 10.

5-aza inhibits expression and activity of matrix metalloproteinases

Cancer cell invasion and intravasation represent a first and limiting step during metastasis that is strictly dependent on a function of matrix metalloproteinases (MMPs) to degrade the extracellular matrix [191, 192]. MMP1 and MMP10 have each been proposed as tumor markers for HNSCC [193]. In addition, MMPs 1 and 10 have been shown to promote tumor cell invasion and metastasis in diverse cancer types, including head and neck, through their degradation of collagens and fibronectin, respectively [194-196]. Treatment of HPV+ UMSCC47 xenograft bearing mice with 5-aza resulted in significantly decreased levels of MMP 10 mRNA in tumors (Fig. 14B). Forty-eight hours

of 5-aza inhibited expression of MMPs 1 and 10 in two HPV-positive head and neck cancer cell lines (Fig. 14C, E) and in HPV-positive tumors from patients treated with 5-7 days of 5-aza on a clinical trial (Fig. 15D). 5-aza treatment also effectively decreased the secretion of functional MMPs into culture media from UMSCC47 and SCC090 cells as measured by the degradation of gelatin (Fig. 14D, F).

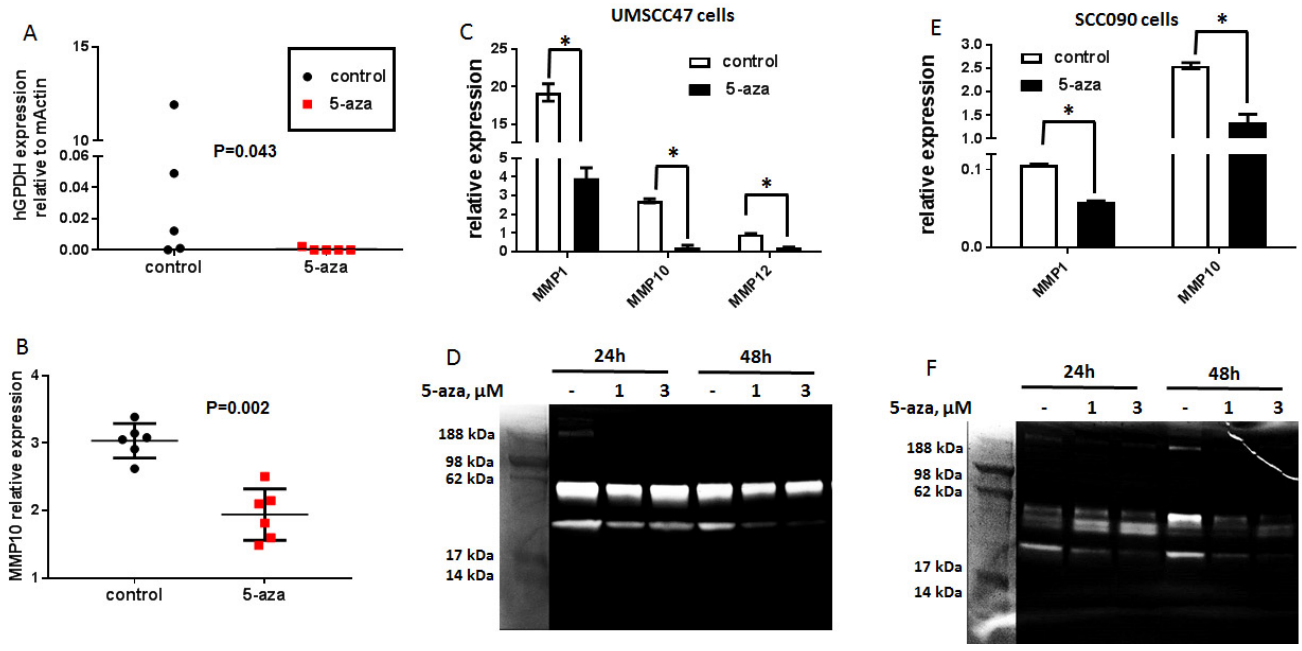

Figure 14: *5-aza inhibits MMPs and HPV+ cancer cell invasion.* (A) Expression of human GAPDH relative to mouse actin gene (%) in blood collected from UMSCC47 tumor-bearing mice on day 25 (p value calculated with 2-tailed T test). (B) Relative to GPDH expression of MMP10 in UMSCC47 tumors derived from mice treated or not with 5-aza. (C) Relative to GPDH MMP1, MM10, and MMP12 mRNA levels in UMSCC47 cells treated or not with 3µM of 5-aza for 48 hours as determined by qRT-PCR. (D) Zymogram gel showing activity of proteases that use gelatin as a substrate in growth medium from UMSCC47 cells treated or untreated with 5-aza for indicated times. (E) Relative to GPDH, MMP1 and MM10 mRNA levels in SCC090 cells treated or not with 3µM of 5-aza for 48 hours as determined by qRT-PCR. (F) Zymogram gel showing activity of gelatinases in growth medium from SCC090 cells treated or untreated with 5-aza for 24 or 48 hours.

5-aza downregulates HPV gene expression, stabilizes p53, and induces apoptosis in HPV+ HNSCC in patients.

Based largely on the cellular and *in vivo* data presented thus far, a window clinical trial was opened at the Yale Cancer Center to assess the tumor cell activity and safety of single agent 5-azacytidine administered at 75mg/m^2/d daily x 5-7 days in patients with HPV+ and HPV- HNSCC [197]. In agreement with results obtained in HPV+ head and neck cancer cells (Fig. 10), 5-aza treatment in patients resulted in the decreased expression of HPV genes, including HPV E6 and E7, in 5 of 5 tumors tested (Fig. 15A). Five to 7 days of patient treatment with 5-aza also significantly increased caspase-3/8 activity (cleavage of the fluorescent substrate AC-Devd-AMC) in 4 of 5 HPV+, but not in an HPV- tumor (Fig. 15B). Importantly, 5-aza therapy resulted in marked increase in p53 protein levels in all HPV+ tumors tested (Fig. 15C). Consistent with 5-aza-induced inhibition of MMP expression and activity in both HPV+ cells and xenografted tumors (Fig. 14B-F), a substantial reduction of MMP1 and MMP10 mRNA levels in tumors from patients after 5-aza treatment (Fig. 15D) was detected.

These data are consistent with findings from cell line, primary culture, and xenograft experiments, which showed that 5-aza is toxic to HPV+ HNSCC, resulting in decreased survival (Fig. 9A), and that 5-aza inhibits the expression of HPV genes (Fig. 10) with increased protein levels of p53 (Fig. 11). Head and neck cancer patients enrolled in the 5-aza clinical trial did not report any treatment-related side effects. Although imaging was not repeated to determine tumor shrinkage as tumor response was not

expected due to the short treatment course, of the five patients analyzed, two patients reported an improvement in swallowing and decreased "fullness" after 5-aza treatment. Furthermore, two patients reported a reduction in pain around the tumor site following treatment with 5-aza.

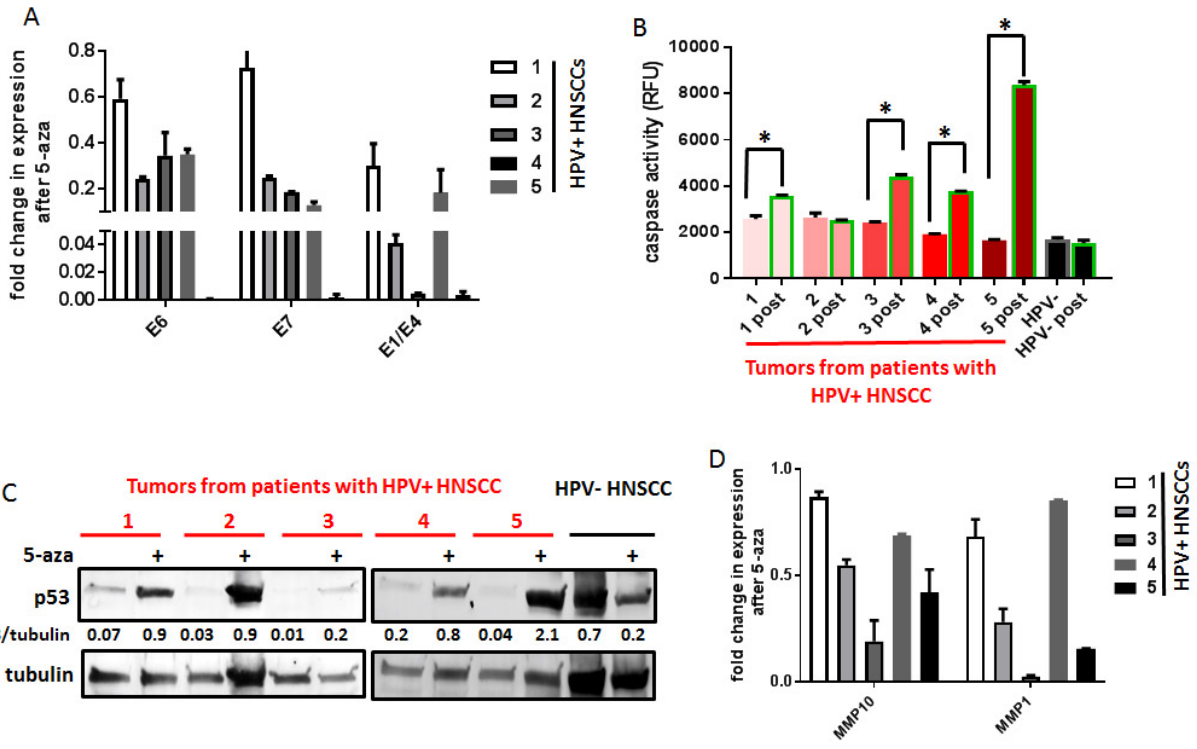

Figure 15: *5-aza downregulates HPV gene and MMPs expression, stabilizes p53, and induces apoptosis in HPV+ HNSCC in patients.* (A) Fold change in expression of HPV E6, E7, and E1/4 splice variant in tumors from 5 different HPV+ patient tumors after 5 days of 5-aza treatment. (B) Caspase 3/8 activity in tumors from 5 HPV+ and 1 HPV- patients after 5-aza treatment. Assay was performed in duplicate. (C) p53 protein levels in tumors from patients after 5-aza treatment. (D) Fold change in expression of MMP1 and MMP10 in tumors from 5 different patients with HPV+ HNSCC after 5 days of 5-aza treatment.

Discussion

As previously shown in Specific Aim 1, treatment with 5-aza shows promising cytoxicity with formation of irreparable DNA damage in HPV+ HNSCC. The cellular response to 5-aza in cells, xenograft models, and head and neck cancer patients was then necessary to further evaluate the clinical activity of 5-aza as a novel treatment for HPV+ HNSCC. Further solidifying its use as a targeted therapeutic, treatment with 5-aza caused the downregulation of HPV gene expression, including the major oncoproteins E6 and E7, as well as E1, E5, L1, and L2 (Fig. 10). This is in line with previous research demonstrating the decitabine-induced downregulation of E6 and E7 in both HPV+ cervical and HPV+ head and neck cancer cells [176]. The link between E6 and E7 expression, increased methylation status of gene promoters, and tumor invasiveness has been described previously in the cervical cancer literature [198-202]. Although uterine cervical cancer and HNSCC are distinct diseases, demethylating the host genome through 5-aza or decitabine treatment may begin to reverse the fundamental steps of HPV-driven carcinogenesis and remove protective measures that allow the expression of viral genes. This has interesting implications, as demethylation treatment may even play a role in preventing HPV+ carcinogenesis if a patient has an active HPV oropharyngeal infection or theoretical HPV+ premalignant lesion. Given that 5-aza treatment stimulates the upregulation of APOBEC3B (Fig. 7B) and that APOBEC3 enzymes are known to restrict viral ssDNA [46, 50, 51, 146, 147], it would be informative to test the effect of 5-aza on the expression of HPV genes in HPV+ APOBEC3B depleted HNSCC cells utilized in Specific Aim 1 as a possible mechanism behind HPV gene downregulation.

The finding that p53 activity is stimulated by 5-aza treatment (Fig. 9) is exciting and further speaks to the potential role of 5-aza in the treatment of HPV+ HNSCC, as the reactivation of p53 has been long been an attractive goal in cancer therapy [203]. p53 is arguably the most potent tumor suppressor and is the most commonly mutated gene in cancer [204, 205]. Though p53 is mutated in 84% of HPV- HNSCC tumors, it is rarely mutated in HPV+ HNSCC and is instead suppressed by the HPV E6 viral oncoprotein [43]. Thus, in HPV+ HNSCC, 5-aza treatment leads to the reactivation of wild-type p53 (Fig. 9A, 15C), with subsequent apoptosis (Fig. 9D, 15B) and inhibition of proliferation (Fig. 12 and 13). Mechanistically, the 5-aza induced p53 reactivation is likely secondary to the downregulation of HPV E6 and release of p53 suppression in the setting of DNA damage, and provides yet another axis through which HPV+ HNSCC cells are targeted despite the systemic distribution of treatment.

The key to improved patient survival in head and neck cancer is the management of regional metastases to the neck, as the presence of nodal disease is the most important negative predictor of patient survival [206]. This is reflected in the importance of nodal status in the staging of head and neck cancer, as a single positive node less than 3 cm automatically confers a stage 3 disease, while more than one node or a single node greater than 3 cm defines the cancer as stage 4, regardless of primary tumor size. Matrix metalloproteinases (MMPs) are key regulators of the tumor microenvironment, including promoting angiogenesis and tumor growth, but perhaps most importantly, the ability of MMPs to degrade the extracellular matrix is the primary way in which tumors intravasate, the first step in metastasis [207, 208]. Given how critical the presence of regional metastases is in head and neck cancer outcomes, the finding that 5-aza reduces

both MMP (MMP1 and 10) expression and activity in HPV+ HNSCC cells (Fig. 14C-F), as well as in patient tumors (Fig. 15D), was very promising. 5-aza also completely abolished the detection of human RNA in the blood of xenografted mice (Fig. 14A), which provided further evidence of 5-aza's role in reducing the metastatic potential HPV+ HNSCC. Because 5-aza significantly slowed the HPV+ HNSCC tumor growth in these mice (Fig. 11A), it is possible that the evidence of reduced intravasation in treated mice (Fig. 14A) resulted from the decreased tumor size rather than a reduced ability of cancer cells to penetrate mouse blood vessels. While the reduced expression and activity of MMPs in 5-aza treated cells provides a mechanistic explanation for reduced metastatic potential, this needs to be tested further and represents a limitation of the study. This can be accomplished by xenografting a larger number of mice and normalizing human GPDH expression (as a surrogate measure of tumor intravasation) to tumor volume. Though it is theoretically possible that the human RNA detected in the mouse blood was from exosomes rather than tumor cells and that 5-aza decreased exosome formation, it is highly unlikely that exosomes from tumor cells are able to gain access to the blood stream.

A major impetus of the study was to develop a treatment for HPV+ HNSCC that carries less morbidity than current treatment paradigms. Importantly, 5-aza treatment stabilized p53, reduced the expression of HPV genes, and MMPs in HPV+ head and neck tumors from patients enrolled in the 5-aza window clinical trial. The activation of caspases in 4/5 of HPV+ tumors following treatment indicates that 5-aza induced apoptosis after only 5 days of treatment and 2 patients had improved symptoms. These preliminary results are encouraging and in contrast to the extended treatment time

required to see an effect in MDS and AML [209]. The major side effects seen after extended 5-aza and decitabine treatments in MDS and AML are associated with bone marrow suppression. Although not tested, it is possible that head and neck cancer patients will not experience these effects due to their underlying pathology not involving hematologic abnormalities and due to a potential shorter treatment regimen. The 5-aza trial continues to recruit patients. Upon completion of this trial, if results remain favorable, we will consider a trial to look for efficacy of 5-aza in HPV+ HNSCC patients.

4. **SPECIFIC AIM 3: To discover biomarkers that identify a subset of HPV+ HNSCC patients that may be amenable to de-escalation therapy**

Methods

Analysis of TRAF3, CYLD, and PIK3CA mutations

To analyze TRAF3, CYLD, and phosphatidylinositol-4,5-bisphosphae 3-kinase catalytic subunit α (PIK3CA) genetic alterations in HNSCC and other types of cancer, we obtained data using the cBioPortal for Cancer Genomics (available at: www.cbioportal.org) [1, 2]. Figures 16 through 18 and Supplemental Figure 8 were downloaded and adapted from the portal.

Association of TRAF3, CYLD, and PIK3CA, Mutations with Smoking and HPV Integration

Contingency graphs representing the distribution of patients with HPV-positive HNSCC among smokers or nonsmokers (Fig. 18A) and among those with HPV-positive HNSCC with or without HPV integration (Fig. 18B, C), in the TRAF3/CYLD or PIK3CA wild-type and mutant groups were produced using GraphPad Prism 6 software, and *P* values were calculated using Fisher exact tests and chi-square tests. Patients' smoking status and the absence or presence of HPV integration (HPV and human breakpoints) for each TCGA sample were obtained from the Table S2 in reference [27].

Survival

Kaplan-Meier curves illustrating the overall survival of patients who had HPV-associated HNSCC with or without alterations in the TRAF3/CYLD or PIK3CA genes were produced using GraphPad Prism 6 software, and the log-rank (Mantel-Cox) test was used for statistical analyses. Overall patient survival data were obtained from the Table S2 in reference [27].

Gene Set Enrichment Analysis

The list of genes that had significantly different expression ($P < .05$) in HPV-positive TRAF3/CYLD or PIK3CA mutant and wild-type HNSCC was downloaded from the cBioPortal for Cancer Genomics [1, 2] Gene set enrichment analysis (GSEA) (Figs. 20 and 21; Supplemental Figure 10) was performed using software available from The Broad Institute (available at: http://software.broadinstitute.org/gsea/index.jsp) [210, 211].

Results and Discussion

One-third of HPV-positive head and neck tumors harbor TRAF3 or CYLD gene defects

One unexpected discovery from TCGA head and neck cancer project was the finding of deletions and/or mutations of TRAF3 in 25% of HPV-associated HNSCCs [5, 212]. The majority of TRAF3 alterations were homozygous gene deletions (55%), whereas the remainder were truncating mutations (45%), consistent with TRAF3 inactivation in these tumors (Fig. 16A, left). Notably, 2 mutations, namely, p.R310*/c.928C>T and p.R505*/c.1513C>T, have been reported previously in diffuse large-B cell (DLBC) lymphoma [213] and gastric adenocarcinoma, respectively (Fig. 1B). In contrast, alterations in the TRAF3 gene were infrequently detected (2%) in HPV-negative HNSCCs, and amplification and deletion/truncating mutations were equally represented, suggesting no functional requirement for TRAF3 activation or inhibition in HNSCCs lacking HPV (Fig. 16A, right). TRAF3 is an important component of both innate and acquired immune responses against many viruses [214], including Epstein-Barr virus (EBV) [215], human immunodeficiency virus [216], and HPV [217]. It is noteworthy that antiviral functions of TRAF3 are unique and cannot be substituted by other members of the TRAF family. Because the antiviral activity of TRAF3 requires a full-length, wild-type TRAF3 protein [218, 219], alterations in the TRAF3 gene observed in HPV-positive HNSCC most likely result in the loss of TRAF3 antiviral activity.

TRAF3 functions as a ubiquitin ligase to activate the type I IFN response while simultaneously inhibiting non-canonical and canonical NF-κB activation [53, 55, 218]. Type I IFN signaling is a potent and first-line cellular defense against viral infection, and

this response relies on pattern recognition receptors (PRRs) that also activate NF-κB signaling. Although NF-κB is required for constitutive IFN expression, it is not required for IFN expression late in viral infection, in which a major role for NF-κB is to promote cell survival [219-221].

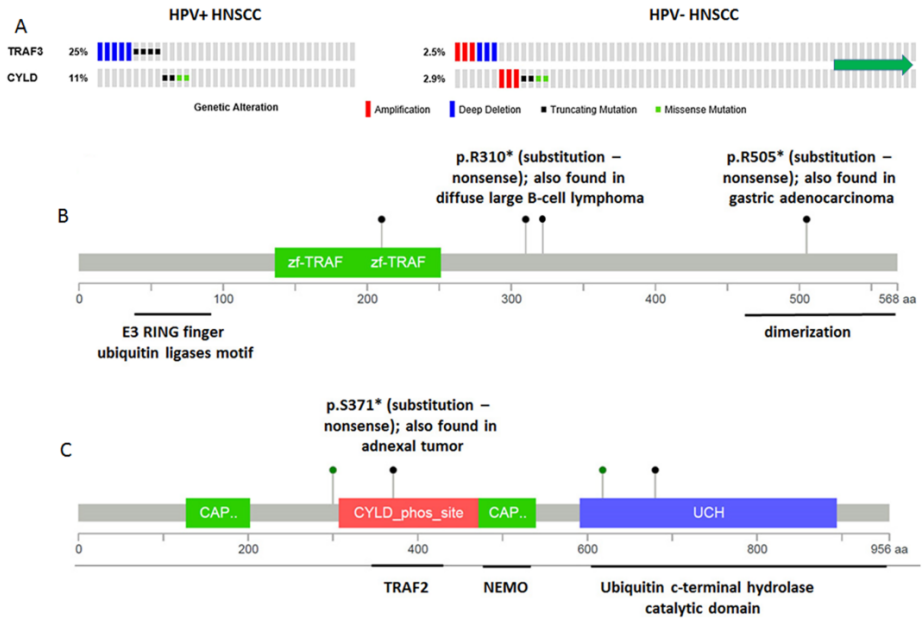

Figure 16: *Tumor necrosis factor receptor-associated factor 3 (TRAF3) or cylindromatosis lysine 63 deubiquitinase (CYLD) is mutated in 36% of human papillomavirus-positive HPV+HNSCCs.* (A) Genetic alterations in the TRAF3 and CYLD genes were identified in patients with HPV-positive (n = 36) and HPV-negative (n = 243) HNSCC. Columns represent individual tumors. The green arrow indicates that several tumors without alterations were omitted to fit the figure (A). Schematic representations of missense point (green) and truncating (black) mutations in the (B) TRAF3 and (C) CYLD genes identified in HPV-positive HNSCC. NEMO indicates NF-κB essential modulator; phos_site, phosphorylation site; UCH, ubiquitin C-terminal hydrolase; zf, zinc finger domain; CAP, cytoskeletal-associated protein domain. Adapted from the cBioPortal for Cancer Genomics

To determine whether additional genes regulating IFN and NF-κB responses were also altered in HPV-positive HNSCC, TCGA data were queried. These analyses revealed that the tumor suppressor CYLD, which inhibits NF-κB pathways at various steps, was mutated in 11% of HPV-positive HNSCCs (Fig. 16A, left). One-half of identified CYLD genetic variations were truncating mutations, whereas the other half included missense point mutations occurring within either its ubiquitin hydrolase catalytic domain or situated in close proximity to the TRAF2 binding site (Fig. 16C). The p.S371*/ c.1112C>A, nonsense substitution, has been described previously in adnexal skin tumors [222]. In addition, another amino acid 618 substitution in the CYLD gene, an aspartic acid-to-asparagine substitution at codon 618 (D618N) (identified in HPV-positive HNSCC) has been recently reported in cutaneous squamous cell carcinoma [223]. It is noteworthy that, the copy number status of mutated CYLD indicates a shallow loss (a possible heterozygous deletion) in all 4 CYLD-mutant samples (Table 1). Notably, CYLD mutations have been identified in another cohort of HPV-associated head and neck cancer [224]. As with TRAF3, few CYLD mutations occurred in HPV-negative HNSCCs from the TCGA cohort, and there was roughly equal representation of amplification and truncating/ missense mutations suggesting no striking functional consequences in HPV-negative tumors (Fig. 16A, right). It is also worth noting that TRAF3 mutations were not observed in CYLD-mutant tumors (Fig. 16A), revealing strong, mutual exclusivity (log odds ratio, < -3), although the difference was not statistically significant because of the relatively small number of events ($P = .29$). A tendency toward mutual exclusivity suggests that TRAF3 and CYLD mutations may be impacting the same downstream activities. Like TRAF3, CYLD inhibits NF-κB pathways

at various steps including, binding, deubiquitinating, and inhibiting the NF-κB essential modulator (NEMO). It was initially believed that CYLD inhibited IFN signaling by deubiquitinating the PRR, RIG-1, and downstream kinases TANK-binding kinase 1 (TBK-1) and inhibitor of NF-κB kinase E (IKKE) [225]; but, surprisingly, IFN response to vesicular stomatitis virus in CYLD knockout mice or cells from these mice was abrogated [226]. On the basis of these reports, TRAF3 and CYLD may serve similar functions after viral infection, namely, to inhibit NF-κB and activate IFN. These findings suggest that up to 36% of HPV-positive HNSCCs harboring defective TRAF3 or CYLD may rely on overactive NF-κB and defective innate immunity.

TRAF3 and CYLD genetic abnormalities are not frequent in HPV-positive uterine cervical cancer

The above data suggest that a portion of HPV-positive HNSCCs may rely on TRAF3 or CYLD mutations. Because high-risk HPV is the primary etiologic agent of uterine cervical cancer, sequencing data from these tumors was examined to determine whether they also contained TRAF3 or CYLD gene defects. Surprisingly, TRAF3 defects detected in uterine cervical cancer, which is associated with high-risk HPVs in about 93% of cases, were reminiscent of the pattern observed in HPV-negative HNSCCs. Uterine cervical cancers had infrequent TRAF3 alterations that included both amplifications and deletions (Fig. 17A). Alterations of the CYLD gene in uterine cervical cancer were even less frequent (2%), comprising 1 missense mutation and 2 deletions (Fig. 17A). Compared with HPV-positive HNSCC, in which TRAF3 and CYLD defects were

mutually exclusive, TRAF3 and CYLD defects overlapped in 2 of the 9 uterine cervical cancers that had alterations in either gene.

To extend these analyses, deep-sequencing data from multiple tumor types was queried for mutations in the TRAF3 and CYLD genes. Tumor types with > 10% alterations of TRAF/CYLD were: breast (data from xenografted tumors), neuroendocrine prostate cancer (NEPC), DLBC lymphoma, and lung squamous cell carcinoma. Breast cancer and NEPC contained only amplifications of TRAF3/CYLD, suggesting that, unlike HPV-positive HNSCC, TRAF and CYLD or some adjacent genes are activated in these tumor types. DLBC lymphoma and lung squamous cancer each had a significant proportion of total TRAF/CYLD alterations (mutations and deletions) and relatively few samples had amplification. It is noteworthy that, although lung squamous cancer is not connected to viral infection, DLBC lymphoma can be associated with EBV, suggesting that TRAF3/CYLD inactivation may be serving a similar role in DLBC lymphoma and HPV-positive HNSCC. A recent study of another EBV-associated cancer, nasopharyngeal carcinoma, identified numerous inactivating mutations in NF-κB–negative regulators, including CYLD, NF-κB inhibitor a (NFKBIA), and tumor necrosis factor a-induced protein 3 (TNFAIP3), in 17% of these tumors [227].

Across all solid tumor types, frequent inactivating TRAF3 and CYLD alterations, which are predicted to constitutively activate NF-κB pathways while inhibiting innate immunity, occur only in HPV-positive HNSCC. This is surprising, because such a high percentage of HPV-positive HNSCCs harbored defects in these genes (36%). It is particularly striking that HPV-associated uterine cervical cancer did not exhibit a similar

pattern of TRAF3/CYLD mutation, suggesting that HPV-driven carcinogenesis in the uterine cervix may be distinct from HPV-driven carcinogenesis in the head and neck.

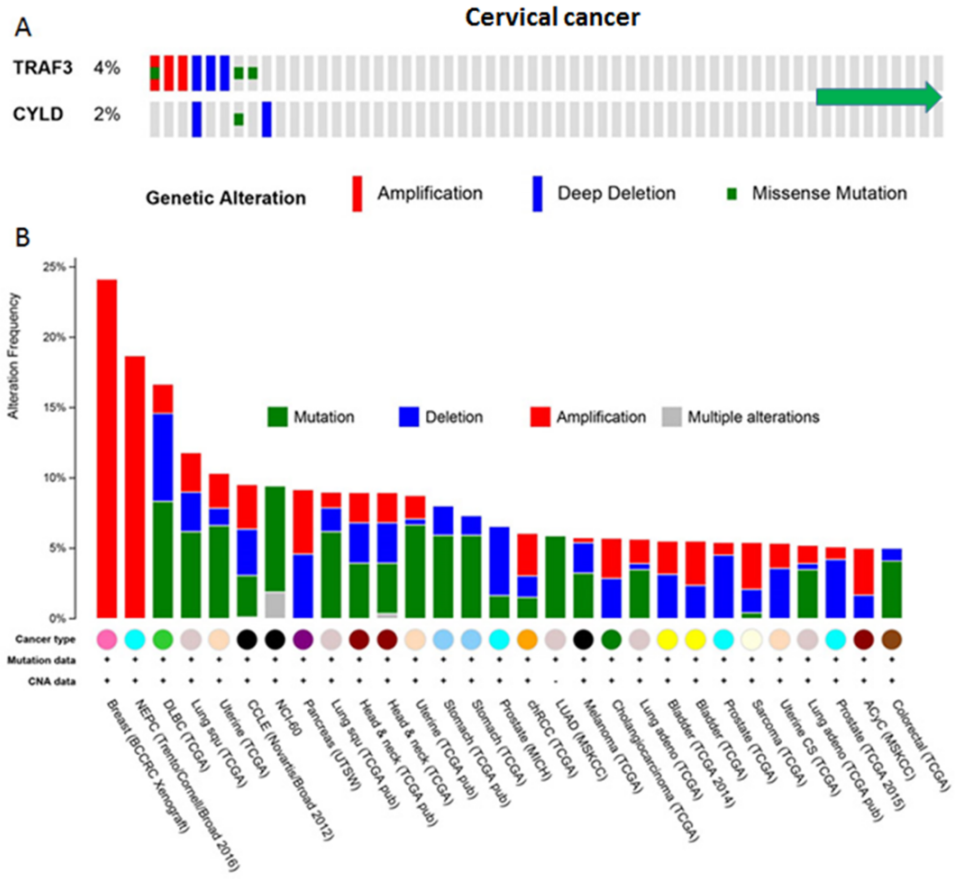

Figure 17: *Tumor necrosis factor receptor-associated factor 3 (TRAF3) or cylindromatosis lysine 63 deubiquitinase (CYLD) genetic abnormalities are not present in human papillomavirus (HPV)-positive uterine cervical cancer.* (A) Alterations in the TRAF3 and CYLD genes are illustrated in cervical cancer (n = 191). The green arrow indicates several tumors without alterations that were omitted to fit the figure. (B) Cross-cancer alterations are summarized for the TRAF3 and CYLD genes (combined) from 126 studies; studies that included < 5% alterations in genes were omitted to fit the figure. Adeno indicates adenocarcinoma; BCCRC, breast cancer patient xenografts; ACyC, adenoid cystic carcinoma; CCLE, Cancer Cell Line Encyclopedia; chRCC, chromophobe renal cell carcinoma; CNA, copy number alteration; CS, carcinosarcoma; DLBC, diffuse large B-cell lymphoma; LUAD, lung adenocarcinoma; MICH, University of Michigan; MSKCC, Memorial Sloan Kettering Cancer Center; NCI, National Cancer Institute; NEPC, neuroendocrine prostate cancer; TCGA, The Cancer Genome Atlas; squ, squamous; UTSW, University of Texas Southwestern Medical Center. Adapted from the cBioPortal for Cancer Genomics.

We and others previously reported that HPV-associated head and neck cancer more frequently, although not exclusively, contained alterations in the PIK3CA gene [145, 228]. In contrast to TRAF3/CYLD mutations, PIK3CA mutations or amplifications are commonly detected in cervical and head and neck cancers regardless of HPV status (Supp. Fig. 8A-C). It is noteworthy that, among 20 HPV+ head and neck tumors with alterations in PIK3CA gene, 4 samples harbored mutations in TRAF3/CYLD; whereas, among 16 tumors without PIK3CA mutations, 9 contained alterations in TRAF3/ CYLD, indicating a tendency toward mutual exclusivity (log odds ratio, -1.1; p = .25) (Supp. Fig. 8A).

TRAF3 and CYLD gene defects in HPV-positive HNSCC correlate with the absence of HPV integration and improved survival

In addition to high-risk HPV infection, several cofactors are associated with uterine cervical tumorigenesis, including alcohol consumption, coinfection with other infectious agents, and smoking [229-231]. In contrast, tobacco smoking is not etiologically implicated in HPV-positive head and neck cancer, but it is associated with decreased survival in patients who have HPV+ HNSCC [232, 233]. It is noteworthy that there were relatively high numbers of patients who had a history of smoking in the HPV-positive TCGA cohort [43]. Querying the TCGA cohort for TRAF3/CYLD mutations and smoking history revealed a correlation between the absence of smoking and

TRAF3/CYLD gene defects, but this association did not reach statistical significance (p = .064) (Fig. 18A).

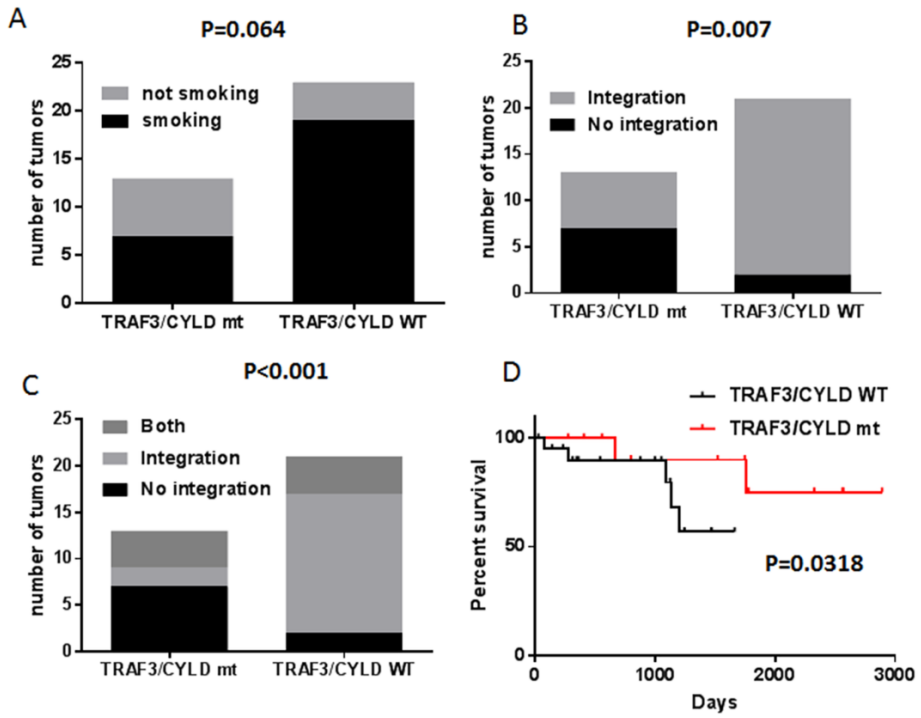

Figure 18: Tumor necrosis factor receptor-associated factor 3 (*TRAF3*) or cylindromatosis lysine 63 deubiquitinase (*CYLD*) mutations correlate with the absence of human papillomavirus (HPV) integration and improved survival in HPV-associated head and neck squamous cell carcinoma (HNSCC). Contingency graphs represent (A) the distribution of smokers or nonsmokers in the TRAF3/CYLD wild-type (WT) and mutant (mt) groups (the P value was calculated using a 2-sided Fisher exact test); (B) the distribution of tumors with or without HPV integration in the TRAF3/CYLD WT and mt groups (the P value was calculated using a 2-sided Fisher exact test); and (C) the distribution of tumors with episomal HPV only, with HPV integration only, or containing both integrated and episomal HPV DNA in the TRAF3/CYLD WT and mt groups (the P value was calculated using a 2-sided chi-square test). (D) Kaplan-Meier curves illustrate the overall survival of patients who had HPV-associated HNSCC with or without alterations in TRAF3/CYLD. Statistics were calculated using the log-rank (Mantel-Cox) test. Adapted from the cBioPortal for Cancer Genomics

Although both head and neck cancer and uterine cervical cancer are driven by high-risk HPV types, these tumor types have many differences, including gene and

protein expression profiles [234]. The classic cervical HPV tumorigenesis model is based on enhanced expression of the E6 and E7 oncogenes, which depends on HPV genome integration and loss of HPV E2 and other HPV genes [42]. In opposition to this classic HPV carcinogenesis model, HPV integration into the cellular genome was not identified in approximately 30% of HPV-positive HNSCCs [27]. The subset of HPV-positive HNSCCs that lacked integration had a distinct methylation profile as well as unambiguous differences in cellular and HPV gene expression compared with tumors that had integration. DNA methylation and somatic gene expression profiles of integration-positive tumors were analogous to those of HPV-negative HNSCCs and normal tissues, whereas tumors that lacked integration were different from the other groups [27]. The expression of HPV genes was also different between tumors with and without integration, because HPV integration-negative tumors had lower expression of the HPV E6 and E7 oncogenes and increased expression of HPV E2, E4, and E5 [27]. Expression of the early genes E2, E4, and E5 with lower expression of E6 and E7 is a pattern observed in the HPV lifecycle, in which HPV exists as an episome in basal, undifferentiated cells [235].

Although HPV uses defenses to dampen immune recognition and to suppress innate immunity in infected cells, episomal HPV activates innate immune responses [236-238]. To determine whether the maintenance of episomes in HPV-positive HNSCC was associated with inhibition of immune responses or NF-κB activation, HPV integration was associated with TRAF3/CYLD gene defects. The majority of TRAF3/CYLD mutant tumors (54%) had no HPV integration, whereas only 10% of TRAF3/CYLD wild-type samples lacked HPV integration (Fig. 18B). These data suggest that defects in TRAF3/ CYLD may not be required if tumors contain integrated HPV or,

alternatively, that the maintenance of episomal HPV pressures cells to mutate TRAF3/CYLD. To begin distinguishing these possibilities, cells with both episomal and integrated HPV would be ideal to correlate with TRAF3/CYLD defects. Although there are no direct sequencing data available that identify episomal and integrated forms in HPV-positive HNSCC, a subset of tumors with HPV DNA integrated into the human genome were identified as having somatic and HPV gene expression profiles reminiscent of tumors lacking integration. These data led our group and our collaborators in a previous publication to propose that a subset of HPV-positive HNSCC tumors contain both episomal and integrated HPV DNA [27]. The incorporation of tumors suspected to harbor both integrated and episomal forms of HPV into the TRAF3/CYLD mutation analyses revealed that 11 of 13 tumors (85%) with mutant TRAF3/CYLD contained episomal HPV, whereas 6 of 21 (29%) TRAF3/CYLD wild-type tumors harbored episomal HPV DNA (Fig. 18C). These data suggest that the presence of episomal HPV in HNSCC, regardless of the presence of integrated copies, may drive the dependence of these tumors on TRAF3 or CYLD gene defects. Mechanistically, mutations in TRAF3 or CYLD may create a cellular microenvironment needed to support the maintenance of the HPV episome. HPV episomal maintenance could then drive carcinogenesis as an alternative mechanism to classic HPV carcinogenesis, which depends on the HPV genome integration.

Studies from EBV-related cancers or hepatocellular carcinoma, along with HNSCC, suggest that PIK3CA mutations are common in virally associated cancers and may be mediated by viral infection. However, in contrast to TRAF3/CYLD mutants, altered PIK3CA did not significantly correlate with the presence or absence of HPV

integration sites (Supp. Fig. 9A-C), suggesting no requirement for PIK3CA activation in HPV episome maintenance.

Irrespective of HPV status, current therapy for advanced HNSCC includes concomitant radiation therapy (66-70 Gy) and chemotherapy as a radiation sensitizer. Although HPV-positive head and neck tumors respond better to conventional chemotherapy and radiotherapy than HPV-negative HNSCCs, patients are prone to short- and long-term deleterious side effects of this aggressive treatment. In addition, up to 25% of HPV-positive HNSCCs recur at regional or distant metastatic sites. To begin assessing the possible biologic or prognostic potential of TRAF3/CYLD genetic alterations in HPV-positive tumors, Kaplan-Meier survival analyses of 34 patients with HPV-positive HNSCC who had available survival data was performed based on the presence or absence of TRAF3 or CYLD mutations (Fig. 18D). Remarkably, TRAF3/CYLD alterations significantly correlated with improved overall survival. These data suggest that somatic defects in the CYLD or TRAF3 gene may be used to identify a subset of patients who have HPV-positive HNSCC with a significantly improved prognosis. In contrast, PIK3CA mutations did not influence the overall survival of patients in this cohort (Supp. Fig. 9D).

HPV+ HNSCC patients with tumors harboring TRAF3/CYLD mutations may also represent a subset of HPV+ HNSCC that may respond favorably to demethylation therapy, as described in Specific Aims 1 and 2. These tumors with episomal HPV express E6 and E7 at lower levels than other HPV+ HNSCC [27], and are thus likely more dependent on other HPV genes to retain the HPV genome in the episomal form. Both the downregulation of HPV genes (Figs. 10 and 15A) and the induction of APOBEC3B

expression (Fig. 7B), which is known to restrict HPV DNA [147], provide possible mechanisms through which these tumors may be more susceptible to demethylation therapy. This can be best tested by examining the sensitivity of early passage, primary HPV+ HNSCC cells harboring TRAF3/CYLD mutations to 5-aza, as knocking out TRAF3 or CYLD in HPV+ HNSCC cell lines may not induce the formation of episomal HPV DNA. This would provide additional utility in using TRAF3/CYLD mutational status as an important biomarker in head and neck cancer.

Mutations in TRAF3 or CYLD activate NF-κB Signaling in HPV-Positive HNSCC

Inactivating abnormalities in TRAF3 and CYLD lead to constitutive activation of both canonical and alternative NF-κB signaling, as reported in multiple myeloma [58, 59]. Because of its ability to induce expression of immune response genes, NF-κB signaling was initially viewed as a protector against viral infection; however, it became evident that viruses co-opt NF-κB activity to increase viral replication, elevate expression of viral genes, promote virion assembly, and block apoptosis in infected cells, allowing completion of the viral life cycle [239-241]. To assess whether the genetic alterations in TRAF3 and CYLD genes identified in HPV-positive HNSCC were associated with activation of NF-κB, we performed GSEA using 615 data sets focusing on transcription factor target genes and a list of genes with significantly different expression in TRAF3/CYLD-mutant compared versus wild-type tumors. Genes that were highly expressed in tumors with TRAF3/CYLD mutations were enriched for those that shared NF-κB or epidermal growth factor 1 (EGR-1) binding sites (Fig. 19A). Although the role

of EGR-1 in relation to NF-κB is not well defined, similar to NF-κB, it has been demonstrated that EGR-1 promotes cell survival and proliferation in B-cell lymphoma and prostate cancer cells [242]. Consistent with these data, previous gene expression analyses revealed that HPV-positive HNSCC with episomal HPV DNA had differential expression of genes involved in NF-κB signaling [27].

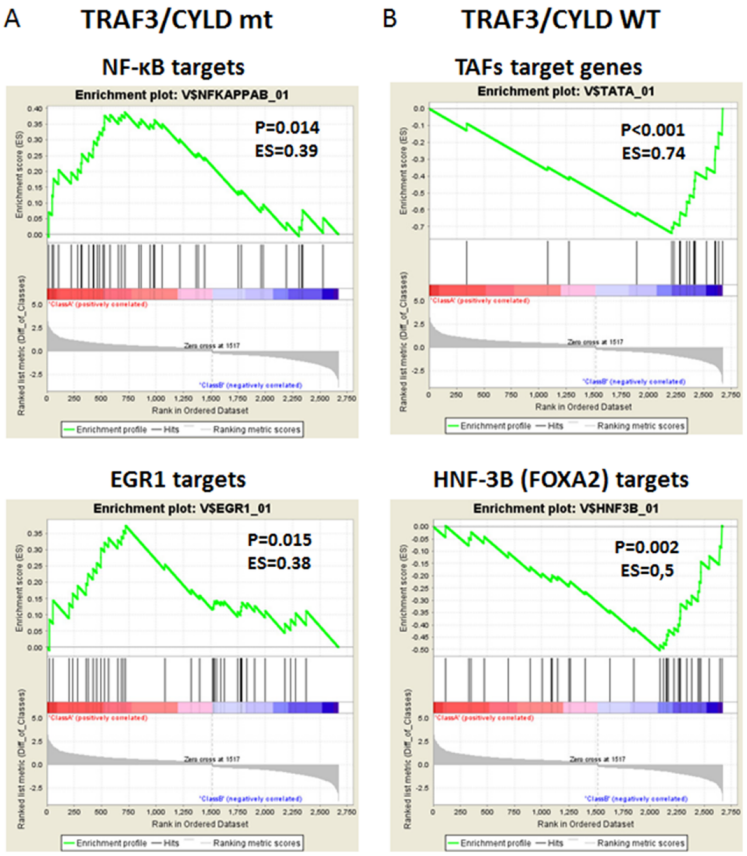

Figure 19: Mutations in tumor necrosis factor receptor-associated factor 3 (*TRAF3*) and cylindromatosis lysine 63 deubiquitinase (*CYLD*) are associated with activated nuclear factor κB (NF-κB) in human papillomavirus (HPV)-positive head and neck squamous cell carcinoma. The results from transcription factor target genes gene set enrichment analysis are illustrated for genes that had significantly different expression in (A) the *TRAF3*/*CYLD*-mutant (mt) group versus (B) the wild-type (WT) group. EGR1 indicates Early Growth Response 1; ES, enrichment score; TAF, TATA box binding protein associated factor; HNF-3B (FOXA2), hepatocyte nuclear factor 3β; hits, genes from the dataset; P, nominal *P* value.

In contrast to the TRAF3/CYLD-mutant group, genes commonly expressed in TRAF3/CYLD wild-type tumors encode for TATA-binding proteins or contain a forkhead box A2 (FOXA2) binding site in the promoter region (Fig. 19B), whereas genes that are highly expressed in tumors with altered PIK3CA are enriched for those that share androgen receptor or hypoxia-inducible factor 1a binding sites (Supp. Fig. 10A).

These data reveal that HPV-positive HNSCC with TRAF3 or CYLD gene defects have increased transcription of targets on the NF-κB pathway and are consistent with the known roles of TRAF3 and CYLD as negative regulators of NF-κB. Combined with data correlating the maintenance of episomal forms with TRAF3 and CYLD gene alterations, these data suggest that NF-κB activation may be required for episomal maintenance in HPV+ HNSCC.

Classification of Tumors Based on TRAF3/CYLD Mutation Status

The differences between the transcriptomes of HNSCC with mutant versus wild-type TRAF3/CYLD may lead to diverse clinical and biologic features, such as improved survival (Fig. 18D). To identify additional biologic functions or pathways associated with TRAF3/CYLD mutations, we ran GSEA using data sets of oncogenic and immunologic signatures as well as hallmark gene sets for differentially expressed genes. Remarkably, HPV-positive HNSCCs that harbored TRAF3 or CYLD defects expressed genes that were up-regulated in well versus poorly differentiated, HPV-negative HNSCC [243], whereas TRAF3/CYLD wild-type tumors were enriched in genes that were down-regulated in well differentiated, HPV-negative HNSCC (Fig. 20A, B). In addition,

TRAF3/CYLD-mutant tumors were characterized by up-regulation of a gene cluster associated with adhesion, motility, proliferation, and differentiation; whereas TRAF3/CYLD wild-type HNSCCs were linked to genes involved in the immune response and development (Fig. 20A, B) [243]. Confirming these observations, we observed a substantial correlation between genes expressed in the TRAF3/CYLD wild-type group with several data sets containing immune and inflammatory response genes. Conversely, mutant tumors were enriched in DNA replication genes [234, 244], in genes that distinguished HPV+ from HPV- HNSCC [234], and in genes that were up-regulated in nasopharyngeal carcinoma compared with normal tissue (Fig. 20C) [245]. Notably, the majority of TRAF3-mutant and CYLD-mutant tumors did not contain HPV integration (Fig. 3B), and tumors without integration had a gene expression profile different from that of HPV-negative HNSCC and normal tissue. Conversely, expression profiles of HPV integration-positive HNSCC were similar to HPV-negative HNSCC and normal samples [27]. In addition, genes expressed in nasopharyngeal carcinoma that were enriched in TRAF3-defective or CYLD-defective, HPV-positive HNSCC (Fig. 20C) had a high representation of DNA repair and replication genes [245].

Confirming our previous finding that mutant PIK3CA in HPV-positive tumors correlated with activation of the mechanistic target of rapamycin (mTOR) pathway, tumors with altered PIK3CA in the TCGA cohort overexpressed genes that were up-regulated by activation of the mTORC1 complex or during the unfolded protein response (Supp. Fig. 10B).

Many reports have highlighted differences between HPV-positive and HPV-negative HNSCC. The data presented here suggest that, within HPV-positive tumors,

there are 2 major subgroups that can be distinguished based on TRAF3 or CYLD mutations. Comparison of HPV-positive tumors with and without TRAF3 or CYLD mutations revealed that mutant tumors had improved survival and expressed genes that were enriched in HPV+ gene sets, suggesting that the tumors harboring TRAF3 or CYLD defects are the drivers of differences in gene expression between HPV-positive versus HPV-negative HNSCC and contribute significantly to the improved survival of patients with HPV-positive tumors. Our data also suggest that TRAF3 or CYLD mutations harbor episomal HPV and have activated NF-κB, which may be required for episomal maintenance.

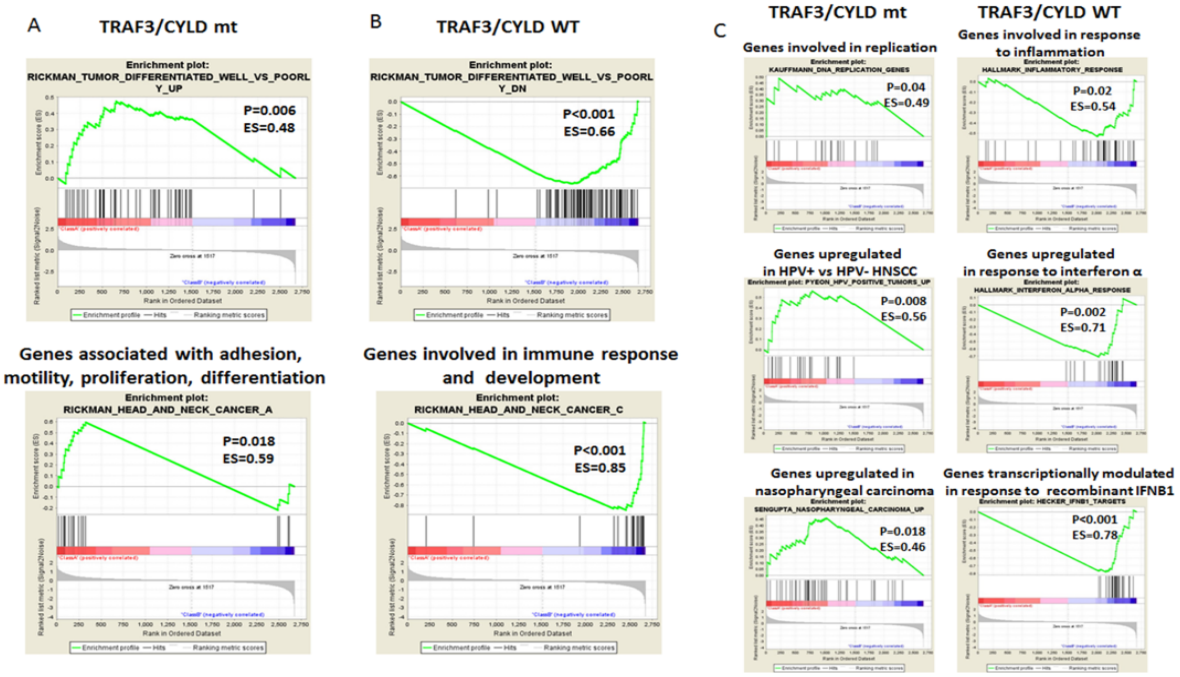

Figure 20: Classification of head and neck squamous cell carcinoma (HNSCC) based on tumor necrosis factor receptor-associated factor 3 (*TRAF3*) and cylindromatosis lysine 63 deubiquitinase (*CYLD*) mutation status is illustrated. Results are shown from gene set enrichment analysis using data sets of (A,B) oncogenic and (C) hallmark and immunologic signatures for genes had significantly different expression in the TRAF3/CYLD mutant (mt) group versus the wild-type (WT) group. ES indicates enrichment score; HPV−, human papillomavirus-negative; HPV+, human papillomavirus-positive; IFNB1, interferon β1; P, nominal *P* value.

The normal life cycle of HPV is linked to epithelial differentiation, with viral DNA maintained at a low copy number in basal cells, amplified and encapsidated only in more differentiated cells, and finally shed from the epithelial surface. It is noteworthy that the transcriptome of tumors with altered TRAF3/CYLD is highly enriched in genes that are overexpressed in well differentiated squamous cells (Fig. 20A). Because the majority of these tumors contained episomal HPV DNA (Fig. 18B, C), the data suggest that they may maintain replicating viral DNA and that differentiation signals may trigger encapsidation. Supporting our hypothesis, tumors with episomal HPV, regardless of the presence or absence of integration sites, overexpress the HPV E2, E4, and E5 genes [27], which control viral replication.

Treatment of cells with IFN causes resistance to radiation [246, 247], and an IFN-related DNA damage-resistance gene signature (IRDS) is associated with resistance to chemotherapy and radiation in various cancer cells and in patients with breast cancer [248, 249]. A significant feature of TRAF3/CYLD wild-type tumors was the expression of genes involved in the type I interferon and inflammatory response. We observed that patients who had wild-type TRAF3 and CYLD tumors had worse survival, which may implicate IFN signaling in therapeutic resistance (Fig. 18D).

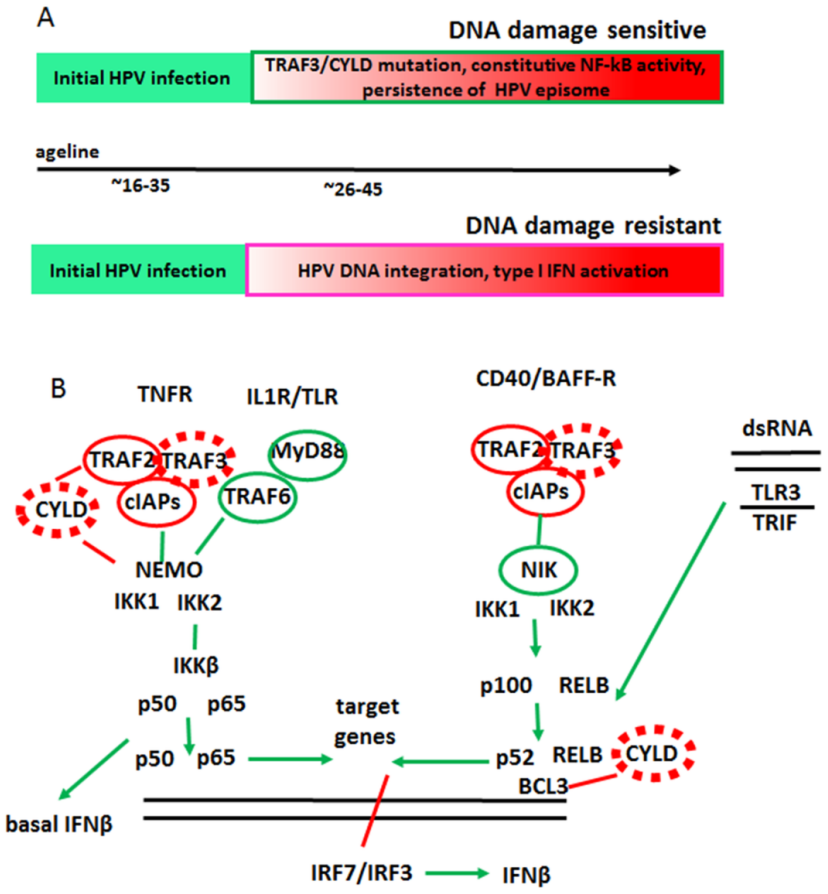

Figure 21: The etiology of HPV+ HNSCC is illustrated. (A) This is a model for the etiology of HPV+ HNSCC. (*Top*) After initial HPV infection, mutations in TRAF3 and CYLD, or in other genes, lead to constitutively active NF-κB, which supports persistence of the HPV episome; these tumors will be sensitive to DNA damage. (*Bottom*) Initial HPV infection activates type I interferon (IFN) signaling that selects for DNA damage-resistant tumors with HPV DNA integrated into the human genome. (B) This is a schematic model of (*left*) canonical and (*right*) noncanonical NF-κB pathways. Inactivating mutations in TRAF3/CYLD (dashed red ovals) identified in HPV-positive HNSCC result in the activation of both NF-κB pathways. Inactivating (solid red ovals) or activating (green ovals) mutations that activate NF-κB identified in other types of human cancer are shown. BAFF-R indicates B-cell activating factor receptor; BCL3, B-cell leukemia/lymphoma 3; CD40, cluster of differentiation 40 (costimulatory protein on antigen-presenting cells); cIAPs, cellular inhibitor of apoptosis proteins; dsRNA, double-stranded RNA; IKK, inhibitor of NF-κB kinase; IL1R, interleukin 1 receptor; MyD88, myeloid differentiation primary response 88; NEMO indicates NF-κB essential modulator; NIK, NF-κB B-inducing kinase; RELB, RELB proto-oncogene, NF-κB subunit; Toll-like receptor; TNFR, tumor necrosis factor receptor; TRIF, Toll/interleukin-1 receptor (TIR)-domain–containing adapter-inducing interferon β.

The major limitation of this study is the relatively small number of HPV-positive HNSCCs in the data set. Further profiling of HPV-associated head and neck samples is needed to confirm the significance of TRAF3/ CYLD mutations in HNSCC and to determine whether additional regulators of NF-κB, which is known to be mutated in human cancer (Fig. 21B), are genetically altered in HNSCC. Although additional data may improve biomarker selection for predicting prognosis, these studies suggest that TRAF3 and CYLD mutations are useful for selecting patients who have HPV-positive HNSCC with an improved outcome and suggest that these patients may be most appropriate for trials of therapeutic de-escalation. Targeted therapy, such as NF-κB inhibitors, may also be a rational option for preclinical studies. The unique characteristics of these TRAF3- and CYLD- mutant tumors, such as episomal HPV status and likely reliance on HPV genes other than E6 and E7, may also increase their susceptibility to demethylation therapy. Furthermore, integration negative HPV+ HNSCC tumors are associated with hypermethylated genomes [27], which would theoretically increase sensitivity to 5-aza through demethylation-induced double strand break formation, as modeled in Figure 8.

In summary, using TCGA data, we identified and characterized 2 groups of HPV-positive HNSCCs (Fig. 21A). These groups are distinguished by the presence or absence of TRAF3/CYLD mutations, which are associated with the presence of HPV episomes and a lack of HPV genome integration, respectively. Future studies are needed, but these data suggest that the activation of NF-κB signaling and the inhibition of innate immunity through TRAF3/ CYLD mutations may be required for episomal maintenance. The presence of HPV episomes is not well described in other HPV-associated cancers, and

uterine cervical cancers do not have frequent mutations in TRAF3 or CYLD. The co-occurrence of episomal HPV with TRAF3 or CYLD mutations suggests an alternative route of HPV carcinogenesis based on selection for HPV integration and high levels of HPV E6 and E7 expression (classic) or for TRAF3 or CYLD mutations with low HPV oncogene expression (alternative). The major difference between the classic and alternative HPV carcinogenesis pathways is how the innate immune reaction to episomal HPV is relieved. In the classic pathway, HPV integrates to avoid recognition by pattern recognition receptors; whereas, in the alternative pathway, episomal HPV can be recognized, but somatic mutations that block innate immune response while activating NF-κB to promote cell survival are selected. Significantly, HNSCC with defects in the TRAF3/ CYLD genes have a better prognosis compared with tumors that lack mutations (Fig. 18D). One of the major goals of head and neck oncology is personalization of treatment so that resistant tumors are aggressively treated and sensitive tumors can be less aggressively treated. Our data suggest that constitutively active NF-κB resulting from somatic mutations in TRAF3 or CYLD may serve as a biomarker to predict an improved prognosis for patients with HPV-positive head and neck cancer.

Summary and Conclusions

Current treatment paradigms for head and neck cancer are associated with major morbidity. Despite the growing evidence that HPV+ and HPV- head and neck cancer comprise two distinct diseases, guidelines state that the HPV status of a tumor should not affect treatment decisions. HPV+ HNSCC patients tend to be diagnosed younger and

have a significantly improved prognosis compared to HPV- patients; therefore, a major goal in the head and neck oncology community is to develop de-escalation therapy for HPV+ HNSCC. The demethylating drugs 5-aza and decitabine are FDA approved, used to treat AML and MDS, and have markedly improved side-effect profiles compared to current head and neck cancer treatments. Our data suggests that the unique epigenetic and gene expression profiles in HPV+ HNSCC renders these cancer cells exceptionally susceptible to demethylation therapy with 5-azacytidine. We found that 5-aza selectively induces widespread, pathologic DNA double strand break formation only in HPV+ HNSCC cells through a synthetic lethal-like mechanism. Furthermore, our data suggests that demethylation therapy reactivates p53, downregulates HPV genes, reduces the expression of matrix metalloproteinases, and reduces the metastatic potential of HPV+ HNSCC cells. We propose demethylation therapy as a novel, targeted approach to HPV+ HNSCC.

A key to implementing such treatments in HNSCC is to determine which patients will benefit from the therapeutic de-escalation. We have identified a previously unreported subset of HPV+ HNSCC marked by inactivating mutations in TRAF3 or CYLD. This subset of HPV+ HNSCC is associated with an improved prognosis and the viral genome existing in its episomal form. We suggest that mutations in these genes represents a patient cohort that may benefit from demethylation therapy as an alternative to current treatments.

References

1. Gao, J., et al., *Integrative analysis of complex cancer genomics and clinical profiles using the cBioPortal.* Sci Signal, 2013. **6**(269): p. pl1.
2. Cerami, E., et al., *The cBio cancer genomics portal: an open platform for exploring multidimensional cancer genomics data.* Cancer Discov, 2012. **2**(5): p. 401-4.
3. Kamangar, F., G.M. Dores, and W.F. Anderson, *Patterns of cancer incidence, mortality, and prevalence across five continents: defining priorities to reduce cancer disparities in different geographic regions of the world.* J Clin Oncol, 2006. **24**(14): p. 2137-50.
4. Fitzmaurice, C., et al., *Global, Regional, and National Cancer Incidence, Mortality, Years of Life Lost, Years Lived With Disability, and Disability-Adjusted Life-years for 32 Cancer Groups, 1990 to 2015: A Systematic Analysis for the Global Burden of Disease Study.* JAMA Oncol, 2016.
5. Miller, K.D., et al., *Cancer treatment and survivorship statistics, 2016.* CA Cancer J Clin, 2016.
6. Leemans, C.R., B.J. Braakhuis, and R.H. Brakenhoff, *The molecular biology of head and neck cancer.* Nat Rev Cancer, 2011. **11**(1): p. 9-22.
7. Brugere, J., et al., *Differential effects of tobacco and alcohol in cancer of the larynx, pharynx, and mouth.* Cancer, 1986. **57**(2): p. 391-5.
8. Rodriguez, T., et al., *Risk factors for oral and pharyngeal cancer in young adults.* Oral Oncol, 2004. **40**(2): p. 207-13.
9. Gillison, M.L., et al., *Evidence for a causal association between human papillomavirus and a subset of head and neck cancers.* J Natl Cancer Inst, 2000. **92**(9): p. 709-20.
10. Chaturvedi, A.K., et al., *Human papillomavirus and rising oropharyngeal cancer incidence in the United States.* J Clin Oncol, 2011. **29**(32): p. 4294-301.
11. Sturgis, E.M. and P.M. Cinciripini, *Trends in head and neck cancer incidence in relation to smoking prevalence: an emerging epidemic of human papillomavirus-associated cancers?* Cancer, 2007. **110**(7): p. 1429-35.
12. Viens, L.J., et al., *Human Papillomavirus-Associated Cancers - United States, 2008-2012.* MMWR Morb Mortal Wkly Rep, 2016. **65**(26): p. 661-6.
13. Gillison, M.L., *Current topics in the epidemiology of oral cavity and oropharyngeal cancers.* Head Neck, 2007. **29**(8): p. 779-92.
14. Goon, P.K., et al., *HPV & head and neck cancer: a descriptive update.* Head Neck Oncol, 2009. **1**: p. 36.
15. Hama, T., et al., *Prevalence of human papillomavirus in oropharyngeal cancer: a multicenter study in Japan.* Oncology, 2014. **87**(3): p. 173-82.
16. Goldenberg, D., et al., *Cystic lymph node metastasis in patients with head and neck cancer: An HPV-associated phenomenon.* Head Neck, 2008. **30**(7): p. 898-903.
17. Wagner, S., et al., *[HPV-associated head and neck cancer : mutational signature and genomic aberrations].* Hno, 2015. **63**(11): p. 758-67.
18. Fakhry, C., et al., *Improved survival of patients with human papillomavirus-positive head and neck squamous cell carcinoma in a prospective clinical trial.* J Natl Cancer Inst, 2008. **100**(4): p. 261-9.

19. Pfister, D.G., S. Spencer, and e. al., *(Version 1. 2017). NCCN Clinical Practice Guidelines in Oncology: Head and Neck Cancers.* 2017.
20. Gillison, M.L., et al., *Epidemiology of Human Papillomavirus-Positive Head and Neck Squamous Cell Carcinoma.* J Clin Oncol, 2015. **33**(29): p. 3235-42.
21. Gillison, M.L., et al., *Prevalence of oral HPV infection in the United States, 2009-2010.* Jama, 2012. **307**(7): p. 693-703.
22. Wyss, A., et al., *Cigarette, cigar, and pipe smoking and the risk of head and neck cancers: pooled analysis in the International Head and Neck Cancer Epidemiology Consortium.* Am J Epidemiol, 2013. **178**(5): p. 679-90.
23. Maier, H., et al., *Tobacco and alcohol and the risk of head and neck cancer.* Clin Investig, 1992. **70**(3-4): p. 320-7.
24. Burd, E.M., *Human papillomavirus and cervical cancer.* Clin Microbiol Rev, 2003. **16**(1): p. 1-17.
25. McMurray, H.R., et al., *Biology of human papillomaviruses.* Int J Exp Pathol, 2001. **82**(1): p. 15-33.
26. Munoz, N., et al., *Epidemiologic classification of human papillomavirus types associated with cervical cancer.* N Engl J Med, 2003. **348**(6): p. 518-27.
27. Parfenov, M., et al., *Characterization of HPV and host genome interactions in primary head and neck cancers.* Proc Natl Acad Sci U S A, 2014. **111**(43): p. 15544-9.
28. Graham, S.V., *Human papillomavirus: gene expression, regulation and prospects for novel diagnostic methods and antiviral therapies.* Future Microbiol, 2010. **5**(10): p. 1493-506.
29. zur Hausen, H., *Papillomaviruses and cancer: from basic studies to clinical application.* Nat Rev Cancer, 2002. **2**(5): p. 342-50.
30. Zheng, Z.M. and C.C. Baker, *Papillomavirus genome structure, expression, and post-transcriptional regulation.* Front Biosci, 2006. **11**: p. 2286-302.
31. Hoffman, W.H., et al., *Transcriptional repression of the anti-apoptotic survivin gene by wild type p53.* J Biol Chem, 2002. **277**(5): p. 3247-57.
32. Mihara, M., et al., *p53 has a direct apoptogenic role at the mitochondria.* Mol Cell, 2003. **11**(3): p. 577-90.
33. Bargonetti, J. and J.J. Manfredi, *Multiple roles of the tumor suppressor p53.* Curr Opin Oncol, 2002. **14**(1): p. 86-91.
34. el-Deiry, W.S., *Regulation of p53 downstream genes.* Semin Cancer Biol, 1998. **8**(5): p. 345-57.
35. Slebos, R.J., et al., *p53-dependent G1 arrest involves pRB-related proteins and is disrupted by the human papillomavirus 16 E7 oncoprotein.* Proc Natl Acad Sci U S A, 1994. **91**(12): p. 5320-4.
36. Cam, H. and B.D. Dynlacht, *Emerging roles for E2F: beyond the G1/S transition and DNA replication.* Cancer Cell, 2003. **3**(4): p. 311-6.
37. Moody, C.A. and L.A. Laimins, *Human papillomavirus oncoproteins: pathways to transformation.* Nat Rev Cancer, 2010. **10**(8): p. 550-60.
38. Snijders, P.J., et al., *HPV-mediated cervical carcinogenesis: concepts and clinical implications.* J Pathol, 2006. **208**(2): p. 152-64.

39. Egawa, N., et al., *Human Papillomaviruses; Epithelial Tropisms, and the Development of Neoplasia.* Viruses, 2015. **7**(7): p. 3863-90.
40. Wentzensen, N., S. Vinokurova, and M. von Knebel Doeberitz, *Systematic review of genomic integration sites of human papillomavirus genomes in epithelial dysplasia and invasive cancer of the female lower genital tract.* Cancer Res, 2004. **64**(11): p. 3878-84.
41. Luft, F., et al., *Detection of integrated papillomavirus sequences by ligation-mediated PCR (DIPS-PCR) and molecular characterization in cervical cancer cells.* Int J Cancer, 2001. **92**(1): p. 9-17.
42. Hudelist, G., et al., *Physical state and expression of HPV DNA in benign and dysplastic cervical tissue: different levels of viral integration are correlated with lesion grade.* Gynecol Oncol, 2004. **92**(3): p. 873-80.
43. *Comprehensive genomic characterization of head and neck squamous cell carcinomas.* Nature, 2015. **517**(7536): p. 576-82.
44. Gubanova, E., et al., *Downregulation of SMG-1 in HPV-positive head and neck squamous cell carcinoma due to promoter hypermethylation correlates with improved survival.* Clin Cancer Res, 2012. **18**(5): p. 1257-67.
45. Slebos, R.J., et al., *Gene expression differences associated with human papillomavirus status in head and neck squamous cell carcinoma.* Clin Cancer Res, 2006. **12**(3 Pt 1): p. 701-9.
46. Henderson, S., et al., *APOBEC-mediated cytosine deamination links PIK3CA helical domain mutations to human papillomavirus-driven tumor development.* Cell Rep, 2014. **7**(6): p. 1833-41.
47. Agrawal, N., et al., *Exome sequencing of head and neck squamous cell carcinoma reveals inactivating mutations in NOTCH1.* Science, 2011. **333**(6046): p. 1154-7.
48. Stransky, N., et al., *The mutational landscape of head and neck squamous cell carcinoma.* Science, 2011. **333**(6046): p. 1157-60.
49. Burns, M.B., et al., *APOBEC3B is an enzymatic source of mutation in breast cancer.* Nature, 2013. **494**(7437): p. 366-70.
50. Vieira, V.C. and M.A. Soares, *The role of cytidine deaminases on innate immune responses against human viral infections.* Biomed Res Int, 2013. **2013**: p. 683095.
51. Roberts, S.A., et al., *An APOBEC cytidine deaminase mutagenesis pattern is widespread in human cancers.* Nat Genet, 2013. **45**(9): p. 970-6.
52. Chiu, Y.L. and W.C. Greene, *The APOBEC3 cytidine deaminases: an innate defensive network opposing exogenous retroviruses and endogenous retroelements.* Annu Rev Immunol, 2008. **26**: p. 317-53.
53. Hacker, H., P.H. Tseng, and M. Karin, *Expanding TRAF function: TRAF3 as a tri-faced immune regulator.* Nat Rev Immunol, 2011. **11**(7): p. 457-68.
54. Ghosh, S. and M. Karin, *Missing pieces in the NF-kappaB puzzle.* Cell, 2002. **109 Suppl**: p. S81-96.
55. Hoebe, K. and B. Beutler, *TRAF3: a new component of the TLR-signaling apparatus.* Trends Mol Med, 2006. **12**(5): p. 187-9.
56. Harhaj, E.W. and V.M. Dixit, *Regulation of NF-kappaB by deubiquitinases.* Immunol Rev, 2012. **246**(1): p. 107-24.

57. Hajek, M., et al., *TRAF3/CYLD mutations identify a distinct subset of human papilloma virus-associated head and neck squamous cell carcinoma.* Cancer, 2017.
58. Annunziata, C.M., et al., *Frequent engagement of the classical and alternative NF-kappaB pathways by diverse genetic abnormalities in multiple myeloma.* Cancer Cell, 2007. **12**(2): p. 115-30.
59. Keats, J.J., et al., *Promiscuous mutations activate the noncanonical NF-kappaB pathway in multiple myeloma.* Cancer Cell, 2007. **12**(2): p. 131-44.
60. Berger, S.L., et al., *An operational definition of epigenetics.* Genes Dev, 2009. **23**(7): p. 781-3.
61. Sharp, A.J., et al., *DNA methylation profiles of human active and inactive X chromosomes.* Genome Res, 2011. **21**(10): p. 1592-600.
62. Dillon, N., *Gene regulation and large-scale chromatin organization in the nucleus.* Chromosome Res, 2006. **14**(1): p. 117-26.
63. Illingworth, R., et al., *A novel CpG island set identifies tissue-specific methylation at developmental gene loci.* PLoS Biol, 2008. **6**(1): p. e22.
64. Leenen, F.A., C.P. Muller, and J.D. Turner, *DNA methylation: conducting the orchestra from exposure to phenotype?* Clin Epigenetics, 2016. **8**: p. 92.
65. Jones, P.A., *Functions of DNA methylation: islands, start sites, gene bodies and beyond.* Nat Rev Genet, 2012. **13**(7): p. 484-92.
66. Smith, I.M., et al., *DNA global hypomethylation in squamous cell head and neck cancer associated with smoking, alcohol consumption and stage.* Int J Cancer, 2007. **121**(8): p. 1724-8.
67. Richards, K.L., et al., *Genome-wide hypomethylation in head and neck cancer is more pronounced in HPV-negative tumors and is associated with genomic instability.* PLoS One, 2009. **4**(3): p. e4941.
68. Lleras, R.A., et al., *Unique DNA methylation loci distinguish anatomic site and HPV status in head and neck squamous cell carcinoma.* Clin Cancer Res, 2013. **19**(19): p. 5444-55.
69. Lechner, M., et al., *Identification and functional validation of HPV-mediated hypermethylation in head and neck squamous cell carcinoma.* Genome Med, 2013. **5**(2): p. 15.
70. Zhang, H.Z., et al., *Characterization of gene methylation in human papillomavirus associated-head and neck squamous cell carcinoma.* Genet Mol Res, 2016. **15**(3).
71. Hernandez, J.M., et al., *DNA methylation profiling across the spectrum of HPV-associated anal squamous neoplasia.* PLoS One, 2012. **7**(11): p. e50533.
72. Kim, K., et al., *Methylation patterns of papillomavirus DNA, its influence on E2 function, and implications in viral infection.* J Virol, 2003. **77**(23): p. 12450-9.
73. Marsit, C.J., et al., *Hypermethylation of E-cadherin is an independent predictor of improved survival in head and neck squamous cell carcinoma.* Cancer, 2008. **113**(7): p. 1566-71.
74. Melchers, L.J., et al., *Identification of methylation markers for the prediction of nodal metastasis in oral and oropharyngeal squamous cell carcinoma.* Epigenetics, 2015. **10**(9): p. 850-60.
75. Virmani, A.K., et al., *Aberrant methylation during cervical carcinogenesis.* Clin Cancer Res, 2001. **7**(3): p. 584-9.

76. Cicchini, L., et al., *Suppression of Antitumor Immune Responses by Human Papillomavirus through Epigenetic Downregulation of CXCL14.* MBio, 2016. **7**(3).
77. Keating, G.M., *Azacitidine: a review of its use in higher-risk myelodysplastic syndromes/acute myeloid leukaemia.* Drugs, 2009. **69**(17): p. 2501-18.
78. Estey, E.H., *Epigenetics in clinical practice: the examples of azacitidine and decitabine in myelodysplasia and acute myeloid leukemia.* Leukemia, 2013. **27**(9): p. 1803-12.
79. Issa, J.P. and H.M. Kantarjian, *Targeting DNA methylation.* Clin Cancer Res, 2009. **15**(12): p. 3938-46.
80. Navada, S.C., et al., *Clinical development of demethylating agents in hematology.* J Clin Invest, 2014. **124**(1): p. 40-6.
81. Li, L.H., et al., *Cytotoxicity and mode of action of 5-azacytidine on L1210 leukemia.* Cancer Res, 1970. **30**(11): p. 2760-9.
82. Stresemann, C. and F. Lyko, *Modes of action of the DNA methyltransferase inhibitors azacytidine and decitabine.* Int J Cancer, 2008. **123**(1): p. 8-13.
83. Aimiuwu, J., et al., *RNA-dependent inhibition of ribonucleotide reductase is a major pathway for 5-azacytidine activity in acute myeloid leukemia.* Blood, 2012. **119**(22): p. 5229-38.
84. Chiappinelli, K.B., et al., *Inhibiting DNA Methylation Causes an Interferon Response in Cancer via dsRNA Including Endogenous Retroviruses.* Cell, 2015. **162**(5): p. 974-86.
85. Orta, M.L., et al., *5-Aza-2'-deoxycytidine causes replication lesions that require Fanconi anemia-dependent homologous recombination for repair.* Nucleic Acids Res, 2013. **41**(11): p. 5827-36.
86. Palii, S.S., et al., *DNA methylation inhibitor 5-Aza-2'-deoxycytidine induces reversible genome-wide DNA damage that is distinctly influenced by DNA methyltransferases 1 and 3B.* Mol Cell Biol, 2008. **28**(2): p. 752-71.
87. Schneider-Stock, R., et al., *5-Aza-cytidine is a potent inhibitor of DNA methyltransferase 3a and induces apoptosis in HCT-116 colon cancer cells via Gadd45- and p53-dependent mechanisms.* J Pharmacol Exp Ther, 2005. **312**(2): p. 525-36.
88. Nie, J., et al., *Decitabine, a new star in epigenetic therapy: the clinical application and biological mechanism in solid tumors.* Cancer Lett, 2014. **354**(1): p. 12-20.
89. Abraham, R.T., *Cell cycle checkpoint signaling through the ATM and ATR kinases.* Genes Dev, 2001. **15**(17): p. 2177-96.
90. Hakem, R., *DNA-damage repair; the good, the bad, and the ugly.* EMBO J, 2008. **27**(4): p. 589-605.
91. Denning, G., et al., *Cloning of a novel phosphatidylinositol kinase-related kinase: characterization of the human SMG-1 RNA surveillance protein.* J Biol Chem, 2001. **276**(25): p. 22709-14.
92. Brumbaugh, K.M., et al., *The mRNA surveillance protein hSMG-1 functions in genotoxic stress response pathways in mammalian cells.* Mol Cell, 2004. **14**(5): p. 585-98.
93. Abraham, R.T., *PI 3-kinase related kinases: 'big' players in stress-induced signaling pathways.* DNA Repair (Amst), 2004. **3**(8-9): p. 883-7.
94. Abraham, R.T., *The ATM-related kinase, hSMG-1, bridges genome and RNA surveillance pathways.* DNA Repair (Amst), 2004. **3**(8-9): p. 919-25.

95. Gubanova, E., et al., *SMG-1 suppresses CDK2 and tumor growth by regulating both the p53 and Cdc25A signaling pathways.* Cell Cycle, 2013. **12**(24): p. 3770-80.
96. Pierce, A.J., et al., *Double-strand breaks and tumorigenesis.* Trends Cell Biol, 2001. **11**(11): p. S52-9.
97. Thompson, L.H. and D. Schild, *Homologous recombinational repair of DNA ensures mammalian chromosome stability.* Mutat Res, 2001. **477**(1-2): p. 131-53.
98. Ferguson, D.O. and F.W. Alt, *DNA double strand break repair and chromosomal translocation: lessons from animal models.* Oncogene, 2001. **20**(40): p. 5572-9.
99. Aguilera, A., *Double-strand break repair: are Rad51/RecA--DNA joints barriers to DNA replication?* Trends Genet, 2001. **17**(6): p. 318-21.
100. West, S.C., *Molecular views of recombination proteins and their control.* Nat Rev Mol Cell Biol, 2003. **4**(6): p. 435-45.
101. West, S.C., *Cross-links between Fanconi anaemia and BRCA2.* DNA Repair (Amst), 2003. **2**(2): p. 231-4.
102. Petermann, E. and T. Helleday, *Pathways of mammalian replication fork restart.* Nat Rev Mol Cell Biol, 2010. **11**(10): p. 683-7.
103. Gary, C., et al., *Selective antitumor activity of roscovitine in head and neck cancer.* Oncotarget, 2016. **7**(25): p. 38598-38611.
104. Dok, R., et al., *p16INK4a impairs homologous recombination-mediated DNA repair in human papillomavirus-positive head and neck tumors.* Cancer Res, 2014. **74**(6): p. 1739-51.
105. Kraakman-van der Zwet, M., et al., *Brca2 (XRCC11) deficiency results in radioresistant DNA synthesis and a higher frequency of spontaneous deletions.* Mol Cell Biol, 2002. **22**(2): p. 669-79.
106. Issaeva, N., et al., *6-thioguanine selectively kills BRCA2-defective tumors and overcomes PARP inhibitor resistance.* Cancer Res, 2010. **70**(15): p. 6268-76.
107. Weaver, A.N., et al., *DNA double strand break repair defect and sensitivity to poly ADP-ribose polymerase (PARP) inhibition in human papillomavirus 16-positive head and neck squamous cell carcinoma.* Oncotarget, 2015. **6**(29): p. 26995-7007.
108. Lobrich, M., et al., *gammaH2AX foci analysis for monitoring DNA double-strand break repair: strengths, limitations and optimization.* Cell Cycle, 2010. **9**(4): p. 662-9.
109. Kuo, H.K., J.D. Griffith, and K.N. Kreuzer, *5-Azacytidine induced methyltransferase-DNA adducts block DNA replication in vivo.* Cancer Res, 2007. **67**(17): p. 8248-54.
110. Jiang, Y., et al., *Aberrant DNA methylation is a dominant mechanism in MDS progression to AML.* Blood, 2009. **113**(6): p. 1315-25.
111. Daskalakis, M., et al., *Demethylation of a hypermethylated P15/INK4B gene in patients with myelodysplastic syndrome by 5-Aza-2'-deoxycytidine (decitabine) treatment.* Blood, 2002. **100**(8): p. 2957-64.
112. Sugimura, K., et al., *Cell cycle-dependent accumulation of histone H3.3 and euchromatic histone modifications in pericentromeric heterochromatin in response to a decrease in DNA methylation levels.* Exp Cell Res, 2010. **316**(17): p. 2731-46.
113. Mehta, A. and J.E. Haber, *Sources of DNA double-strand breaks and models of recombinational DNA repair.* Cold Spring Harb Perspect Biol, 2014. **6**(9): p. a016428.

114. Tobey, R.A., et al., *Life cycle analysis of mammalian cells. 3. The inhibition of division in Chinese hamster cells by puromycin and actinomycin.* Biophys J, 1966. **6**(5): p. 567-81.
115. Vispe, S., et al., *Triptolide is an inhibitor of RNA polymerase I and II-dependent transcription leading predominantly to down-regulation of short-lived mRNA.* Mol Cancer Ther, 2009. **8**(10): p. 2780-90.
116. Koba, M. and J. Konopa, *[Actinomycin D and its mechanisms of action].* Postepy Hig Med Dosw (Online), 2005. **59**: p. 290-8.
117. Zandomeni, R., et al., *Mechanism of action of dichloro-beta-D-ribofuranosylbenzimidazole: effect on in vitro transcription.* Proc Natl Acad Sci U S A, 1982. **79**(10): p. 3167-70.
118. Ross, W.E. and M.O. Bradley, *DNA double-stranded breaks in mammalian cells after exposure to intercalating agents.* Biochim Biophys Acta, 1981. **654**(1): p. 129-34.
119. Prado, F. and A. Aguilera, *Impairment of replication fork progression mediates RNA polII transcription-associated recombination.* Embo j, 2005. **24**(6): p. 1267-76.
120. Tuduri, S., et al., *Topoisomerase I suppresses genomic instability by preventing interference between replication and transcription.* Nat Cell Biol, 2009. **11**(11): p. 1315-24.
121. Gottipati, P., et al., *Transcription-associated recombination is dependent on replication in Mammalian cells.* Mol Cell Biol, 2008. **28**(1): p. 154-64.
122. Helmrich, A., et al., *Transcription-replication encounters, consequences and genomic instability.* Nat Struct Mol Biol, 2013. **20**(4): p. 412-8.
123. Petermann, E., et al., *Hydroxyurea-stalled replication forks become progressively inactivated and require two different RAD51-mediated pathways for restart and repair.* Mol Cell, 2010. **37**(4): p. 492-502.
124. Bartek, J., C. Lukas, and J. Lukas, *Checking on DNA damage in S phase.* Nat Rev Mol Cell Biol, 2004. **5**(10): p. 792-804.
125. Zeman, M.K. and K.A. Cimprich, *Causes and consequences of replication stress.* Nat Cell Biol, 2014. **16**(1): p. 2-9.
126. Ide, H., et al., *Formation, Repair, and Biological Effects of DNA-Protein Cross-Link Damage, Advances in DNA Repair, Prof. Clark Chen (Ed.).* Intech, 2015.
127. Gowher, H. and A. Jeltsch, *Mechanism of inhibition of DNA methyltransferases by cytidine analogs in cancer therapy.* Cancer Biol Ther, 2004. **3**(11): p. 1062-8.
128. Kiianitsa, K. and N. Maizels, *A rapid and sensitive assay for DNA-protein covalent complexes in living cells.* Nucleic Acids Res, 2013. **41**(9): p. e104.
129. Nakano, T., et al., *Homologous recombination but not nucleotide excision repair plays a pivotal role in tolerance of DNA-protein cross-links in mammalian cells.* J Biol Chem, 2009. **284**(40): p. 27065-76.
130. Hartsuiker, E., M.J. Neale, and A.M. Carr, *Distinct requirements for the Rad32(Mre11) nuclease and Ctp1(CtIP) in the removal of covalently bound topoisomerase I and II from DNA.* Mol Cell, 2009. **33**(1): p. 117-23.
131. Dupre, A., et al., *A forward chemical genetic screen reveals an inhibitor of the Mre11-Rad50-Nbs1 complex.* Nat Chem Biol, 2008. **4**(2): p. 119-25.
132. Lopez-Contreras, A.J. and O. Fernandez-Capetillo, *The ATR barrier to replication-born DNA damage.* DNA Repair (Amst), 2010. **9**(12): p. 1249-55.

133. Sorensen, C.S. and R.G. Syljuasen, *Safeguarding genome integrity: the checkpoint kinases ATR, CHK1 and WEE1 restrain CDK activity during normal DNA replication.* Nucleic Acids Res, 2012. **40**(2): p. 477-86.
134. Ward, I.M. and J. Chen, *Histone H2AX is phosphorylated in an ATR-dependent manner in response to replicational stress.* J Biol Chem, 2001. **276**(51): p. 47759-62.
135. Zou, L. and S.J. Elledge, *Sensing DNA damage through ATRIP recognition of RPA-ssDNA complexes.* Science, 2003. **300**(5625): p. 1542-8.
136. Sirbu, B.M., et al., *Analysis of protein dynamics at active, stalled, and collapsed replication forks.* Genes Dev, 2011. **25**(12): p. 1320-7.
137. Bermejo, R., M.S. Lai, and M. Foiani, *Preventing replication stress to maintain genome stability: resolving conflicts between replication and transcription.* Mol Cell, 2012. **45**(6): p. 710-8.
138. Durkin, S.G. and T.W. Glover, *Chromosome fragile sites.* Annu Rev Genet, 2007. **41**: p. 169-92.
139. Casper, A.M., et al., *ATR regulates fragile site stability.* Cell, 2002. **111**(6): p. 779-89.
140. Vendetti, F.P., et al., *The orally active and bioavailable ATR kinase inhibitor AZD6738 potentiates the anti-tumor effects of cisplatin to resolve ATM-deficient non-small cell lung cancer in vivo.* Oncotarget, 2015. **6**(42): p. 44289-305.
141. Ying, S., F.C. Hamdy, and T. Helleday, *Mre11-dependent degradation of stalled DNA replication forks is prevented by BRCA2 and PARP1.* Cancer Res, 2012. **72**(11): p. 2814-21.
142. Satoh, M.S. and T. Lindahl, *Role of poly(ADP-ribose) formation in DNA repair.* Nature, 1992. **356**(6367): p. 356-8.
143. Berti, M., et al., *Human RECQ1 promotes restart of replication forks reversed by DNA topoisomerase I inhibition.* Nat Struct Mol Biol, 2013. **20**(3): p. 347-54.
144. Zellweger, R., et al., *Rad51-mediated replication fork reversal is a global response to genotoxic treatments in human cells.* J Cell Biol, 2015. **208**(5): p. 563-79.
145. Sewell, A., et al., *Reverse-phase protein array profiling of oropharyngeal cancer and significance of PIK3CA mutations in HPV-associated head and neck cancer.* Clin Cancer Res, 2014. **20**(9): p. 2300-11.
146. Vartanian, J.P., et al., *Evidence for editing of human papillomavirus DNA by APOBEC3 in benign and precancerous lesions.* Science, 2008. **320**(5873): p. 230-3.
147. Warren, C.J. and D. Pyeon, *APOBEC3 in papillomavirus restriction, evolution and cancer progression.* Oncotarget, 2015. **6**(37): p. 39385-6.
148. Alexandrov, L.B., et al., *Signatures of mutational processes in human cancer.* Nature, 2013. **500**(7463): p. 415-21.
149. Landry, S., et al., *APOBEC3A can activate the DNA damage response and cause cell-cycle arrest.* EMBO Rep, 2011. **12**(5): p. 444-50.
150. Suspene, R., et al., *Somatic hypermutation of human mitochondrial and nuclear DNA by APOBEC3 cytidine deaminases, a pathway for DNA catabolism.* Proc Natl Acad Sci U S A, 2011. **108**(12): p. 4858-63.
151. Nowarski, R. and M. Kotler, *APOBEC3 cytidine deaminases in double-strand DNA break repair and cancer promotion.* Cancer Res, 2013. **73**(12): p. 3494-8.

152. Park, C., W. Qian, and J. Zhang, *Genomic evidence for elevated mutation rates in highly expressed genes.* EMBO Rep, 2012. **13**(12): p. 1123-9.
153. Mugal, C.F., H.H. von Grunberg, and M. Peifer, *Transcription-induced mutational strand bias and its effect on substitution rates in human genes.* Mol Biol Evol, 2009. **26**(1): p. 131-42.
154. D'Alessandro, G. and F. d'Adda di Fagagna, *Transcription and DNA Damage: Holding Hands or Crossing Swords?* J Mol Biol, 2016.
155. Duch, A., E. de Nadal, and F. Posas, *Dealing with transcriptional outbursts during S phase to protect genomic integrity.* J Mol Biol, 2013. **425**(23): p. 4745-55.
156. Aguilera, A. and H. Gaillard, *Transcription and recombination: when RNA meets DNA.* Cold Spring Harb Perspect Biol, 2014. **6**(8).
157. Huertas, P. and A. Aguilera, *Cotranscriptionally formed DNA:RNA hybrids mediate transcription elongation impairment and transcription-associated recombination.* Mol Cell, 2003. **12**(3): p. 711-21.
158. Skourti-Stathaki, K. and N.J. Proudfoot, *A double-edged sword: R loops as threats to genome integrity and powerful regulators of gene expression.* Genes Dev, 2014. **28**(13): p. 1384-96.
159. Kumar, A., et al., *ATR mediates a checkpoint at the nuclear envelope in response to mechanical stress.* Cell, 2014. **158**(3): p. 633-46.
160. Bermejo, R., et al., *The replication checkpoint protects fork stability by releasing transcribed genes from nuclear pores.* Cell, 2011. **146**(2): p. 233-46.
161. Chanoux, R.A., et al., *ATR and H2AX cooperate in maintaining genome stability under replication stress.* J Biol Chem, 2009. **284**(9): p. 5994-6003.
162. Milligan, J.R., et al., *DNA repair by thiols in air shows two radicals make a double-strand break.* Radiat Res, 1995. **143**(3): p. 273-80.
163. Puigvert, J.C., K. Sanjiv, and T. Helleday, *Targeting DNA repair, DNA metabolism and replication stress as anti-cancer strategies.* Febs j, 2016. **283**(2): p. 232-45.
164. Groth, P., et al., *Homologous recombination repairs secondary replication induced DNA double-strand breaks after ionizing radiation.* Nucleic Acids Res, 2012. **40**(14): p. 6585-94.
165. Helleday, T., *Cancer phenotypic lethality, exemplified by the non-essential MTH1 enzyme being required for cancer survival.* Ann Oncol, 2014. **25**(7): p. 1253-5.
166. Arnaudeau, C., C. Lundin, and T. Helleday, *DNA double-strand breaks associated with replication forks are predominantly repaired by homologous recombination involving an exchange mechanism in mammalian cells.* J Mol Biol, 2001. **307**(5): p. 1235-45.
167. Saleh-Gohari, N., et al., *Spontaneous homologous recombination is induced by collapsed replication forks that are caused by endogenous DNA single-strand breaks.* Mol Cell Biol, 2005. **25**(16): p. 7158-69.
168. Hartwell, L.H., et al., *Integrating genetic approaches into the discovery of anticancer drugs.* Science, 1997. **278**(5340): p. 1064-8.
169. Helleday, T., *The underlying mechanism for the PARP and BRCA synthetic lethality: clearing up the misunderstandings.* Mol Oncol, 2011. **5**(4): p. 387-93.
170. Vieira, V.C., et al., *Human papillomavirus E6 triggers upregulation of the antiviral and cancer genomic DNA deaminase APOBEC3B.* MBio, 2014. **5**(6).

171. Kavli, B., et al., *Uracil in DNA--general mutagen, but normal intermediate in acquired immunity.* DNA Repair (Amst), 2007. **6**(4): p. 505-16.
172. Nowosielska, A. and M.G. Marinus, *DNA mismatch repair-induced double-strand breaks.* DNA Repair (Amst), 2008. **7**(1): p. 48-56.
173. Cortazar, D., et al., *The enigmatic thymine DNA glycosylase.* DNA Repair (Amst), 2007. **6**(4): p. 489-504.
174. Robertson, A.B., et al., *DNA repair in mammalian cells: Base excision repair: the long and short of it.* Cell Mol Life Sci, 2009. **66**(6): p. 981-93.
175. Chen, J., B.F. Miller, and A.V. Furano, *Repair of naturally occurring mismatches can induce mutations in flanking DNA.* Elife, 2014. **3**: p. e02001.
176. Stich, M., et al., *5-aza-2'-deoxycytidine (DAC) treatment downregulates the HPV E6 and E7 oncogene expression and blocks neoplastic growth of HPV-associated cancer cells.* Oncotarget, 2016.
177. Hietanen, S., et al., *Activation of p53 in cervical carcinoma cells by small molecules.* Proc Natl Acad Sci U S A, 2000. **97**(15): p. 8501-6.
178. Kochetkov, D.V., et al., *[Transcriptional inhibition of human papilloma virus in cervical carcinoma cells reactivates functions of the tumor suppressor p53].* Mol Biol (Mosk), 2007. **41**(3): p. 515-23.
179. Dymalla, S., et al., *A novel peptide motif binding to and blocking the intracellular activity of the human papillomavirus E6 oncoprotein.* J Mol Med (Berl), 2009. **87**(3): p. 321-31.
180. Issaeva, N., et al., *Small molecule RITA binds to p53, blocks p53-HDM-2 interaction and activates p53 function in tumors.* Nat Med, 2004. **10**(12): p. 1321-8.
181. Zhao, C.Y., et al., *Rescue of p53 function by small-molecule RITA in cervical carcinoma by blocking E6-mediated degradation.* Cancer Res, 2010. **70**(8): p. 3372-81.
182. Vogelstein, B., D. Lane, and A.J. Levine, *Surfing the p53 network.* Nature, 2000. **408**(6810): p. 307-10.
183. Komarov, P.G., et al., *A chemical inhibitor of p53 that protects mice from the side effects of cancer therapy.* Science (New York, N.Y.), 1999. **285**(5434): p. 1733-7.
184. Rampias, T., et al., *E6 and e7 gene silencing and transformed phenotype of human papillomavirus 16-positive oropharyngeal cancer cells.* J Natl Cancer Inst, 2009. **101**(6): p. 412-23.
185. Morrison, M.A., et al., *Targeting the human papillomavirus E6 and E7 oncogenes through expression of the bovine papillomavirus type 1 E2 protein stimulates cellular motility.* J Virol, 2011. **85**(20): p. 10487-98.
186. Boulet, G., et al., *Human papillomavirus: E6 and E7 oncogenes.* Int J Biochem Cell Biol, 2007. **39**(11): p. 2006-11.
187. Leechanachai, P., et al., *The E5 gene from human papillomavirus type 16 is an oncogene which enhances growth factor-mediated signal transduction to the nucleus.* Oncogene, 1992. **7**(1): p. 19-25.
188. Ganguly, N., *Human papillomavirus-16 E5 protein: oncogenic role and therapeutic value.* Cell Oncol (Dordr), 2012. **35**(2): p. 67-76.
189. Venuti, A., et al., *Papillomavirus E5: the smallest oncoprotein with many functions.* Mol Cancer, 2011. **10**: p. 140.

190. Bellanger, S., et al., *Tumor suppressor or oncogene? A critical role of the human papillomavirus (HPV) E2 protein in cervical cancer progression.* Am J Cancer Res, 2011. **1**(3): p. 373-389.
191. Gialeli, C., A.D. Theocharis, and N.K. Karamanos, *Roles of matrix metalloproteinases in cancer progression and their pharmacological targeting.* FEBS J, 2011. **278**(1): p. 16-27.
192. Shay, G., C.C. Lynch, and B. Fingleton, *Moving targets: Emerging roles for MMPs in cancer progression and metastasis.* Matrix Biol, 2015. **44-46**: p. 200-6.
193. Stott-Miller, M., et al., *Tumor and salivary matrix metalloproteinase levels are strong diagnostic markers of oral squamous cell carcinoma.* Cancer Epidemiol Biomarkers Prev, 2011. **20**(12): p. 2628-36.
194. Zhang, G., et al., *Matrix metalloproteinase-10 promotes tumor progression through regulation of angiogenic and apoptotic pathways in cervical tumors.* BMC Cancer, 2014. **14**: p. 310.
195. Jiang, H., et al., *Helicobacter pylori infection promotes the invasion and metastasis of gastric cancer through increasing the expression of matrix metalloproteinase-1 and matrix metalloproteinase-10.* Exp Ther Med, 2014. **8**(3): p. 769-774.
196. Foley, C.J., et al., *Matrix metalloprotease-1a promotes tumorigenesis and metastasis.* J Biol Chem, 2012. **287**(29): p. 24330-8.
197. ; Available from: http://home.ccr.cancer.gov/lco/ripcord.htm.
198. Yin, F., et al., *HPV16 oncogenes E6 or/and E7 may influence the methylation status of RASSFIA gene promoter region in cervical cancer cell line HT-3.* Oncol Rep, 2017.
199. Laurson, J., et al., *Epigenetic repression of E-cadherin by human papillomavirus 16 E7 protein.* Carcinogenesis, 2010. **31**(5): p. 918-26.
200. Henken, F.E., et al., *Sequential gene promoter methylation during HPV-induced cervical carcinogenesis.* Br J Cancer, 2007. **97**(10): p. 1457-64.
201. Li, L., et al., *E6 and E7 gene silencing results in decreased methylation of tumor suppressor genes and induces phenotype transformation of human cervical carcinoma cell lines.* Oncotarget, 2015. **6**(27): p. 23930-43.
202. Mazumder Indra, D., et al., *Genetic and epigenetic changes of HPV16 in cervical cancer differentially regulate E6/E7 expression and associate with disease progression.* Gynecol Oncol, 2011. **123**(3): p. 597-604.
203. Zawacka-Pankau, J. and G. Selivanova, *Pharmacological reactivation of p53 as a strategy to treat cancer.* J Intern Med, 2015. **277**(2): p. 248-59.
204. Selivanova, G. and K.G. Wiman, *Reactivation of mutant p53: molecular mechanisms and therapeutic potential.* Oncogene, 2007. **26**(15): p. 2243-54.
205. Sjoblom, T., et al., *The consensus coding sequences of human breast and colorectal cancers.* Science, 2006. **314**(5797): p. 268-74.
206. Layland, M.K., D.G. Sessions, and J. Lenox, *The influence of lymph node metastasis in the treatment of squamous cell carcinoma of the oral cavity, oropharynx, larynx, and hypopharynx: N0 versus N+.* Laryngoscope, 2005. **115**(4): p. 629-39.
207. Liotta, L.A., et al., *Metastatic potential correlates with enzymatic degradation of basement membrane collagen.* Nature, 1980. **284**(5751): p. 67-8.
208. Bhowmick, N.A., E.G. Neilson, and H.L. Moses, *Stromal fibroblasts in cancer initiation and progression.* Nature, 2004. **432**(7015): p. 332-7.

209. Silverman, L.R., et al., *Randomized controlled trial of azacitidine in patients with the myelodysplastic syndrome: a study of the cancer and leukemia group B.* J Clin Oncol, 2002. **20**(10): p. 2429-40.
210. Mootha, V.K., et al., *PGC-1alpha-responsive genes involved in oxidative phosphorylation are coordinately downregulated in human diabetes.* Nat Genet, 2003. **34**(3): p. 267-73.
211. Subramanian, A., et al., *Gene set enrichment analysis: a knowledge-based approach for interpreting genome-wide expression profiles.* Proc Natl Acad Sci U S A, 2005. **102**(43): p. 15545-50.
212. Hunter, K.D., E.K. Parkinson, and P.R. Harrison, *Profiling early head and neck cancer.* Nat Rev Cancer, 2005. **5**(2): p. 127-35.
213. Pasqualucci, L., et al., *Analysis of the coding genome of diffuse large B-cell lymphoma.* Nat Genet, 2011. **43**(9): p. 830-7.
214. Oganesyan, G., et al., *Critical role of TRAF3 in the Toll-like receptor-dependent and -independent antiviral response.* Nature, 2006. **439**(7073): p. 208-11.
215. Eliopoulos, A.G., et al., *CD40-induced growth inhibition in epithelial cells is mimicked by Epstein-Barr Virus-encoded LMP1: involvement of TRAF3 as a common mediator.* Oncogene, 1996. **13**(10): p. 2243-54.
216. Imbeault, M., et al., *Acquisition of host-derived CD40L by HIV-1 in vivo and its functional consequences in the B-cell compartment.* J Virol, 2011. **85**(5): p. 2189-200.
217. Karim, R., et al., *Human papillomavirus (HPV) upregulates the cellular deubiquitinase UCHL1 to suppress the keratinocyte's innate immune response.* PLoS Pathog, 2013. **9**(5): p. e1003384.
218. Guven-Maiorov, E., et al., *The Architecture of the TIR Domain Signalosome in the Toll-like Receptor-4 Signaling Pathway.* Sci Rep, 2015. **5**: p. 13128.
219. Chan, Y.K. and M.U. Gack, *Viral evasion of intracellular DNA and RNA sensing.* Nat Rev Microbiol, 2016. **14**(6): p. 360-73.
220. Balachandran, S. and A.A. Beg, *Defining emerging roles for NF-kappaB in antivirus responses: revisiting the interferon-beta enhanceosome paradigm.* PLoS Pathog, 2011. **7**(10): p. e1002165.
221. Stetson, D.B. and R. Medzhitov, *Recognition of cytosolic DNA activates an IRF3-dependent innate immune response.* Immunity, 2006. **24**(1): p. 93-103.
222. Sima, R., et al., *Brooke-Spiegler syndrome: report of 10 patients from 8 families with novel germline mutations: evidence of diverse somatic mutations in the same patient regardless of tumor type.* Diagn Mol Pathol, 2010. **19**(2): p. 83-91.
223. Pickering, C.R., et al., *Mutational landscape of aggressive cutaneous squamous cell carcinoma.* Clin Cancer Res, 2014. **20**(24): p. 6582-92.
224. Seiwert, T.Y., et al., *Integrative and comparative genomic analysis of HPV-positive and HPV-negative head and neck squamous cell carcinomas.* Clin Cancer Res, 2015. **21**(3): p. 632-41.
225. Friedman, C.S., et al., *The tumour suppressor CYLD is a negative regulator of RIG-I-mediated antiviral response.* EMBO Rep, 2008. **9**(9): p. 930-6.
226. Zhang, M., et al., *Regulation of antiviral innate immunity by deubiquitinase CYLD.* Cell Mol Immunol, 2011. **8**(6): p. 502-4.

227. Zheng, H., et al., *Whole-exome sequencing identifies multiple loss-of-function mutations of NF-kappaB pathway regulators in nasopharyngeal carcinoma.* Proc Natl Acad Sci U S A, 2016. **113**(40): p. 11283-11288.
228. Yarbrough, W.G., et al., *Phosphoinositide kinase-3 status associated with presence or absence of human papillomavirus in head and neck squamous cell carcinomas.* Int J Radiat Oncol Biol Phys, 2007. **69**(2 Suppl): p. S98-101.
229. Mzarico, E., et al., *Relationship between smoking, HPV infection, and risk of Cervical cancer.* Eur J Gynaecol Oncol, 2015. **36**(6): p. 677-80.
230. Austin, D.F., *Smoking and cervical cancer.* Jama, 1983. **250**(4): p. 516-7.
231. Fonseca-Moutinho, J.A., *Smoking and cervical cancer.* ISRN Obstet Gynecol, 2011. **2011**: p. 847684.
232. Ang, K.K., et al., *Human papillomavirus and survival of patients with oropharyngeal cancer.* N Engl J Med, 2010. **363**(1): p. 24-35.
233. D'Souza, G., et al., *Case-control study of human papillomavirus and oropharyngeal cancer.* N Engl J Med, 2007. **356**(19): p. 1944-56.
234. Pyeon, D., et al., *Fundamental differences in cell cycle deregulation in human papillomavirus-positive and human papillomavirus-negative head/neck and cervical cancers.* Cancer Res, 2007. **67**(10): p. 4605-19.
235. Nakahara, T. and P.F. Lambert, *Induction of promyelocytic leukemia (PML) oncogenic domains (PODs) by papillomavirus.* Virology, 2007. **366**(2): p. 316-29.
236. Amador-Molina, A., et al., *Role of innate immunity against human papillomavirus (HPV) infections and effect of adjuvants in promoting specific immune response.* Viruses, 2013. **5**(11): p. 2624-42.
237. Stanley, M., *Immune responses to human papillomavirus.* Vaccine, 2006. **24 Suppl 1**: p. S16-22.
238. Scott, M., M. Nakagawa, and A.B. Moscicki, *Cell-mediated immune response to human papillomavirus infection.* Clin Diagn Lab Immunol, 2001. **8**(2): p. 209-20.
239. Amici, C., et al., *Activation of I kappa b kinase by herpes simplex virus type 1. A novel target for anti-herpetic therapy.* J Biol Chem, 2001. **276**(31): p. 28759-66.
240. Schwarz, E.M., et al., *NF-kappaB-mediated inhibition of apoptosis is required for encephalomyocarditis virus virulence: a mechanism of resistance in p50 knockout mice.* J Virol, 1998. **72**(7): p. 5654-60.
241. Santoro, M.G., A. Rossi, and C. Amici, *NF-kappaB and virus infection: who controls whom.* Embo j, 2003. **22**(11): p. 2552-60.
242. Parra, E., J. Ferreira, and A. Ortega, *Overexpression of EGR-1 modulates the activity of NF-kappaB and AP-1 in prostate carcinoma PC-3 and LNCaP cell lines.* Int J Oncol, 2011. **39**(2): p. 345-52.
243. Rickman, D.S., et al., *Prediction of future metastasis and molecular characterization of head and neck squamous-cell carcinoma based on transcriptome and genome analysis by microarrays.* Oncogene, 2008. **27**(51): p. 6607-22.
244. Kauffmann, A., et al., *High expression of DNA repair pathways is associated with metastasis in melanoma patients.* Oncogene, 2008. **27**(5): p. 565-73.

245. Dodd, L.E., et al., *Genes involved in DNA repair and nitrosamine metabolism and those located on chromosome 14q32 are dysregulated in nasopharyngeal carcinoma.* Cancer Epidemiol Biomarkers Prev, 2006. **15**(11): p. 2216-25.
246. Kita, K., et al., *Involvement of LEU13 in interferon-induced refractoriness of human RSa cells to cell killing by X rays.* Radiat Res, 2003. **160**(3): p. 302-8.
247. Sirota, N.P., et al., *Modifying effect in vivo of interferon alpha on induction and repair of lesions of DNA of lymphoid cells of gamma-irradiated mice.* Radiat Res, 1996. **146**(1): p. 100-5.
248. Weichselbaum, R.R., et al., *An interferon-related gene signature for DNA damage resistance is a predictive marker for chemotherapy and radiation for breast cancer.* Proc Natl Acad Sci U S A, 2008. **105**(47): p. 18490-5.
249. Khodarev, N.N., et al., *STAT1 is overexpressed in tumors selected for radioresistance and confers protection from radiation in transduced sensitive cells.* Proc Natl Acad Sci U S A, 2004. **101**(6): p. 1714-9.

Supplemental Figures and Tables

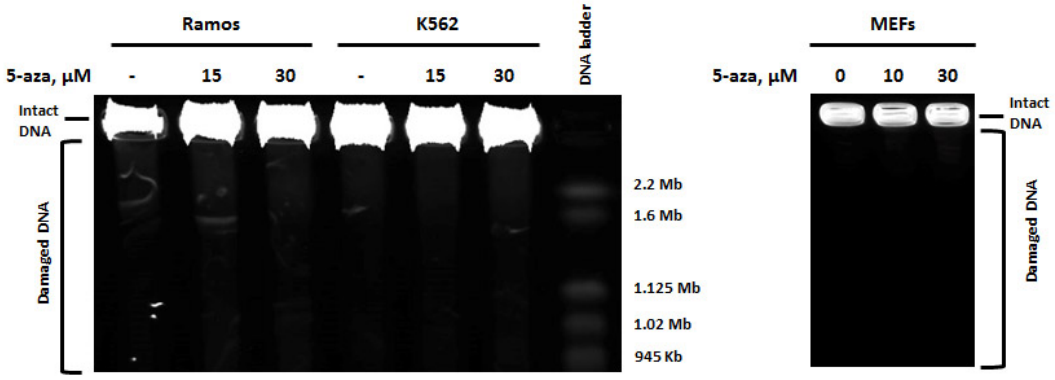

Supplementary Figure 1: *5-aza does not induce DSBs in lymphoma or AML cells* (left) PFGE depicting Ramos (Burkitt's lymphoma) and K562 (AML) cells treated with 72 hours of 0, 15, or 30μM 5-aza as indicated. (right) PFGE depicting MEFs (mouse embryonic fibroblasts) treated with 72 hours of 0, 10, or 30μM 5-aza as indicated

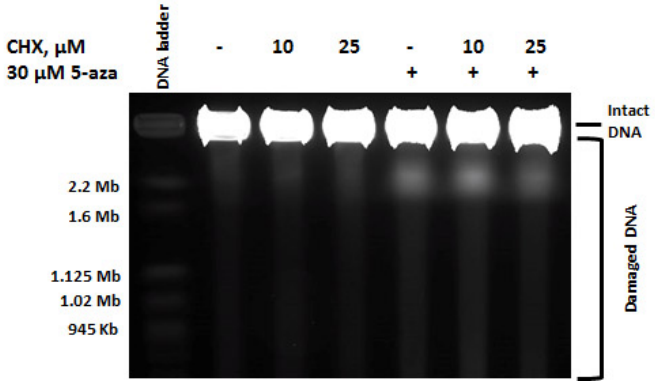

Supplementary Figure 2: *5-aza induced DSBs do not depend on de-novo protein translation.* PFGE depicting HPV+ UMSCC47 cells treated for 24 hours with 0, 10 or 25μM cycloheximide (CHX) as indicated, without or without 72 hours of 30μM 5-aza as indicated.

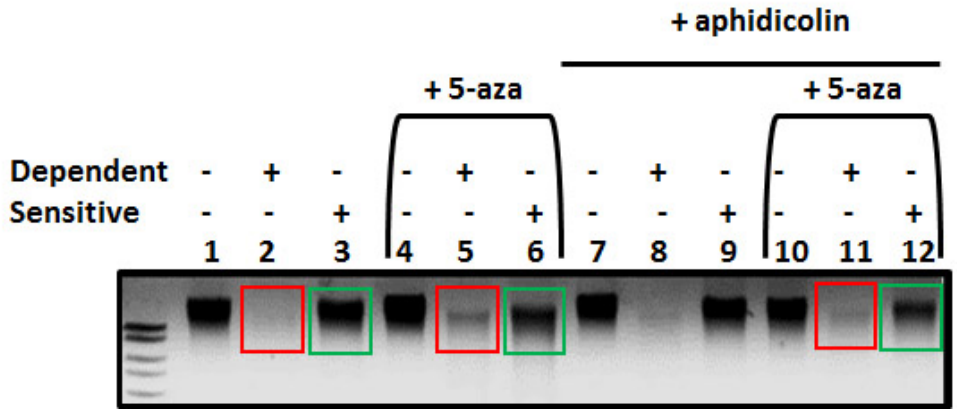

Supplementary Figure 3: *Replication inhibition does not prevent 5-aza induced demethylation.* Ethidium Bromide stained DNA gel after restriction of DNA from HPV+ UMSCC47 cells treated with 30μM 5-aza for 72 hrs, aphidicolin (aph) for last 24 hrs, or a combination of the two (last 24 hr of 5-aza treatment) with methylation dependent (red squares) or methylation sensitive (green squares) enzymes. Methylation dependent restriction can cut DNA only at methylated CpG loci, while sensitive can only cut DNA at unmethylated CpG loci.

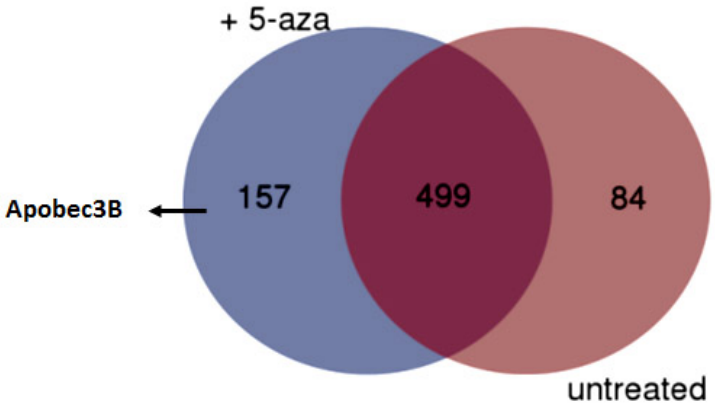

Supplementary Figure 4: *APOBEC3B is found only on 5-aza treated chromatin in HPV+ HNSCC cells.* Venn diagram depicting numbers of peptides found with 95% confidence via mass spectrometry on HPV+ UMSCC47 cells treated with 20μM 5-aza for 72 hours.

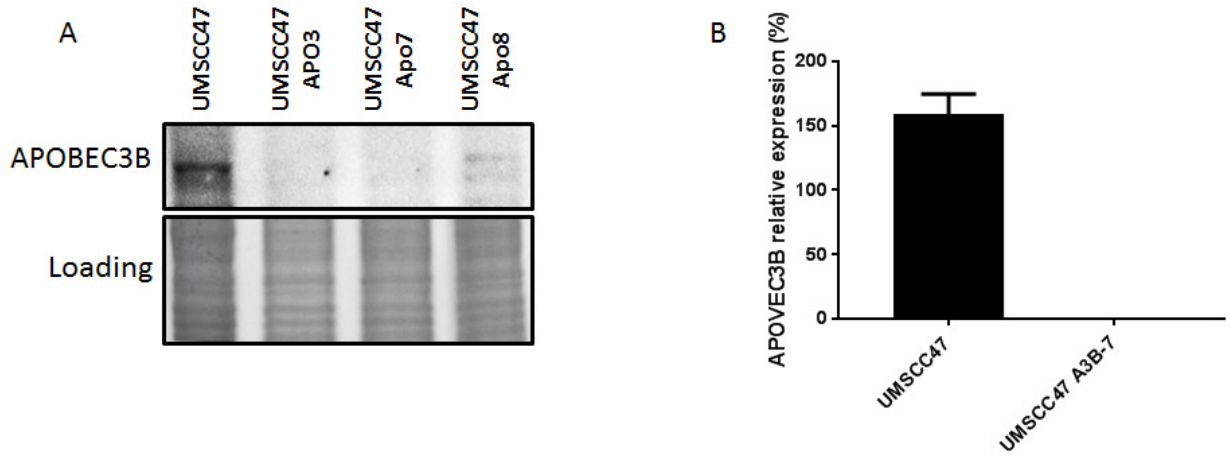

Supplementary Figure 5: *APOBEC3B knockout.* (A) Immunoblot showing APOBEC3B protein levels in cell lysates of HPV+ UMSCC47 and three APOBEC3B CRISPR clones. "UMSCC47 Apo7" was used in Figure 7. (B) Relative expression of APOBEC3B mRNA in HPV+ UMSCC47 cells and APOBEC3B CRISPR cells, as determined by qRT-PCR.

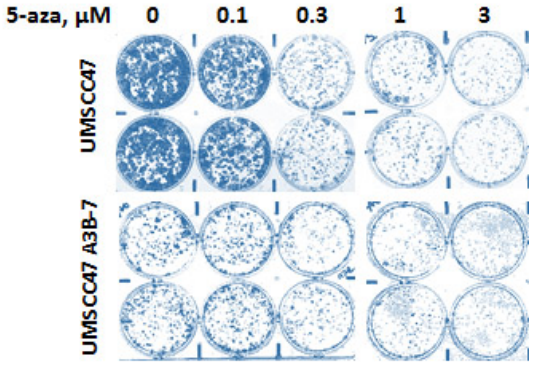

Supplementary Figure 6: *Clonogenic survival in HPV+ HNSCC with APOBEC3B knockout after 5-aza.* Clonogenic survival assay showing HPV+ UMSCC47 cells (top two rows) and UMSCC47 cells with APOBEC3B CRISPR (A3B-7) (bottom two rows) after treatment with increasing doses of 5-aza.

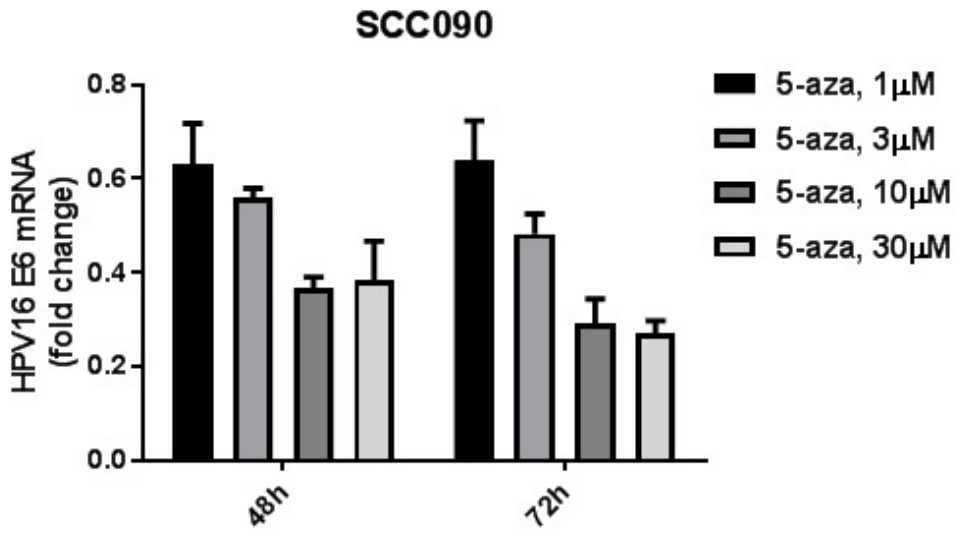

Supplementary Figure 7: *5-aza downregulates HPV E6 in HPV+ HNSCC.* Fold change in HPV16 E6 expression after 48 and 72 hours of varying doses of 5-aza in HPV+ SCC090 cells as determined by qRT-PCR

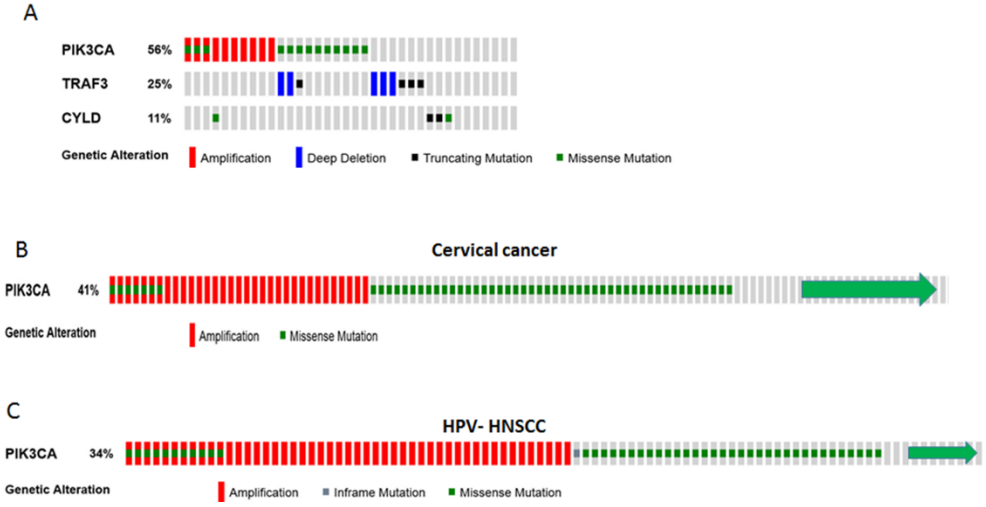

Supplementary Figure 8: (A) Genetic alterations in PIK3CA, TRAF3 and CYLD genes found in HPV-positive (n=36) HNSCC. (B) Genetic alterations in PIK3CA found in cervical cancer (n=191) and (C) in HPV-negative HNSCC (n=243). Individual tumors are represented as columns. The green arrow indicates that several tumors without alterations were cut to fit the figure. Figures were adapted from www.cbioportal.org

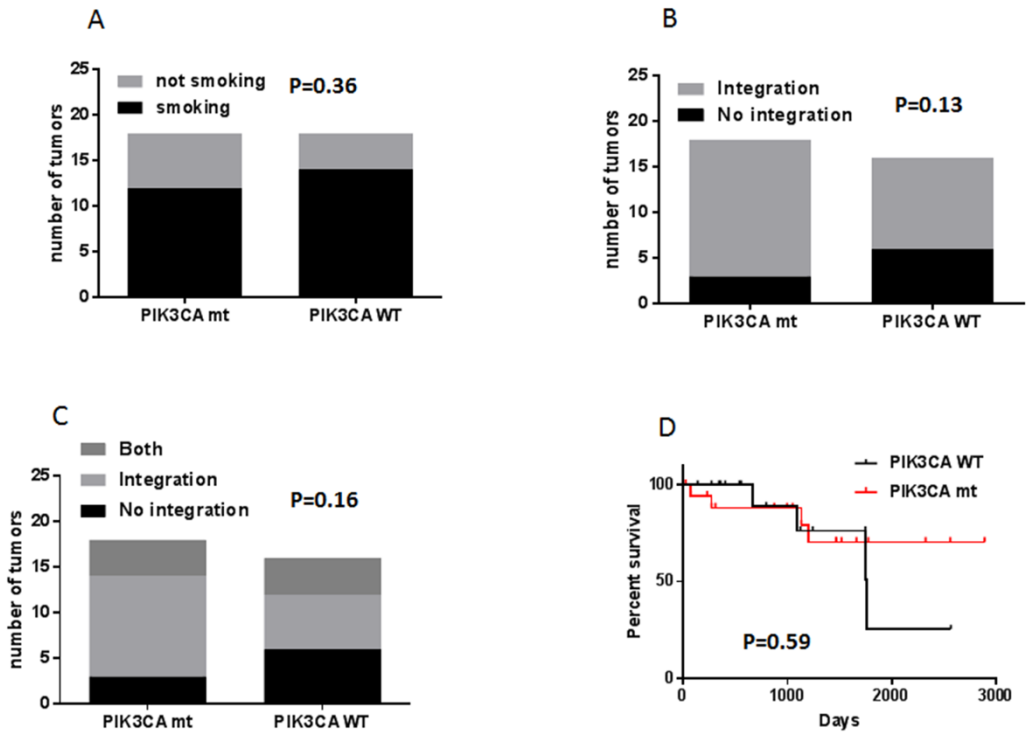

Supplementary Figure 9: *(*A) Contingency graph representing the distribution of smokers or non-smokers in PIK3CA wt and mt groups; p value was calculated using two-sided Fisher's exact test. (B) Contingency graph representing the distribution of tumors with or without HPV integration in PIK3CA wt and mt groups; p value was calculated using a two-sided Fisher exact test. (C) Contingency graph representing the distribution of tumors with episomal HPV only, with HPV integrations only, or containing both integrated and episomal HPV DNA in PIK3CA wt and mt groups; p value was calculated using two sided Chi-square test. (D) Kaplan-Meier curves showing overall survival of HPV-associated HNSCC patients with or without alterations in PIK3CA; statistic was done using Log-rank (Mantel-Cox) test.

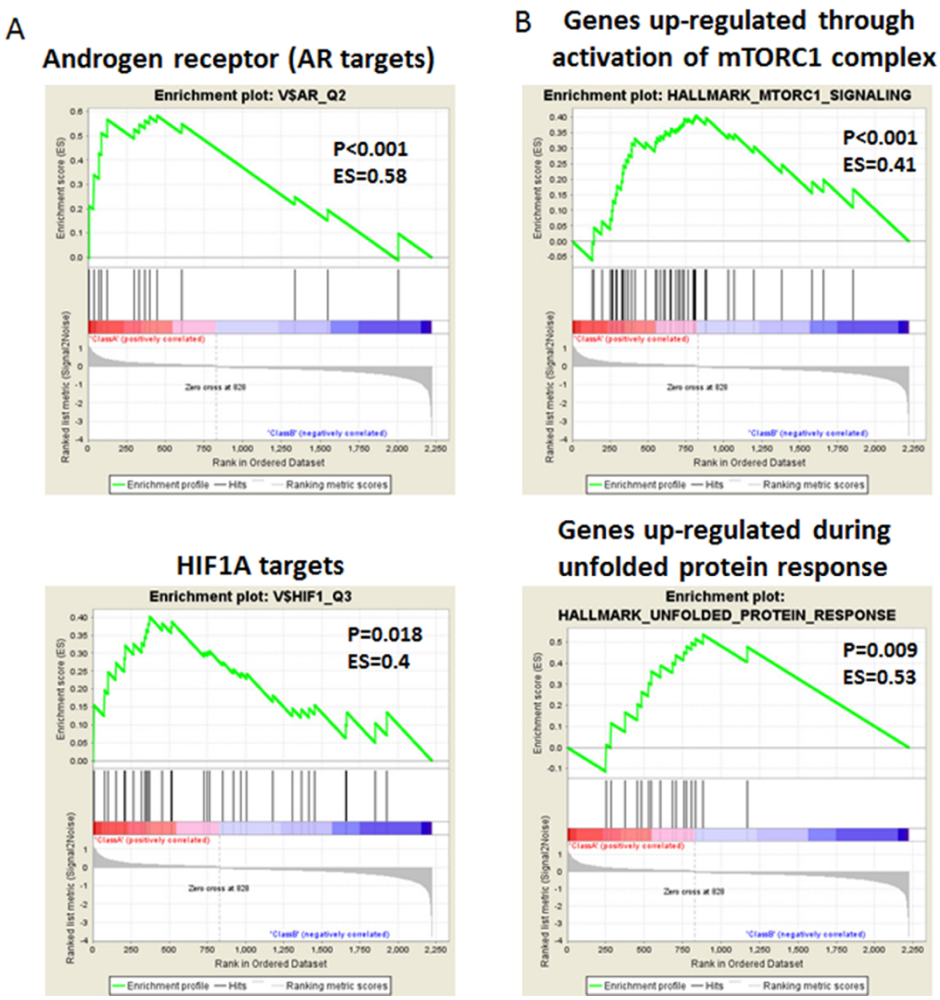

Supplementary Figure 10: Results of transcription factor (A) target genes or (B) data sets of oncogenic and hallmark GSEA for genes that are significantly differently expressed in PIK3CA mutant (vs the wild type group). ES = enrichment score; p = nominal p value.

Table 1: CYLD mutations in HPV+ HNSCC

Amino Acid Change	Type	Copy Number
K680*	Nonsense	Shallow Deletion
S371*	Nonsense	Shallow Deletion
D618A	Missense	Shallow Deletion
N300S	Missense	Shallow Deletion